Master's thesis

Next-to-leading order QCD corrections to the Drell-Yan process

Submitted by

Oliver Ledwig

October 4, 2017

First examiner

Prof. Dr. Michael Klasen

Second examiner

Dr. Karol Kovařík

Westfälische Wilhelms-Universität Münster

Fachbereich Physik

Institut für theoretische Physik

Contents

1 Introduction

Since antiquity, philosophers have been pondering, what the inner structure and the building blocks of matter are. Even then the idea existed that matter consists of small, indivisible constituents, however, it was only in the 19th century given a scientific basis by John Dalton in his Atomic theory. It gradually gained more and more recognition by chemist and physicists, and almost a decade later in 1906 Thomson found the first experimental evidence for an elementary particle in his investigation of cathode rays. However, the mass of the particles, he had observed, was only a small fraction of the predicted mass of an atom. He had not observed atoms, but smaller particles, the electrons. His findings led Thomson and other scientists to discard the hitherto accepted atom model, and replace it by the so-called plum pudding model, where he postulated that the negatively charged electrons were distributed throughout the atom in a uniform sea of positive charge.

He was proven wrong by Rutherford only some years later. Rutherford showed that atoms contain highly condensed positively charged nuclei with an size of less than about 10^{-14} m. The basis for his analysis was the famous gold foil experiment, where Hans Geiger and Ernest Marsden under his direction bombarded a metal foil with $\alpha-$particles and measured the deflection angle of the particles. From the fact that a substantial amount of particles was deflected by angles of more than $90°$, he concluded that there must be positive charge concentrated in a very small nucleus in the center of the atom.

Rutherford's experiment might be considered the first prototype experiment of modern particle physics. Since then, the so-called scattering experiments have been one of the main instruments to investigate the structure and interaction of particles. The main idea is that particles are accelerated and collided, and the distribution of outcoming particles is measured. By comparison with models and their theoretical predictions, theories can be tested and properties of particles can be inferred. While Rutherford scattering is an example of elastic scattering, in the 1950 the first particle accelerators that collide particles in inelastic collisions were built, where exited particle states or even additional particles are created according to the energy-mass equivalence. In the last decades, numerous accelerators reaching to higher and higher collision energies have been built, revealing new particles and evidence for deeper constituents of matter. Today we know that atoms are made of protons and neutrons, which are not elementary particles, but consist of the elementary quarks and gluons.

Up to now the search for the most fundamental particles has culminated in the standard model of particle physics, which was formulated in its current form already in the 1970s. The standard model does not only classify all known elementary particles, but also describes their interactions among each other by the fundamental weak, strong, and electromagnetic force. It has been a huge success in predicting particles and their properties, such as the W and Z Boson, and has been experimentally confirmed with high precision. Nevertheless it cannot explain certain phenomena, such as neutrino masses or dark matter. To find solutions to these problems and further test the standard model, the Large Hadron Collider (LHC) was built, which collides protons at unmatched energies. But to do this to high precision, an accurate understanding of the proton is essential.

This thesis focuses on the theoretical treatment of one of the processes, which provides essential information on the structure of the proton, the Drell-Yan process,

$$H_a + H_b \to l^- l^+ + X$$

where two hadrons ($H_{a/b}$) are collided to form a lepton-antilepton pair ($l^- l^+$) and additional debris particles X, which are usually of less interest then the lepton pair. It is one of the best explored processes at hadron-hadron colliders, because precise theoretic predictions can be made, and the experimental signal is very clear, with two leptons in the final state. The process was used to design the experiments at CERN that discovered the W and Z bosons [1], and was also a crucial background process in the discovery of the top quark at Fermilab [2].

Today, the Drell-Yan process is still one of the main tools to probe the partonic structure of hadrons, where at the current LHC beam energy of 14 TeV even contributions from heavier quark flavors such as strange or charm can be resolved. It can therefore be used to further constrain the information on the partonic structure of the proton, which is important for the discovery of new phenomena and high precision measurements at all recent and future hadron-hadron colliders. It also opens a window to new physics, as extensions of the standard model such as new neutral (Z') or charged (W') currents can be tested.

The aim of this thesis, is the detailed calculation of the hadronic Drell-Yan cross section at next-to-leading order in QCD. The outline is the following:

In chapter 2, the theoretical foundations of how cross sections are computed generally in a quantum field theory are discussed. This includes how cross sections can be reduced to the fundamental object of the theory, the Green's function, and how these can be calculated perturbatively using Feynman rules. In chapter 3, the quantum field theory of the strong interaction, QCD, is introduced. The basic Feynman rules of QCD are given and it is shown how divergences that occur in next-to-leading order calculations are treated. Subsequently we discuss how hadronic cross sections can be calculated using QCD and the parton model in chapter 4. Using the techniques described in the preceding chapters, the main part of the thesis, the calculation of the Drell-Yan cross section to next-to-leading order will be presented in chapter 5. We start with the leading-order partonic contributions, and then cover the contributions of $\mathcal{O}(\alpha_s)$. Finally we show, how a finite prediction for the cross section $\frac{\mathrm{d}\sigma}{\mathrm{d}q^2}$ can be obtained from the calculation.

2 Cross sections

As mentioned in the introduction, starting with Rutherford's discovery of the nucleus in 1911, scattering experiments have been the main source of information about the properties and interactions of elementary particles. Since then colliders have been the tool of choice to perform scattering experiments, as they provide a way to carefully set up well-defined initial states $|i\rangle$ and then produce non-interacting final states $|f\rangle$ that can be observed in detectors. The distribution and number of final state particles carries the information about the scattering process. A measure for the strength of the interaction is the cross section

$$\sigma = \frac{1}{T\Phi}N,$$

where N is the total number of particles scattered, T the duration of the experiment and Φ the incoming flux. In quantum theories, the cross section can be written in terms of the S-Matrix $\langle f|S|i\rangle$, the overlap between both states of the experiment. We will first show this relation, then further reduce the S-Matrix to Green's functions and finally demonstrate how these Green's function can be computed.

2.1 Cross sections and the S-Matrix

To relate the formula for the cross section to the S-matrix, we consider a $2 \to n$ scattering process, where two particles with momenta p_a and p_b are scattered into final state particles with momenta k_j:

$$p_a + p_b \to \{k_j\}.$$

We can expect the cross section to be closely related to the quantum transition probabilities $|\langle f; t_f|i; t_i\rangle|^2$, where i is the initial state at time t_i and f denotes the final state at a later time t_f. In collider physics, we assume all interactions to happen during a finite time interval so that at asymptotic times $t_{i/f} = \mp\infty$ the initial and final state can be assumed to be composed of momentum eigenstates $|p\rangle$. One defines the S-matrix as

$$\langle f|S|i\rangle_{\text{Heisenberg}} = \langle f; \infty|i; -\infty\rangle_{\text{Schrödinger}}\,,$$

where S is the Operator that evolves the initial state into the final state. The S-Matrix contains all information about the scattering process, and can be calculated from a given theory. It is usually calculated perturbatively, such that it can be split up as

$$S = \mathbb{1} + i\mathcal{T},$$

with the identity representing the free part of the S matrix, where no interactions happen, and the transfer matrix $\mathcal{T}$, which describes deviations from the free theory. The S-matrix will always vanish, unless initial and final state fulfill four-momentum conservation

$$\sum p = \sum p_i - \sum k_j = 0.$$

Hence one factors a momentum conserving factor off the transfer matrix

$$\langle f|\mathcal{T}|i\rangle = (2\pi)^4\delta^4(\Sigma p)\mathcal{M}.$$

Thus the interesting part for scattering, namely the matrix element $\mathcal{M}$ can be related to the S-matrix,

$$\langle f|S-1|i\rangle = i(2\pi)^4\delta^4(\sum p)\mathcal{M}.$$

We can convert this into a normalized differential transition probability, by taking the absolute value squared and multiplying with the phase space for the final momenta,

$$\mathrm{d}\tilde{P} = \frac{\mathrm{d}^3k_1}{(2\pi)^3 2E_1}\cdots\frac{\mathrm{d}^3k_n}{(2\pi)^3 2E_n}\left|\langle f|S-1|i\rangle\right|^2.$$

This yields a differential probability which still has to be normalized, because the initial and final states may not be normalized. By analyzing the normalization of these momentum eigenstates, one finds the normalization factor VT, which is the space-time volume in which the scattering takes place. In symbolic notion, it can be written as

$$VT = (2\pi)^4\delta^4(0),$$

so the normalized probability for the scattering takes the form

$$\begin{aligned}\mathrm{d}P &= \frac{\mathrm{d}^3k_1}{(2\pi)^3 2E_1}\cdots\frac{\mathrm{d}^3k_n}{(2\pi)^3 2E_n}(2\pi)^4\delta^4(\sum p)|\mathcal{M}|^2\\ &= \mathrm{dPS}^{(n)}|\mathcal{M}|^2,\end{aligned}$$

where the phase space, together with the factor of $(2\pi)^4\delta^4(\sum p)$, is called the Lorentz-invariant phase space $\mathrm{dPS}^{(n)}$. The transition probability can be directly transformed into a quantity with the dimension of an area by dividing by the flux factor

$$\mathrm{d}\sigma = \frac{1}{F}\mathrm{d}P = \frac{1}{F}\mathrm{dPS}^{(n)}|\mathcal{M}|^2$$

which is given by

$$F = 4E_aE_b|v_a^z - v_b^z|.$$

Here $E_{a/b}$ is the energy of the respective incoming particle, and $v_{a/b}^z$ the velocity in the beam direction, which is conventionally chosen to be z. One can write the flux factor using only Lorentz invariants as

$$F = 2\lambda^{\frac{1}{2}}(s, m_a^2, m_b^2),$$

where the Källeén function

$$\lambda(x,y,z) \equiv x^2 + y^2 + z^2 - 2xy - 2yz - 2zx$$

was used. We can now compute differential or total cross sections by partially or fully integrating out the final state kinematical variables $\vec{k}_j$. To do so, the S-matrix is required, which we will further reduce to a more fundamental object, the Green's functions in the next section.

It should be noted that cross sections are typically understood as unpolarized cross section, unless stated otherwise. These are cross sections where no spin information about the incoming and outgoing particles is recorded. In this case, one has to sum over all final state spins and average over initial states spins, so one has to replace

$$|\mathcal{M}|^2 \to |\overline{\mathcal{M}}|^2 = \frac{1}{N} \sum_{\text{spin states}} |\mathcal{M}|^2$$

where N is the number of initial, unobserved spin states.

2.2 Reduction of the S-Matrix

In a quantum field theory, one does not compute the S-matrix directly, but instead one computes more fundamental objects, the Green's functions,

$$G(x_1, ..., x_n) = \langle T\{\phi(x_1)...\phi(x_n)\}\rangle ,$$

which are given as time-ordered correlation functions of the fields. The Green's functions contain all physical information about the fields of the theory and contributions to the S-matrix can be projected out using the LSZ (Lehmann-Symanik-Zimmermann) reduction formula [4]. The procedure is the following:

According to the LSZ formula, S-Matrix elements are obtained from the Green's Function $G(x_1, ..., x_n)$ by first taking the Fourier transform:

$$\begin{aligned} G(p_1, ..., p_n) &= \int \mathrm{d}^4x_1...\mathrm{d}^4x_n e^{-i(p_1x_1+...+p_nx_n)} G(x_1, ..., x_n) \\ &= (2\pi)^4 \delta(p_1 + ... + p_n) G(p_1, ..., p_n) \end{aligned}$$

Then the poles have to be removed by multiplying with $-i(p_i^2 - M_i^2)$. Finally, the particles can be put on-shell by taking $p^2 = M^2$. For scalar particles, the LSZ formula thus reads

$$\langle -p_{s+1}.... - p_n|S|p_1....p_s\rangle = R^{-n/2}(-i)^n(p_1^2 - M_1^2)...(p_n^2 - M_n^2)\, \widetilde{G}(p_1, ..., p_n)|_{p^2=M^2} \tag{2.1}$$

where the wave function renormalization constants R are required for a correct normalization of the S-matrix. They are given as the expectation value of the field operators for generating a one-particle state, or equivalently by the residues of the two-point function at the physical mass,

$$R = |\langle M, p|\psi(x)|0\rangle|^2 = -i(p^2 - M^2)G(p, -p)|_{p^2=M^2}. \tag{2.2}$$

We can use this relation to replace the factors $p_i^2 - M_i^2$ in (2.1) to get

$$\langle -p_{s+1}.... - p_n|S|p_1....p_s\rangle = R^{n/2}\, \widetilde{G}_{\text{trunc}}(p_1, ..., p_n)|_{p_i^2=M_i^2} \tag{2.3}$$

which states that S-matrix elements are given by Fourier-transformed, truncated Green's functions

$$\widetilde{G}_{\text{trunc}}(p_1, ..., p_n) = G^{-1}(p_1, -p_1)...G^{-1}(p_n, -p_n)\widetilde{G}(p_1, ..., p_n) \tag{2.4}$$

taken on-shell.

For $2 \to 2$ processes, the LSZ Formula can be illustrated like this

$$\langle k_1 k_2 | S | p_1 p_2 \rangle = (\sqrt{R})^4$$

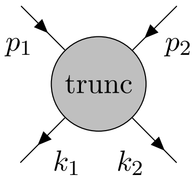

where the blob represents the truncated Green's function, such that the four legs are on-shell.

2.3 Perturbative Expansion of Green's functions

The Green's functions for most interacting quantum field theories, such as QCD cannot be calculated exactly which is why a perturbative expansion in the coupling constant is necessary. As described in the previous section, the starting point is the Green's function

$$G(x_1, ..., x_n) = \langle \Omega | T \{\phi(x_1)...\phi(x_n)\} | \Omega \rangle$$

which then has to be Fourier-transformed and truncated. Here the vacuum state of the interacting theory is denoted as Ω, and the fields $\phi(x_i)$ are fully interacting quantum fields.
There are several equivalent ways to derive a expansion of this Green's function, for example using path integral representation. The starting point is always that the Lagrangian can be separated into a free and an interacting part,

$$\mathcal{L} = \mathcal{L}_0 + \mathcal{L}_{\text{int}}.$$

In the canonical formalism, the most frequently used approach is to first switch to interaction picture and to obtain the Gell-Mann and Low theorem

$$\langle \Omega | T\phi(x_1)...\phi(x_n) | \Omega \rangle = \frac{\langle 0 | T \left\{ \phi_0(x_1)...\phi_0(x_n) \exp\left[i \int \mathrm{d}^4 x \, \mathcal{L}_{\text{int}}[\phi_0(x)] \right] \right\} | 0 \rangle}{\langle 0 | T \left\{ \exp\left[i \int \mathrm{d}^4 x \, \mathcal{L}_{\text{int}}[\phi_0(x)] \right] \right\} | 0 \rangle}, \tag{2.5}$$

which reduces the Green's function to vacuum expectation values (vev) of the free fields ϕ_0 of the theory, which are described by $\mathcal{L}_0$. Here, the Dyson operator

$$\exp\left[i \int \mathrm{d}^4 x \, \mathcal{L}_{\text{int}}[\phi_0(x)] \right] = 1 + i \int \mathrm{d}^4 x \, \mathcal{L}_{\text{int}}[\phi_0(x)] - \int \mathrm{d}^4 x \mathrm{d}^4 y \, \mathcal{L}_{\text{int}}[\phi_0(x)] \mathcal{L}_{\text{int}}[\phi_0(y)] + ..., \tag{2.6}$$

gives a natural starting point for a power expansion in $\mathcal{L}_{\text{int}}$, which reduces the problem to calculating integrals of free n-point Green's functions

$$\langle 0 | T \{\phi_0(x_1)......\phi_0(x_n)\} | 0 \rangle .$$

By applying Wick's Theorem, these $n-$point correlators can be reduced to sums of products of only two-point correlators, the Feynman propagators

$$D_{\text{F}}(x, y) = \langle 0 | T \{\phi_0(x)\phi_0(y)\} | 0 \rangle .$$

Feynman developed a diagrammatic way to calculate this sum, where each propagator is represented by a line and each integration coming out of (2.6)

$$i \int \mathrm{d}^4 x \, \mathcal{L}_{\mathrm{int}}[\phi_0(x)]$$

is represented by a vertex, where the lines meet. The Feynman rules in position-space then simply state, that one has to construct all possible diagrams by connecting the initial and final state using the vertices and propagators of the theory. To give an example, the expansions of a two-point could be

$$G(x_1, x_2) = D_{\mathrm{F}}(x_1, x_2) - g \int \mathrm{d}^4 x \, D_{\mathrm{F}}(x_1, x) D_{\mathrm{F}}(x, x) D_{\mathrm{F}}(x_2, x) + ... \tag{2.7}$$

or diagrammatically

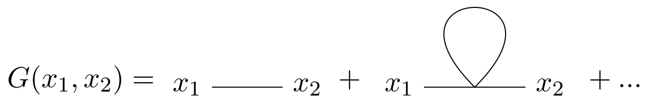

The expression for the propagator can be derived from the free (kinetic) part of the Lagrangian, whereas the coupling g is the prefactor of interaction terms such as

$$\mathcal{L}_{\mathrm{int}} = \frac{g}{4!} \phi^4 .$$

The Feynman rules can be simplified by switching to momentum-space. By using the Fourier-representation of the propagator

$$D_{\mathrm{F}}(x, y) = \int \frac{\mathrm{d}^4 p}{(2\pi)^4} e^{ip(x-y)} \tilde{D}_{\mathrm{F}}(p),$$

these rules can be converted to rules for the Green's function in momentum-space, which is exactly what is required by the LSZ formula. This results in the same lines and vertices, but the integrals

$$i \int \mathrm{d}^4 x$$

can be carried out, leaving momentum-conserving δ-functions of the form

$$\delta \left(\sum p_i^{(\mathrm{in})} - \sum k_j^{(\mathrm{out})} \right)$$

at each vertex multiplied with the coupling. Accordingly, only the momentum integrals over momenta which are undetermined are left over from the propagators. Lines therefore receive a factor $\tilde{D}_{\mathrm{F}}(p)$, unless they are connected to external points. In this case, the propagators are canceled by the LSZ formula as in (2.4). Thus in momentum space, (2.7) takes the form

$$\tilde{G}(p, -p) = \tilde{D}_{\mathrm{F}}(p) - g \int \frac{\mathrm{d}^4 p_1}{(2\pi)^4} \tilde{D}_{\mathrm{F}}(p_1) \tilde{D}_{\mathrm{F}}^2(p) + ... \quad . \tag{2.8}$$

The advantage of the Feynman rules in momentum space is that the propagators $\tilde{D}_{\mathrm{F}}(p)$ have a simpler form than in position space. Thus, for calculations one almost always uses the momentum space rules.

2.4 Structure of Green's functions

Equipped with a basic notion of how Green's functions can be represented and calculated, we examine their general structure. There exists a important subclass of Green's functions, the connected Green's functions $G_c(x_1, ..., x_n)$, which are represented by diagrams where any two points are connected to each other by internal lines. A simple example is the two-point Green's function which is equal to the connected two-point function

$$G(x_1, x_2) = G_c(x_1, x_2) = D_{\mathrm{F}}(x_1, x_2).$$

In general, Green's function can be decomposed into their connected parts by

$$G(x_1, x_n) = \sum_{\text{partitions}} G_c(x_1, ..., x_{k_1}) G_c(x_{k_1+1}, ..., x_{k_1+k_2}) ... G_c(..., x_n).$$

The decomposition of the four-point function reads

$$\begin{aligned} G(x_1, x_2, x_3, x_4) = G_c(x_1, x_2, x_3, x_4) + G_c(x_1, x_2) G_c(x_3, x_4) \\ + G_c(x_1, x_3) G_c(x_2, x_4) + G_c(x_1, x_4) G_c(x_2, x_3) \end{aligned} \tag{2.9}$$

The importance of the connected Green's function arises from a fact, that we suppressed in the previous sections: The only part of the n-point Green's function that contributes to the S-matrix is the respective n-point connected Green's function. On the one hand this is due to the denominator in the Gell-Mann and Low theorem (2.5), which cancels the so-called bubble graphs, a sum of disconnected graphs that factorize in the expansion of the Green's function. On the other hand, products of connected Green's function, such as the last three terms in (2.9) will have the wrong singularity structure to contribute to the S-matrix.

We can decompose the connected Green's functions further into their building blocks, which are propagators and vertex functions. The vertex function $\Gamma(x_1, ..., x_n)$ is defined by the sum of all one-particle irreducible, connected diagrams with n legs. A diagram is one-particle irreducible (1PI), if it can not be decomposed into two parts by cutting one internal line.

If we depict the vertex function as

$\Gamma(x_1, x_2, x_3, x_4) =$ 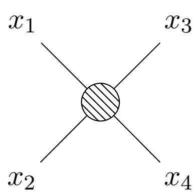

,

the three-point Green's function becomes

$G_c(x_1, x_2, x_3) =$ 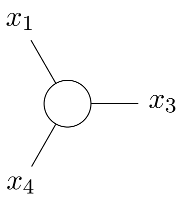

$=$ 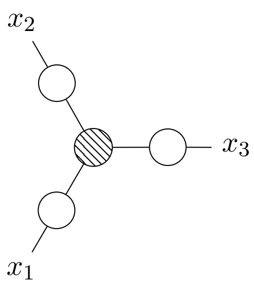

.

Here the blobs on the legs denote two-point functions. The connected four-point Green's function takes the form:

$G_c(x_1, x_2, x_3, x_4) =$

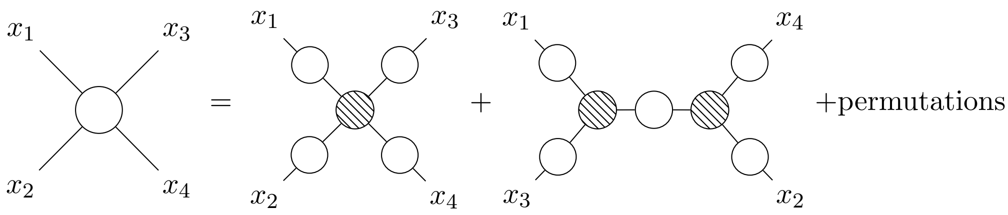

By permutations we denote the additional t and u channel, which are given by the exchange $x_3 \longleftrightarrow x_1$ and $x_3 \longleftrightarrow x_2$, respectively. This concept helps to systematically construct diagrams, and also gives an intuitive understanding of general collision processes: The particles interact in individual processes described by the vertex functions and are propagated in between.

For our final result we have to combine this with the LSZ formula. Note that in this section we argued, that only the connected part of the Green's function contributes to the S-matrix. In the above discussion we therefore included propagators on external legs. But the LSZ formula dictates, that propagators on external legs have to be truncated, so in summary, to compute cross section we need truncated, connected Green's functions, such as

$G_{\mathrm{c,tr}}(x_1, x_2, x_3, x_4) =$

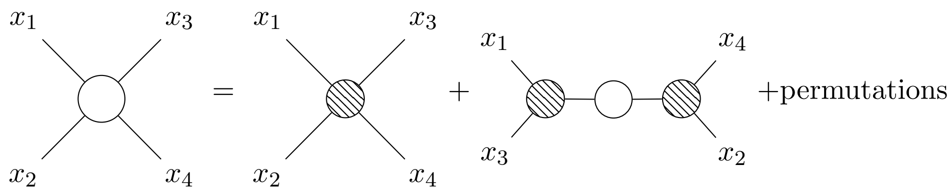

(2.10)

This is the structure, that every four-point Green's function will have and can serve as guidance, which Feynman diagrams to construct for a given process involving four particles.

3 Quantum chromodynamics

One might argue that the grounds for the development of a theory describing the strong interaction were laid by the discovery of nuclei being composed of protons and neutrons. Immediately afterwards, the question arose how the positively charged protons in the nucleus, packed closely together, could form a bound state, despite their strong electromagnetic repulsion. There had to be an unknown force binding protons (and neutrons) together. The first successful attempt to describe this force was made in 1934 by Yukawa, who described the strong force as the exchange of a massive scalar boson. A particle matching the prediction of Yukawa's theory, the pion, was eventually discovered, but while his model could well describe nuclear forces, physicists struggled to apply it to relativistic collisions of baryons and mesons.

Starting in the 50s, through advances in experimental techniques such as the bubble chamber, more and more particles were discovered. In an effort to classify these new particles systematically, Gell-Mann postulated his Eightfold Way in 1961, where hadrons of roughly the same mass are organized into representations of the SU(3) group. Predicting the later discovered Ω^-, his classification became widely accepted.

In 1964, Gell-Mann and Zweig showed that the structure of the Eightfold Way could be readily explained by the assumption that baryons are made out of constituents, the so-called "quarks". They assumed three quarks, up, down and strange (u, d, s) and assigned them fractions of the elementary electric charge and spin $\frac{1}{2}$. In this way, baryons and mesons could be described as bound states of 3 quarks (qqq), while mesons where composed of a quark - antiquark $(q\bar{q})$ pair.

Nevertheless, the quark model generated a problem with certain baryons, like the Δ^{++}, a bound state with spin $\frac{3}{2}$ out of three up quarks with identical quantum numbers. This was clearly a violation of the exclusion principle, which Greenberg, Han, and Nambu resolved in 1965. They introduced a new, unobserved quantum number, the color charge, such that each of the quarks in the Δ^{++} was carrying one of the three different color charges. All observed hadrons were assumed to be colorless states.

While in 1969 still no free quarks had been observed and physicist were debating whether quarks were actual physical entities, observations in high energy scattering of electrons on protons at SLAC showed a so-called scaling invariance, which had been predicted by Bjorken. Subsequently Richard Feynman showed, that this scaling could be explained by the elastic scattering of electrons off almost-free, point-like constituents inside the proton, which he named partons. In the following years, many experimental results indicated that these partons matched the quantum numbers of the quark model. Today it is clear that the partons in Feynman's parton model can be identified as quarks.

The parton model initiated the search for a quantum field theory describing the interaction of quarks. Nevertheless, none of the considered theories exhibited the property of the parton model that the interaction between quarks gets weaker at short distances. In 1973, ‘t Hooft, Gross, Wilczek, and Polizter examined non-abelian gauge theories, and showed that they indeed possessed this property, nowadays called asymptotic freedom.

As a non-abelian gauge theory is based on a gauge symmetry, which is connected to a conservation of charge-currents, the important question about the physical nature of these charges remained. Harald Fritzsch and Heinrich Leutwyler, together with Gell-Mann, proposed that this new charge was the color charge, a quantum number that had been introduced years earlier. With this identification, most of the problems in the quark model could be resolved. A consistent theory for the dynamics between quarks was established and received the name quantum chromodynamics (QCD). It describes the interaction between quarks by the exchange of gauge bosons, the so-called gluons. In contrast to the abelian quantum electrodynamics (QED), the gluons themselves carry color charge and therefore can self-interact and radiate further gluons.

3.1 QCD Lagrangian

As explained in the historic overview, QCD is the established theory to describe the strong interaction. Just as QED, it is a gauge theory, where interactions are mediated by gauge bosons, the gluons. The gauge group is $\mathrm{SU}(3)_\mathrm{C}$ and the index "C" denotes that the gauge transformations act on the color charge of the quarks. The classical gauge-invariant Lagrangian is

$$\mathcal{L}_\mathrm{QCD} = \bar{\psi}_i \left(i\gamma_\mu D^\mu_{ij} - m\,\delta_{ij} \right) \psi_j - \frac{1}{4} G^a_{\mu\nu} G^{\mu\nu}_a,$$

where $\psi_i(x)$ is the quark field in the fundamental representation of the $\mathrm{SU}(3)_\mathrm{C}$ gauge group with mass m. In the first term, the covariant derivative

$$D^\mu_{ij} = \partial^\mu \delta_{ij} - igT^a_{ij} A^\mu_a$$

acts on the quark field. Here, $A^a_\mu(x)$ denotes the gluon (gauge) field and T^a the generator of the fundamental representation of $\mathrm{SU}(3)_\mathrm{C}$. The parameter g_s measures the coupling strength of the strong interaction.

The second term contains the field strength tensor

$$G^a_{\mu\nu} = \partial_\mu \mathcal{A}^a_\nu - \partial_\nu \mathcal{A}^a_\mu + g_s f^{abc} \mathcal{A}^b_\mu \mathcal{A}^c_\nu,$$

and describes the dynamic of the gluon fields, where f^{abc} are the structure constants of SU(3) defined by the commutation relation of its generators T^a through

$$\left[T^a, T^b \right] = i f^{abc} T^c.$$

When quantizing this theory, one runs into a problem because of the gauge freedom of the gluon fields. In the canonical formalism the commutation relations cannot simply be imposed, as they violate the gauge freedom. In the path integral formalism this problem appears as overcounting in the integration and results in singularities, which cannot be resolved ad hoc. The most convenient solution to this problem preserving Lorentz-covariance is introducing "ghost"-fields that cancel the redundant degrees of freedom. Consequently, the ghost Lagrangian

$$\mathcal{L}_\mathrm{Ghost} = \partial_\alpha \eta^{A\dagger} \left(D^\alpha_{AB} \eta^B \right)$$

has to be included, together with a gauge-fixing term

$$\mathcal{L}_{\mathrm{Gauge-Fixing}} = -\frac{1}{2\lambda}\left(\partial^{\alpha} A_{\alpha}^{A}\right)^{2},$$

that fixes the class of covariant gauges with parameter λ. Although this term explicitly breaks the gauge-invariance, observables are independent of λ. The fields η are complex scalar fields, but obey Fermi statistics. At first sight, this seems to be a violation of the spin-statistics-theorem but as a consequence they simply must not appear as external particles, which is why they are called ghosts. For details about the ghost fields or quantization of QCD, see [5].

3.2 Running Coupling and Asymptotic Freedom

The self-interaction of the gluons is responsible for an important feature of QCD, the running of the strong coupling constant $\alpha_s(Q^2) = \frac{g_s^2(Q^2)}{4\pi}$. It can be determined by calculating higher-order corrections to the gluon propagator with the well known result that the coupling decreases at higher energy scales Q^2, and increases at lower energies. The stronger coupling at lower energies is connected to the confinement of the quarks and gluons, while the decrease of the coupling is known as asymptotic freedom which is crucial for the application of perturbation theory to QCD. It is the reason why QCD processes can only be computed perturbatively at sufficiently high energy, where the confined constituents of hadrons act as quasi-free particles.

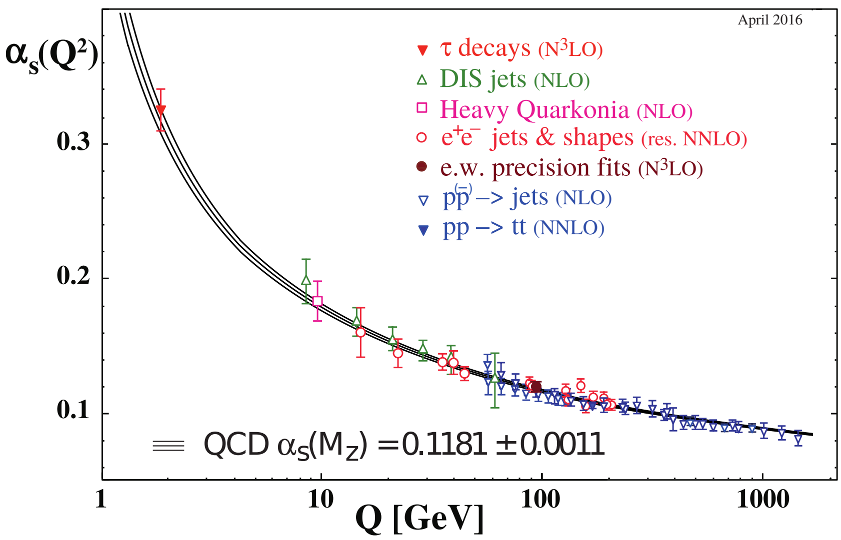

Figure 3.1: Summary of measurements of α_s function of the energy scale Q. The respective degree of QCD perturbation theory used in the extraction of α_s is indicated in brackets (NLO: next-to-leading order; NNLO: next-to-next-to-leading order; res. NNLO: NNLO matched with resummed next-to-leading logs; N^{3}LO: next-to-NNLO). Taken from [27].

At leading-order, the coupling decreases logarithmically as

$$\alpha_{\mathrm{s}}(Q^2) = \frac{1}{\beta_0 \ln\left(\frac{Q^2}{\Lambda_{\mathrm{QCD}}^2}\right)},$$

where

$$\beta_0 = \frac{11}{2} - \frac{1}{3} n_\mathrm{f},$$

is the leading coefficient of the so-called beta-function, and Λ_QCD is the Landau-pole of QCD, which defines the value of the coupling constant at a certain scale. The behavior of the coupling constant extracted from measurements using up to next-to-NNLO calculations is depicted in Figure 3.1.

3.3 Perturbative QCD

The Feynman rules for a perturbative treatment of QCD can be derived from the Lagrangian. The propagator rules originate in the kinetic terms

$$\mathcal{L}_0 = \bar{\psi}_i (i\not{\partial} - m)\psi_i - \frac{1}{4} G^a_{\mu\nu} G^{\mu\nu}_a = \bar{\psi}_i (i\not{\partial} - m\,\psi_i) - \frac{1}{4}(\partial_\mu \mathcal{A}^a_\nu - \partial_\nu \mathcal{A}^a_\mu)^2.$$

The first term leads to the propagator $\tilde{D}_\mathrm{F}(p)$ of the quark field,

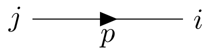

$$= \frac{i\delta_{ij}}{\not{p} - m + i\varepsilon}$$

and the second term to the gluon propagator

$$= \frac{-ig^{\mu\nu} + (1-\xi)\frac{p^\mu p}{p^2}}{p^2 + i\varepsilon} \delta_{ab}.$$

The propagators are identical to the propagator of uncolored fermions and photons, except for a factor of δ_{ij} or δ_{ab} accounting for color conservation.

Expanding the remaining parts of the Lagrangian, we get the interaction terms

$$\mathcal{L}_\mathrm{int} = -g_s f^{abc} (\partial_\mu A^a_\nu) A^b_\mu A^c_\nu - \frac{1}{4} g_s^2 (f^{eab} A^a_\mu A^b_\nu)(f^{ecd} A^c_\mu A^d_\nu) + g_s A^a_\mu \bar{\psi}_i \gamma^\mu T^a_{ij} \psi_j.$$

Using Wick's theorem for the three- and four-point function of the gluons, we can derive the vertex rules

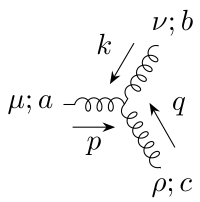

$$= g_s f^{abc} \left[g_s^{\mu\nu} (k-p)^\rho + g_s^{\nu\rho} (p-q)^\mu + g_s^{\rho\mu} (q-k)^\nu \right],$$

and

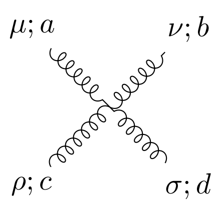

$$\begin{aligned} = \quad & -ig_s^2 [f^{abe} f^{cde} (g_s^{\mu\rho} g_s^{\nu\sigma} - g_s^{\mu\sigma} g_s^{\nu\rho}) \\ & + f^{abe} f^{cde} (g_s^{\mu\rho} g_s^{\nu\sigma} - g_s^{\mu\sigma} g_s^{\nu\rho}) \\ & + f^{abe} f^{cde} (g_s^{\mu\rho} g_s^{\nu\sigma} - g_s^{\mu\sigma} g_s^{\nu\rho})]. \end{aligned}$$

The last term in the interaction Lagrangian generates the quark-gluon vertex

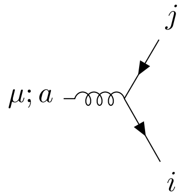

$$= ig\gamma^\mu T^a_{ij}.$$

Here we do not give the Feynman rules for the ghosts, as they only couple to the gluons, and are therefore not relevant for the Drell-Yan process at NLO.

3.4 Divergences and Regularization

When calculating Greens functions at the lowest-order (tree-level), finite results are obtained. Problems arise at higher orders, because virtual particles in the Feynman diagrams can form closed loops. As a consequence, an unconstrained four-momenta emerges, which has to be integrated over according to the Feynman rules. At next-to-leading order (NLO), this leads to loop-integrals of the form

$$(-ig)^2 \int \frac{\mathrm{d}^4 q}{(2\pi)^4} \frac{q^{\mu_1} ... q^{\mu_m}}{(q^2 - m_0^2 + i\varepsilon)\left[(q+p_1)^2 - m_1^2 + i\varepsilon)\right] + ... + \left[(q+p_n)^2 - m_n^2 + i\varepsilon)\right]}, \tag{3.1}$$

where several types of divergences can turn up:

- Through the unconstrained momenta in the integration, divergences can turn up for $q \to \infty$, which are called **ultraviolet (UV)** divergences.
- If one propagator in the loop integral corresponds to a particle with vanishing mass $m_i = 0$, there can be a divergence in the region of low momenta $q \to 0$, called **infrared (IR)** divergence. In QCD, one encounters these divergences often, because the gluon is massless, and the quarks are often assumed to be massless.
- When a massless particle radiates another massless particle and the 3-momenta of these particles are parallel, a **collinear divergence** appears. This can happen in loop integrals of the form
$$\int \frac{\mathrm{d}^4 q}{(2\pi)^4} \frac{1}{q^2\left[(q+p)^2 + i\varepsilon)\right]}$$
in the region $\vec{q} \propto \vec{p}$, when the particle associated with p is a massless on-shell particle ($p^2 = 0$), and also in phase-space integrals, where additional particles are emitted.
- IR and collinear divergences can overlap, resulting in doubly divergent expressions. They will be discussed further in section 3.7

The first step to handle these divergences is to make them explicit by introducing some kind of regularization. Then the key idea to get rid of the divergences, is the simple demand that physical quantities have to be finite. This leads to well-defined procedures to absorb the UV- or IR singularities, which we will discuss later. First we need to introduce a regularization scheme.

Several methods exist, such as the introduction of a momentum cutoff, Pauli-Villars regularization, or the introduction of a lattice. The preferred method nowadays is dimensional regularization [6], which has the main advantage of preserving Lorentz- and gauge invariance. One exploits the fact that by changing the dimension of space-time from $4 \to D$, the divergent behavior of the loop integral changes because of the transition

$$\int \frac{\mathrm{d}^4 q}{(2\pi)^4} \to \int \frac{\mathrm{d}^D q}{(2\pi)^D},$$

and therefore can be regulated. The results are functions of D with poles at $D = 4$. As any regularization prescription, this introduces a scale on which the results will depend. This follows from the fact that the action of the theory

$$S = \int \mathrm{d}^D x \, \mathcal{L}$$

has to be a dimensionless quantity, hence the mass dimension of the Lagrangian has to be $[\mathcal{L}] = -D$. By analyzing the mass dimensions of the fields and couplings of the respective Lagrangian, e.g. the QCD Lagrangian, one finds that for the coupling constant to remain dimensionless, a scale μ with mass dimension $[\mu] = 1$ has to be introduced, and couplings have to be replaced by

$$g \to \mu^{(4-D)/2} g.$$

In this way, the coupling remains a dimensionless quantity, and the results can be consistently expanded with respect to $4 - D$. One often uses the parametrization $D = 4 - 2\varepsilon$ so that in the expansion of divergent results the singularities are located at $\varepsilon \to 0$. UV-divergent integrals will thus converge for $\varepsilon > 0$, IR-divergent integrals for $\varepsilon < 0$. It is useful to distinguish the divergences by writing $\varepsilon = \varepsilon_{\mathrm{UV}}$ for terms that are UV-divergent, and $\varepsilon = \varepsilon_{\mathrm{IR}}$ for the IR-divergent poles, as the cancellation of UV- and IR- poles can be checked separately.

3.4.1 Calculation of Loop-Integrals

The tensor integrals (3.1) in NLO calculations can always be decomposed into basic scalar integrals of the form

$$\mu^{4-D} \int \mathrm{d}^D q \frac{1}{\mathcal{D}_0 ... \mathcal{D}_i},$$

with

$$\mathcal{D}_0 = q^2 - m_0^2 + i\varepsilon, \;\; \mathcal{D}_i = (q + p_i)^2 - m_i^2 + i\varepsilon \;\; \text{for } i \neq 0.$$

Only the first four scalar integrals

$$\begin{aligned} A_0 &= \frac{(2\pi\mu)^{4-D}}{i\pi^2} \int \mathrm{d}^D q \frac{1}{\mathcal{D}_0} = \int_q \frac{1}{\mathcal{D}_0} \\ &\vdots \\ D_0 &= \int_q \frac{1}{\mathcal{D}_0 \mathcal{D}_1 \mathcal{D}_2 \mathcal{D}_3}, \end{aligned}$$

are linearly independent. Using a calculational trick called Feynman parametrization (see Appendix A.2), the scalar integrals can be further reduced to the generic integral

$$I_n(A) = \int \mathrm{d}^D q \frac{1}{(q^2 - A + i\varepsilon)^n},$$

which converges for $D < 2n$ and $A > 0$. It can be solved by exploiting Cauchy's Theorem, which allows the exchange of the integration along the real axis with an integration along the imaginary axis. This procedure is called WICK ROTATION, and allows to render the integral into and euclidean integral

$$I_n(A) = i \int \mathrm{d}^D q_{\mathrm{E}} \frac{(-1)^n}{\left(q_{\mathrm{E}}^2 + A - i\varepsilon\right)^n}.$$

Here, q_{E} is an euclidean vector in D-dimensions, with euclidean metric $q_{\mathrm{E}}^2 = q_{\mathrm{E},0}^2 + \vec{q_{\mathrm{E}}}^2$, such that the integral is spherically symmetric. Therefore, we introduce D-dimensional spherical coordinates

$$\int \mathrm{d}^D q_{\mathrm{E}} = \int \mathrm{d}\Omega_D \int\limits_0^\infty \mathrm{d}q_{\mathrm{E}} q_E^{D-1} = \int \mathrm{d}\Omega_D \int\limits_0^\infty \mathrm{d}q_{\mathrm{E}}^2 \frac{1}{2} (q_E^2)^{D/2-1}$$

resulting in

$$I_n(A) = i(-1)^n \int \mathrm{d}\Omega_D \int\limits_0^\infty \mathrm{d}q_{\mathrm{E}}^2 \frac{1}{2} \frac{(q_E^2)^{D/2-1}}{\left(q_{\mathrm{E}}^2 + A - i\varepsilon\right)^n}.$$

The integral over the solid angle gives

$$\int \mathrm{d}\Omega_D = \Omega_D = \frac{2\pi^{D/2}}{\Gamma(D/2)},$$

such that only the one dimensional integral

$$I_n(A) = i(-1)^n \frac{\pi^{D/2}}{\Gamma(D/2)} \int\limits_0^\infty \mathrm{d}x \frac{x^{D/2-1}}{(x + A - i\varepsilon)^n}.$$

remains. This can now be solved by ordinary methods, and gives the final result

$$I_n(A) = i\,(-1)^n\, \pi^{D/2} \frac{\Gamma(n - \frac{D}{2})}{\Gamma(n)} \,(A - i\varepsilon)^{\frac{D}{2} - n}\,.$$

In calculations, it turns out that factoring in the following way is useful

$$\mu^{4-D} \int \frac{\mathrm{d}^D q}{(2\pi)^D} = \frac{i}{(4\pi)^2} \frac{(2\pi\mu)^{4-D}}{i\pi^2} \int \mathrm{d}^D q = \frac{i}{(4\pi)^2} \int_q,$$

where we introduced the abbreviation $\int_q$ for the q - integral. This motivates a slightly modified version of the generic integral

$$\tilde{I}_n(A) = \int_q \frac{1}{(q^2 - A + i\varepsilon)^n} = \left(4\pi\mu^2\right)^{\frac{4-D}{2}} (-1)^n \,\frac{\Gamma(n - \frac{D}{2})}{\Gamma(n)} \,(A - i\varepsilon)^{\frac{D}{2} - n}\,, \tag{3.2}$$

which includes the conventional factor of $\frac{(2\pi\mu)^{4-D}}{i\pi^2}$.

3.4.2 The quark self-energy

With the techniques established so far, we can calculate next-to-leading order corrections to Green's function. As an example, we consider the two-point function $G(p,-p)$, because as we have seen, it is one of the building blocks of any connected Green's functions. Since this thesis focuses on QCD corrections to the Drell-Yan process, we examine the QCD-corrections of the quark two-point function. The diagrams up to order $\mathcal{O}(g_s^2)$ are:

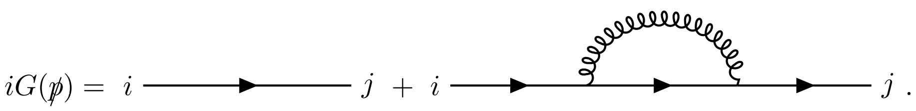

According to the Feynman rules, this results in the expansion

$$iG(\not{p}) = \delta_{ij}\frac{i}{\not{p}-m} + \delta_{ij}\frac{i}{\not{p}-m}i\Sigma(\not{p})\frac{i}{\not{p}-m} + \mathcal{O}(g_s^2),$$

where

$$i\Sigma(\not{p}) = C_{\mathrm{F}}\left(ig_s\right)^2\mu^{4-D}\int\frac{\mathrm{d}^D q}{(2\pi)^D}\gamma^\mu\frac{i(\not{q}+m)}{q^2-m^2+i\varepsilon}\gamma_\mu\frac{-i}{(q-p)^2+i\varepsilon}$$

is the the self-energy loop diagram. Using $m\to 0$ as well as the notation introduced before, we are left with

$$i\Sigma(\not{p}) = -iC_{\mathrm{F}}\frac{g_s^2}{(4\pi)^2}\int_q\frac{\gamma^\mu(\not{q}+m)\gamma_\mu}{\left(q^2-m^2+i\varepsilon\right)\left((q-p)^2+i\varepsilon\right)} = -iC_{\mathrm{F}}\frac{g_s^2}{(4\pi)^2}\underbrace{\int_q\frac{(2-D)\not{q}}{\left(q^2+i\varepsilon\right)\left((q-p)^2+i\varepsilon\right)}}_{I}.$$

This can be reduced to the generic integral using Feynman parametrization

$$I = \int_q\int_0^1\mathrm{d}x\frac{(2-D)\not{q}}{\left[(q-xp)^2+p^2x(1-x)+i\varepsilon\right]^2},$$

where we can now shift the denominator $q\to q+px$ and drop terms that are odd in q, since these vanish under the q-integration. In this way, we arrive at the generic integral

$$I = \int_q\int_0^1\mathrm{d}x\frac{(2-D)\not{p}x}{\left[q^2-A+i\varepsilon\right]^2} \tag{3.3}$$

with $A=-p^2x(1-x)$. Using the result for the generic integral (3.2), this transforms to

$$\begin{aligned}I &= (2-D)\left(4\pi\mu^2\right)^{\frac{4-D}{2}}\frac{\Gamma(2-\frac{D}{2})}{\Gamma(2)}\not{p}\int_0^1\mathrm{d}x\left(-p^2x(1-x)-i\varepsilon\right)^{\frac{D}{2}-2}x\\ &= (2-D)\left(4\pi\frac{\mu^2}{-p^2}\right)^{\frac{4-D}{2}}\Gamma(\frac{4-D}{2})\not{p}\int_0^1\mathrm{d}x\,(1-x)^{\frac{D-4}{2}}x^{\frac{D-2}{2}},\end{aligned}$$

where an UV-singularity in the gamma function $\Gamma(\frac{4-D}{2})$ appears. The remaining integration over x results in a beta function,

$$I = (2-D)\left(4\pi\frac{\mu^2}{-p^2}\right)^{\frac{4-D}{2}}\Gamma(\frac{4-D}{2})\not{p}B(\frac{D-2}{2},\frac{D}{2}),$$

which can be reduced using the properties for the gamma functions (see Appendix A.1). We furthermore introduce $\varepsilon = \frac{4-D}{2}$

$$I = (2-D)\not{p}\left(4\pi\frac{\mu^2}{-p^2}\right)^{\varepsilon}\frac{\Gamma(1+\varepsilon)}{\varepsilon}\frac{\Gamma(1-\varepsilon)\Gamma(2-\varepsilon)}{\Gamma(3-2\varepsilon)}.$$

Expanding

$$\frac{\Gamma(1-\varepsilon)\Gamma(2-\varepsilon)}{\Gamma(3-2\varepsilon)} = -1-\varepsilon+\mathcal{O}(\varepsilon),$$

we arrive at the regularized self-energy of

$$\Sigma(\not{p}) = C_{\mathrm{F}}\frac{g_s^2}{(4\pi)^2}\not{p}\,(4\pi)^{\varepsilon}\Gamma(1+\varepsilon)\left[\frac{1}{\varepsilon_{\mathrm{UV}}}+1+\ln\left(\frac{\mu^2}{p^2}\right)+\mathcal{O}\left(\varepsilon\right)\right] \tag{3.4}$$

$$\Sigma(\not{p}) = C_{\mathrm{F}}\frac{g_s^2}{(4\pi)^2}\not{p}\left[\frac{1}{\varepsilon_{\mathrm{UV}}}-\gamma_{\mathrm{E}}+\ln\left(\frac{4\pi\mu^2}{p^2}\right)+\mathcal{O}\left(\varepsilon\right)\right], \tag{3.5}$$

where the pole was labeled explicitely as UV-pole $\varepsilon = \varepsilon_{\mathrm{UV}}$. To take the limit $\varepsilon \to 0$, the pole has to be removed, which will be discussed in the next section.

3.5 Renormalization

The self-energy graph $\Sigma(\not{p})$ contributing to the quark Green's function diverges. We want to remove this divergence, which can be done systematically order-by-order in perturbation theory, and is called renormalization [6]. The key idea is that physical observables are finite, and in QFT are related to Green's functions which therefore should be finite to. Thus, if infinite quantities appear in the result of the theory, it is not well defined. Looking at the Lagrangian, we can identify parameters of the theory which can be redefined to absorb these infinities in perturbative corrections:

$$\begin{aligned}\mathcal{L}_{\mathrm{QCD}} &= \bar{\psi}_i\left(i\gamma_\mu D^\mu_{ij} - m\,\delta_{ij}\right)\psi_j - \frac{1}{4}G^a_{\mu\nu}G^{\mu\nu}_a\\ &= \bar{\psi}_i\left(\partial^\mu\delta_{ij}\psi_j - ig_sT^a_{ij}A^\mu_a - m\,\delta_{ij}\right)\psi_j - \frac{1}{4}G^a_{\mu\nu}.\end{aligned}$$

It might not immediately be clear in our case, which parameter to redefine. As we set $m \to 0$, the remaining obvious parameter is g_s, but this is needed for the renormalization of the quark-gluon vertex and the three- and four- gluon vertex, which will not be discussed here.
By recalling, that the quark two-point function in position space is just the time ordered vev of the quark fields

$$G(x_1,x_2) = \langle T\left\{\psi(x_1)\psi(x_2)\right\}\rangle,$$

we see that by redefining the normalization of the fields as

$$\psi \to \psi^{\mathrm{R}} = \frac{1}{\sqrt{Z_\psi}}\psi$$

with some formally infinite normalization constants Z_ψ, the Green's function can be modified. It receives the correction

$$G^{\mathrm{R}}(x_1, x_2) = \frac{1}{Z_\psi} G(x_1, x_2),$$

or in momentum space

$$G^{\mathrm{R}}(\not{p}) = \frac{1}{Z_\psi} G(\not{p}).$$

The normalization constant Z_ψ can now be chosen to absorb singularities in G. At leading-order we require $Z_\psi = 1$, as there is no need to renormalize LO Green's functions. At higher orders, we can cancel the infinite corrections by expanding

$$Z_\psi = 1 + \delta_\psi$$

where δ_ψ is called a counterterm, with a series expansion starting at order g_s^2. Inserting this into the Green's function

$$iG^{\mathrm{R}}(\not{p}) = \frac{\delta_{ij}}{Z_\psi}\left(\frac{i}{\not{p}} + \frac{i}{\not{p}} i\Sigma(\not{p})\frac{i}{\not{p}}\right) = \delta_{ij}\left(\frac{i}{\not{p}} + \frac{i}{\not{p}}\left[i\left(\Sigma(\not{p}) + \delta_\psi \not{p}\right)\right]\frac{i}{\not{p}}\right)$$

it can now be rendered finite by choosing δ_ψ to remove the divergent parts of $\Sigma(\not{p})$. We see that

$$\delta_\psi = -C_{\mathrm{F}} \frac{g_s^2}{(4\pi)^2} \frac{1}{\varepsilon_{\mathrm{UV}}}$$

leads to a finite answer for any p. Still, the choice is not unique. Finite parts can be absorbed into the counterterm, where different prescriptions exist for choosing those, which are called subtraction schemes. The choice above corresponds to the minimal subtraction scheme (MS), where only the poles are removed. It is almost always upgraded to modified minimal subtraction ($\overline{\mathrm{MS}}$), where the factors of γ_{E} and $\ln 4\pi$ are also removed. As physical observables should not depend on the subtraction scheme, we will in any scheme demand conditions for the renormalized parameters of the theory, that ensure this. To see how this works, we sum up corrections of the form

$iG(\not{p}) =$ $+$ 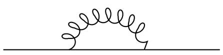 $+$ 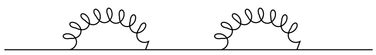 $+ \ldots,$

which just produces the series

$$\begin{aligned}
iG(\not{p}) &= \delta_{ij}\left(\frac{i}{\not{p}} + \frac{i}{\not{p}} i\Sigma(\not{p})\frac{i}{\not{p}} + \frac{i}{\not{p}} i\Sigma(\not{p})\frac{i}{\not{p}} i\Sigma(\not{p})\frac{i}{\not{p}} + \ldots\right) \\
&= \frac{i\delta_{ij}}{\not{p}}\left(1 + \frac{-\Sigma(\not{p})}{\not{p}} + \left(\frac{-\Sigma(\not{p})}{\not{p}}\right)^2 + \ldots\right) \\
&= \frac{i\delta_{ij}}{\not{p}} \frac{1}{1 + \frac{\Sigma(\not{p})}{\not{p}}} = \frac{i\delta_{ij}}{\not{p} + \Sigma(\not{p})}.
\end{aligned}$$

We can again calculate the renormalized Green's function which will give

$$iG^{\mathrm{R}}(\not{p}) = \frac{1}{Z_\psi} iG(\not{p}) = \frac{i\delta_{ij}}{\not{p} + \Sigma(\not{p}) + \delta_\psi \not{p}}.$$

We can conveniently define $\Sigma^{\mathrm{R}}(\not{p}) = \Sigma(\not{p}) + \delta_\psi \not{p}$ to write this simply as

$$iG^{\mathrm{R}}(\not{p}) = \frac{i\delta_{ij}}{\not{p} + \Sigma^{\mathrm{R}}(\not{p})}. \tag{3.6}$$

More generally, we can consider this result as the series of diagrams of the form

$$iG(\not{p}) =$$

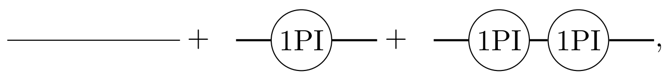

where the blobs are one-particle irreducible (1PI) graphs.

By this summation, it can be seen that the corrections to the propagator change the residuum of the two-point function. As shown previously, the location of the poles of the two-point function are relevant in the LSZ Formula, so we will revisit it for renormalized Green's function in the next section.

3.6 LSZ and renormalization

The LSZ Formula can be used to explain how different renormalization schemes can lead to the same observable, which in this case is the S-matrix. In order to investigate this, we reformulate the LSZ Formula for renormalized n-point Green's functions

$$G_{\mathrm{R}}(p_1, ..., p_n) = Z_\psi^{-n/2} G(p_1, ..., p_n).$$

The S-matrix elements will consequently be calculated using renormalized truncated Green's functions. As in (2.4) they can be obtained by truncating all external legs with renormalized propagators,

$$\begin{aligned} G_{\mathrm{trunc,R}}(p_1, ..., p_n) &= G_{\mathrm{R}}^{-1}(p_1, -p_1) \dots G_{\mathrm{R}}^{-1}(p_n, -p_n) G_{\mathrm{R}}(p_1, ..., p_n) \\ &= Z_\psi^{n/2} G_{\mathrm{trunc}}(k_1, ..., k_n) \end{aligned}$$

and S-matrix elements will then be given by

$$\begin{aligned} \langle -p_{s+1} .... - p_n | S | p_1 .... p_s \rangle &= R_{\mathrm{R}}^{n/2} \, \widetilde{G}_{\mathrm{trunc,R}}(p_1, ..., p_n)|_{p_i^2 = M_i^2} \\ &= R_{\mathrm{R}}^{n/2} Z_\psi^{n/2} \, \widetilde{G}_{\mathrm{trunc}}(p_1, ..., p_n)|_{p_i^2 = M_i^2} \ . \end{aligned} \tag{3.7}$$

This is the correct formula to evaluate S-matrix elements in a renormalized quantum field theory, where R_{R} is determined analogously to (2.2) from the renormalized two-point function. It has the same form as the original formula, but now we encounter the product $R = R_{\mathrm{R}} Z_\psi$, which can be interpreted as the unrenormalized LSZ factor. Different choices for the field renormalization Z_ψ will be exactly compensated by the renormalized LSZ factor R_{R}, which is determined at the physical mass of the external particles, resulting in a factor that is independent of the renormalization scheme.

If we for example renormalize according to the MS-scheme, we have to determine the LSZ factor R_{R} which will be non trivial.

There exists another commonly used scheme, the on-shell scheme, where Z_ψ is determined from the condition that the renormalized propagator has a residue of one at the physical mass. Thus in this case $R_{\mathrm{R}} = 1$ automatically holds.

We won't discuss the renormalization of the coupling constant here, as it is less important for the Drell-Yan process. For a detailed description see [5].

3.7 Mass Divergences

In the previous sections we showed how to eliminate UV-divergences by the procedure of renormalization. In section 3.4 we already mentioned that different types of divergences, the infrared and collinear divergence, can appear in perturbative calculations. These originate in the exchange or emission of massless particles, so they are called mass divergences, and represent a defect in of the theory. The problem in QCD is that quarks and gluons are not the asymptotic states of the theory, which can be prepared and measured with defined momenta in experiments. Considering for example the process

$$e^+e^- \to q(k_1)\bar{q}(k_2),$$

where the two quarks carry momentum k_1 and k_2, then there is no way to distinguish it from the process

$$e^+e^- \to q(k_1')\bar{q}(k_2)g(k_0),$$

where one of the quarks was accompanied by a collinear photon $\vec{k'}_1 \propto \vec{k}_0$, such that $\vec{k}_1 = \vec{k'}_1 + \vec{k}_0$. When computing the first process, we therefore chose one out of many energetically indistinguishable degenerate states. This is unphysical and results in singularities. The same problem could occur in the initial state, e.g. for quark-gluon scattering. The example above already suggests the solution: Looking at the gluon emission process we see that it also yields mass singularities due to the phase space integration of the gluon, and that these singularities exactly cancel. Thus, by summing over the energetically degenerate states, an IR-safe cross section can be obtained in this example.

It has been formally established by the Bloch-Nordsieck [7] and Kinoshita-Lee-Nauenberg [8, 9] theorems, that sufficiently inclusive quantities are finite in the massless limit. Mass divergences cancel exactly between the real, collinear and virtual contributions in the final state, as in the above example. If we had chosen a process, with quarks or gluons in the initial state, there would arise collinear singularities in the initial state. These do not cancel after summing the different contributions and have to be absorbed into parton distribution functions by appropriate factorization theorems. This will be discussed in the calculation of the finite Drell-Yan cross section in section 5.4.

4 Parton Model

In the previous chapter, QCD was presented as the theory of strong interaction. However, it can only be applied to its fundamental particles, the colored quarks and gluons, which can never be observed as free states. How can the scattering of hadrons that are bound states of interacting quarks and gluons be dealt with? Intuitively a perturbative treatment should be possible in the high energy limit because the strong force becomes weak at short distances. This turns out to be the case for many processes at hadron-colliders in certain limits.

4.1 Deep inelastic scattering

The first process that played a fundamental role in developing a framework for hadronic cross sections was deep inelastic scattering (DIS). In DIS, a hadron is probed by a point-like lepton. Usually, one refers to DIS as the specific process

$$e^- + P \to e^- + X,$$

where an electron is scattered off a proton, and additional final state particles X are created. Knowing nothing about the structure of the final state, the cross section can be parametrized by the structure functions $W_1(Q^2, x)$ and $W_2(Q^2, x)$ in the general form

$$\frac{d^2\sigma_{eP}}{dQ^2\, d\nu} = \frac{\pi\alpha^2}{4E^2 \sin^4 \frac{\theta}{2}} \frac{1}{EE'} \left[W_2(Q^2, x) \cos^2 \frac{\theta}{2} + 2W_1(Q^2, x) \sin^2 \frac{\theta}{2} \right]. \tag{4.1}$$

Here $Q^2 = -q^2 = (p_e - p_e')^2$ is the momentum transfer and $\nu = E - E'$ is the energy transfer in the lab frame.

Bjorken predicted [10] that at high energies the structure function should behave like

$$\begin{aligned} MW_1(Q^2, \nu) &\to F_1(x), \\ \nu W_2(Q^2, \nu) &\to F_2(x), \end{aligned}$$

only depending on the scale variable

$$x = \tfrac{Q^2}{2M\nu},$$

which is therefore also called Bjorken x. Here M denotes the mass of the proton. His prediction was verified shortly afterwards in DIS experiments [12]. Feynman interpreted this Bjorken scaling as result of the incoherent scattering on point-like constituents of the nucleon, which he called partons. His parton model gave a simple explanation of the scattering process. The essential assumption is that at large energy and momentum transfers the electron interacts only elastically with quasi-free, point-like constituents of the proton. This seems odd at first, because what makes the proton a bound object is exactly the fact that the partons interact

with each other and are therefore not free. However, looking at the timescales of the scattering in a frame where the proton carries large momentum, this can be justified by the so-called impulse approximation.
If we for example assume that the electron will interact electromagnetically with the proton, then the exchange photon will have a very short lifetime owing to the high momentum transfer Q. On the other hand, the processes that govern the partonic state inside the proton will be time dilated, such that the partons can be regarded as free particles during the interaction. Because of its high virtuality, the photon can only interact with one of the partons, which will carry a definite fraction ξ of the proton's momentum P with $0 < \xi < 1$. If the momentum transfer Q is sufficiently high, the so-called hard interaction between the electron and the parton is perturbatively calculable.

The inelastic hadronic process therefore separates into the hard elastic scattering of the electron on one parton, and everything that happens before and after this hard process on much larger timescales. Because of the different timescales of the so-called short and long distance effects, one assumes the hard and soft processes not to interfere quantum mechanically. The cross section is thus given by a combination of probabilities, where the partonic (hard) cross section $\sigma_{\mathrm{e}i}$ is convoluted with the probability $f_{i/\mathrm{P}}(\xi)$ that a parton carries momentum fraction ξ,

$$\frac{d^2\sigma_{eP}}{dQ^2\,d\nu} = \sum_i \int_0^1 \mathrm{d}\xi\, f_{i/\mathrm{P}}(\xi) \frac{\mathrm{d}\sigma_{\mathrm{e}i}}{dQ^2\,d\nu}. \tag{4.2}$$

As there can be different types of partons, a sum over all partons that participate in the interaction has to be included.

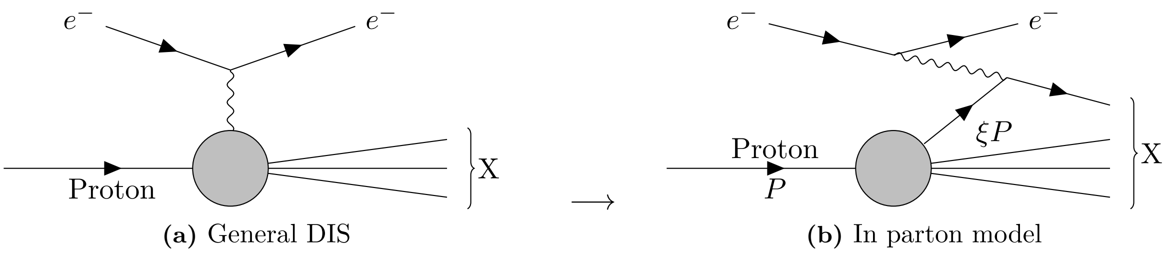

Figure 4.1: Schematic representation of the transition to the parton model for deep inelastic scattering. Instead of inelastic scattering on the proton, the electron scatters elastically on a parton with momentum ξP. The cross section is given by summing over all partons and integrating over the momentum fraction ξ.

The cross section for the partonic process can easily be calculated, as it merely describes the the scattering of point-like particles. If one assumes the parton to be a spin $\frac{1}{2}$ particle, the scattering cross section reads

$$\frac{d^2\sigma_{ei}}{dQ^2\,d\nu} = \frac{\pi\alpha^2 Q_i^2}{4E^2\sin^4\frac{\theta}{2}} \frac{1}{EE'} \left[\cos^2\frac{\theta}{2} + \frac{Q^2}{2m_i^2}\sin^2\frac{\theta}{2}\right] \delta(\nu - \frac{Q^2}{2m_i})$$

where Q_i is the charge of the parton. To obtain the DIS cross section this has to be integrated over the parton momentum fraction ξ according to (4.2). As the four-momentum of the parton is given by $p_i = \xi P$ in the lab frame, with the proton at rest, we have $m_i = \xi M$. In this way, we can modify the $\delta-$function to

$$\delta(\nu - \frac{Q^2}{2m_i}) = \delta(\nu - \frac{Q^2}{2M\xi})$$

and thus the DIS cross section in the parton model simplifies to

$$\frac{d^2\sigma_{eP}}{dQ^2\,d\nu} = \sum_i \int_0^1 f_{i/\mathrm{P}}(\xi) \frac{\pi\alpha^2}{4E^2 \sin^4\frac{\theta}{2}} \frac{1}{EE'} Q_i^2 \left[\cos^2\frac{\theta}{2} + \frac{Q^2}{2M^2x^2}\sin^2\frac{\theta}{2}\right] \delta(\nu - \frac{Q^2}{2M\xi}). \tag{4.3}$$

This can be compared to (4.1) to read off the structure functions

$$F_1(x) = \sum_i \frac{Q_i^2}{2} f_{i/P}(x), \quad F_2(x) = \sum_i Q_i^2 x\, f_{i/P}(x),$$

where the Bjorken scaling emerges as a prediction of the parton model. In Figure 4.2 experimental data demonstrating this to a good extend are shown. At leading-order the structure function are related to each other by the Callan-Gross-relation [15]

$$2xF_1(x) = F_2,$$

which is a consequence of the assumption, that the partons carry spin $\frac{1}{2}$. This assumption was soon supported by experimental data on DIS and together with other observations this gradually led to the *quark parton model*, which today in an enhanced version is an established ingredient for the calculation of hadronic cross sections. Here the partons are identified with quarks and gluons, and the structure function in DIS is a sum of quark (and antiquark) distribution functions $f_f(x)$

$$F_2(x) = x \cdot \sum_f Q_f^2 \left(f_f(x) + \bar{f}_f(x)\right),$$

where $f = \{u, d, c, s, t, b\}$ denotes the quark flavor, and Q_f^2 the corresponding quark charge. The functions $f_i(x)$ are called parton distribution functions (PDFs) and, as probabilities, fulfill a number of sum rules, such as that integrals of the form

$$\int \mathrm{d}\xi \left[f_f(\xi) - f_{\bar{f}}(\xi)\right]$$

have to result in the number of valence quarks of the respective hadron, e.g. for the proton

$$\int \mathrm{d}\xi \left[f_u(\xi) - f_{\bar{u}}(\xi)\right] = 2, \int \mathrm{d}\xi \left[f_d(\xi) - f_{\bar{d}}(\xi)\right] = 1,$$

while all other combinations like

$$\int \mathrm{d}\xi \left[f_s(\xi) - f_{\bar{s}}(\xi)\right] = 0$$

vanish. Additionally, from momentum conservation it follows that

$$\sum_i \int \mathrm{d}\xi \left[\xi f_i(\xi)\right] = 1.$$

It was found that if all quark-PDFs are included in the above sum over i, then

$$\sum_{\text{quark flavors}} \int \mathrm{d}\xi \left[\xi f_i(\xi)\right] \approx 50\%,$$

which means only 50% of the proton's momentum are carried by quarks. What is missing in this sum are the gluon PDFs, which are not relevant for the structure functions of DIS, as they do not couple to the photon. They carry the remaining 50% of the proton momentum.

The PDFs contain non-perturbative information about the respective hadron. As there are no techniques to calculate these from theory, they have to be determined by fitting experimental data. We show example PDFs determined by the CTEQ collaboration [11] in Figure 4.3.

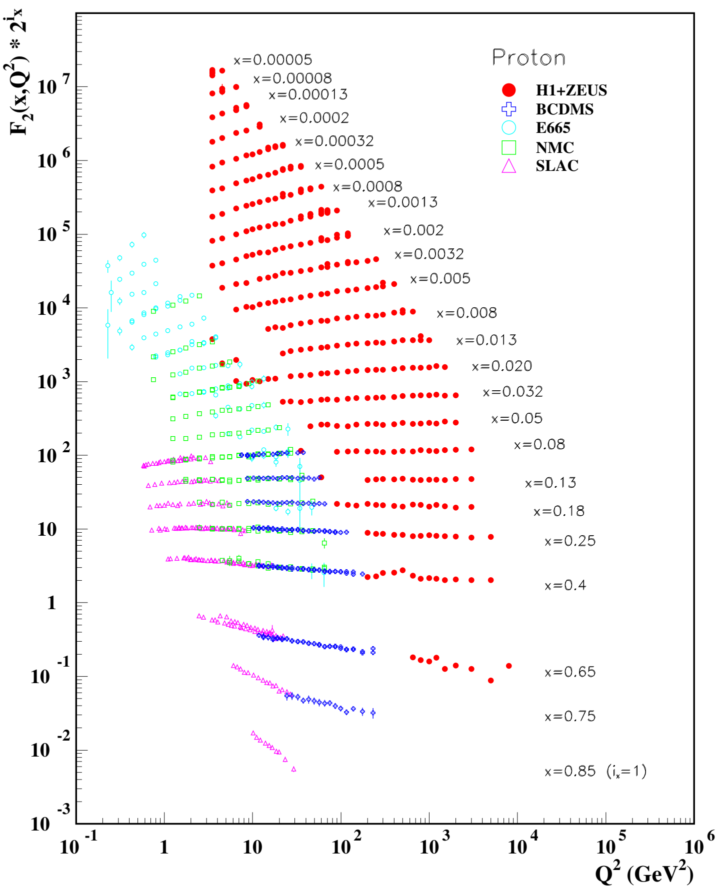

Figure 4.2: The proton structure function F_2 measured in different DIS experiments on protons. Taken from [27].

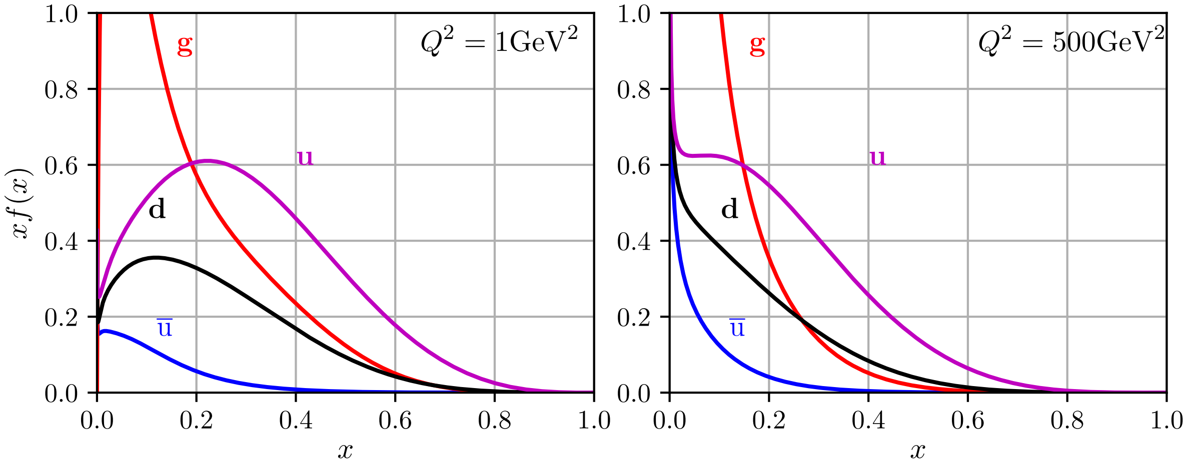

Figure 4.3: CT14 [11] parton distribution function for $u-$, $d-$ and $\bar{u}-$ quarks, and the gluon.

4.2 The Drell-Yan process

In 1970, Christenson et al. reported the first observation of continuous $\mu^+\mu^--$ pairs produced in hadron-hadron collisions. Drell and Yan were the first to give a theoretical description for the process involved by applying the same simple parton picture as in DIS. This was further convincing evidence that the parton model provides the correct framework for high energy collisions of hadrons in general.

In the parton model, the lepton production from two initial hadrons

$$H_A + H_B \to l^+ + l^- + X,$$

is the result of the annihilation of a parton-antiparton pair into an intermediate vector boson, like the γ or Z^0, which then decays into a pair of leptons (dilepton pair).

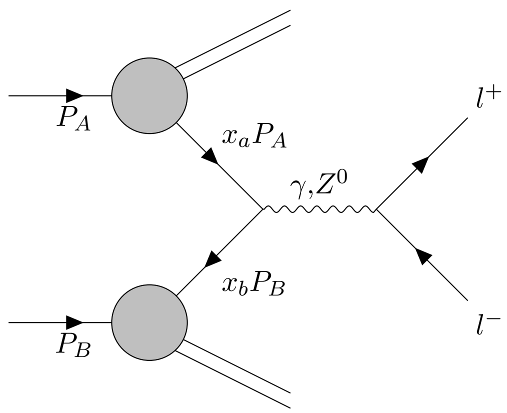

Figure 4.4: Drell-Yan process in the parton model, where two partons with momentum fractions x_a and x_b annihilate into an intermediate vector boson, which then decays into a dilepton pair.

One often uses the term Drell-Yan production in a more general way to describe any process, where an intermediate boson is produced by the annihilation of two initial partons. For example, the process

$$\bar{u} + d \to W^-$$

is one channel of the Drell-Yan W^- production.

The differential cross section of the Drell-Yan process factorizes in an analogous way to DIS, which can also be justified in the impulse-approximation. The hadronic cross section is consequently determined by the same parton ($f_{a/A}$) and antiparton ($f_{b/B}$) distributions measured in deep inelastic lepton scattering and can analogously to DIS be written as a convolution with the partonic cross section $\sigma_{ab}(x_a P_A, x_b P_B)$ resulting in

$$\mathrm{d}\sigma^H_{AB} = \sum_{a,b} \int_0^1 \mathrm{d}x_a \int_0^1 \mathrm{d}x_b \, f_{a/A}(x_a) f_{b/B}(x_b) \mathrm{d}\sigma_{ab}(x_a P_A, x_b P_B). \tag{4.4}$$

Although the cross section can be written differentially in the parton momentum fractions x_a and x_b, these variables are not directly observable. Typically the dilepton energy E and the longitudinal momentum p_l are measured. From these one constructs the kinematic variables Feynman x

$$x_\mathrm{F} = \frac{2p_l}{\sqrt{s}},$$

and the dilepton mass squared

$$M^2 = E^2 - p_l^2.$$

These are directly related to the parton variables x_a and x_b via

$$x_F = x_a x_b, \quad \tau = \frac{M^2}{s} = \frac{Q^2}{x_a x_b s}.$$

Another commonly used variable is the rapidity, given by

$$y = \frac{1}{2} \ln \left(\frac{E + p_l}{E - p_l} \right) = \frac{1}{2} \ln \frac{x_a}{x_b}.$$

Cross sections from experiments are often given differentially in one or two of these kinematic variables, which can be compared to the prediction, e.g.

$$\frac{\mathrm{d}\sigma^H_{AB}}{\mathrm{d}M \mathrm{d}y} = \sum_{a,b} \frac{x_a x_b}{x_a + x_b} \mathrm{d}\sigma_{ab}(x_a, x_b, Q^2) f_{a/A}(\sqrt{\tau}) f_{b/B}(\sqrt{\tau}).$$

4.2.1 Phenomenology of the Drell-Yan process

While first measured in 1970, the Drell-Yan process is still important for hadron colliders such as LHC for several reasons.

1. It is highly sensitive to the parton distribution functions, where
   a) at LHC even sea-quark PDFs can be accessed, for instance anti-down or strange quarks.
   b) nuclear parton distribution functions (nPDFs), meaning PDFs for bound systems of protons and neutrons can be determined. These play an important role at RHIC and LHC in heavy ion collisions.
2. Electroweak observables can be measured to high precision. Examples are
   a) the W boson mass and width (through $W^{\pm}-$production) [16].
   b) the weak mixing angle ($\gamma^*/Z-$production) [17].
   c) the lepton asymmetry (Wproduction) [18].
3. The $W-$ and $Z-$ boson production are used for detector calibration and luminosity monitoring.
4. Because of the clean final state, new gauge bosons, such as Z' or W' may be visible in Drell-Yan production at LHC. For instance, a Z' could appear as additional resonance in the dilepton invariant mass plot.

PDF uncertainty and the strange quark The first point is connected to one of the main uncertainties for hadron-hadron colliders, the uncertainty of the PDFs. The up and down quark contributions are now known to high accuracy, but especially the PDFs for heavier quark flavors still have large uncertainties. Because of the high beam energy at LHC, where lower $x_{a/b}$ can be accessed, Drell-Yan production can give stronger constraints on these PDFs, which in return allows for more precise predictions[1].

Recently, this aspect has for instance been investigated by A. Kusina et al. [19] with focus on the strange quark distribution $f_s(x)$, where in Figure 4.5 the rapidity distribution for $W^{\pm}$ and Z^0 production for beam energies corresponding to Tevatron, LHC 7 and LHC 14 are shown at LO. At Tevatron, the first generation quarks dominate the production processes, while contributions from strange quarks are comparably small with 9% for $W^{\pm}$ and 5% for Z boson production. At the LHC, subprocesses containing strange quarks are considerably more important, and especially at 14 TeV for instance the $s\bar{c}$ channel in W^- production contributes 28% to the cross section.

[1] Of course one must use independent data for further constrains of PDFs and new predictions, to avoid overfitting.

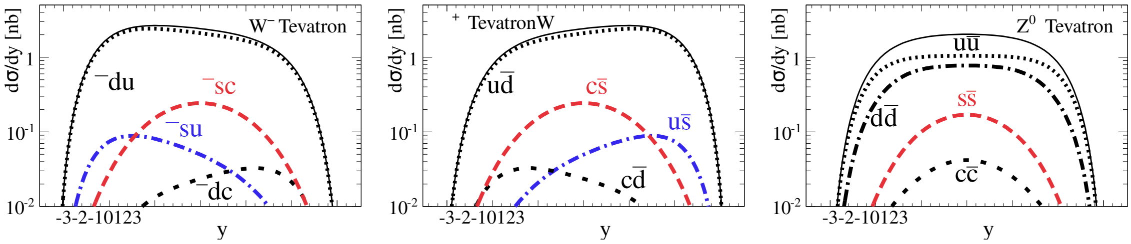

(a) Tevatron

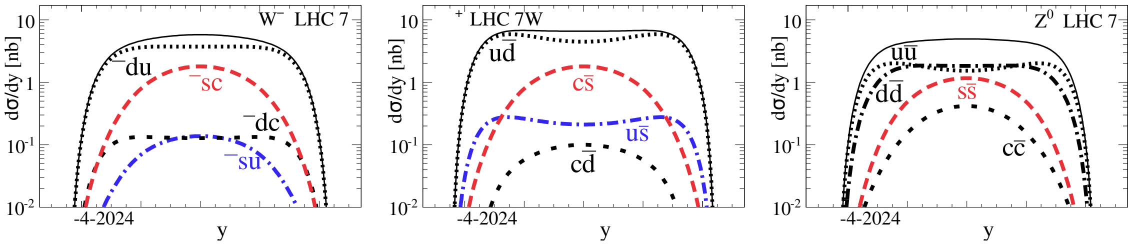

(b) LHC with $\sqrt{s} = 7\,\mathrm{TeV}$

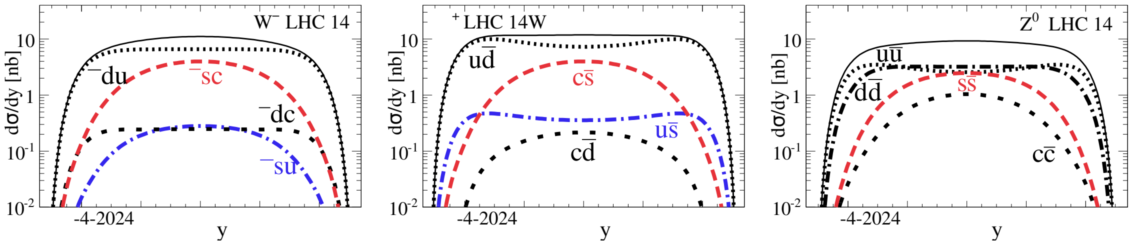

(c) LHC with $\sqrt{s} = 14\,\mathrm{TeV}$

Figure 4.5: Partonic contributions to the differential cross section of on-shell $W^{\pm}/Z$ boson production at LO as a function of the vector boson rapidity. Partonic contributions containing a strange or anti-strange quark are denoted by (red) dashed and (blue) dot-dashed lines. The solid lines show the total contribution. Taken from [19].

Determination of $W-$mass To give an example for the sensitivity for electroweak observables, we refer to the determination of the $W-$mass by the CDF collaboration [16]. The $W-$mass was obtained by fitting MC-events of Drell-Yan $W \to e\nu$ production to the observed transverse mass peak in the differential cross section measured at Tevatron (Figure 4.6). The resonance has the form

$$\frac{\mathrm{d}\sigma}{\mathrm{d}M^2 \mathrm{d}M_{\mathrm{T}}} \propto \frac{\Gamma_W M_W}{(M^2 - M_{\mathrm{T}}^2)^2 + \Gamma_W^2 M_W^2} \frac{1}{M\sqrt{M - M_{\mathrm{T}}}}$$

due to the finite decay width Γ_W of the $W-$boson. Here $M_{(\mathrm{T})}$ is the invariant (transversal) mass of the leptons $(m_e + m_\nu)$. The result from 470 126 $W \to e\nu$ candidates and 624 708 $W \to \mu\nu$ candidates was $M_W = 80387 \pm 19\,\mathrm{MeV/c}$, which to date is the most precise single-experiment measurement of the $W-$boson mass.

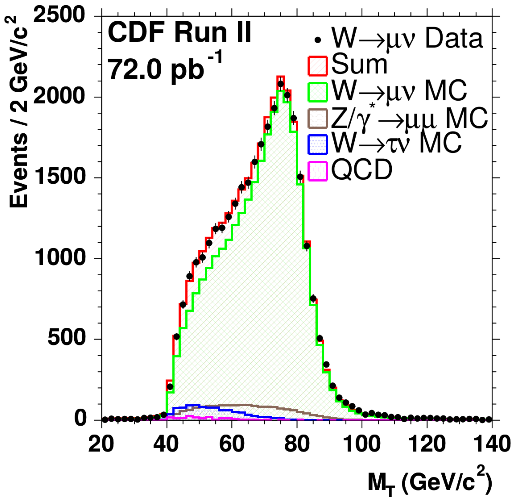

Figure 4.6: The transverse mass peak for a $W \to \mu\nu$ signal observed at CDF. Taken from [20].

Nuclear PDFs Parton distribution functions are universal in the sense that they do not depend on the partonic process. Thus, they can for instance be extracted from DIS experiments and then be used for different processes. As they depend on the hadron under consideration, the question arises, how to extend the notion of hadronic PDFs to PDFs for nuclei. This is for instance especially important for heavy-ion collisions.

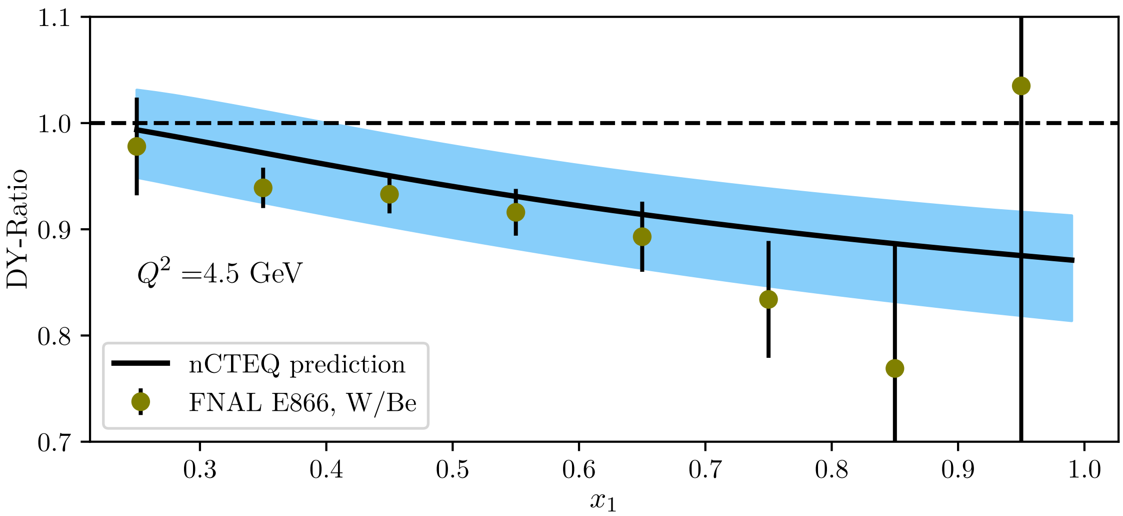

Figure 4.7: Comparison of a theoretical prediction for the Drell-Yan ratio $R = \frac{\sigma^{\mathrm{W}}}{\sigma^{\mathrm{Be}}}$ with data from Fermilab experiment FNAL E866. The ratio was computed using nCTEQ15 PDFs. σ denotes the cross section differential in x_1 and M.

Nuclear PDFs (nPDFs) can of course be defined, but as the nucleus is not an ensemble of free protons and neutrons, the nuclear PDFs will differ from the naive additive combination of free proton and neutron PDFs. As a consequence, the nPDFs have to be determined individually for each nucleus by global fits as well. This is done for instance by the nCTEQ collaboration [21], where experimental DIS and Drell-Yan data with nuclei is fitted and uncertainties are determined.

In Figure 4.7, we used the LO results that will be derived in the next section to compare the ratio of the Drell-Yan cross section between different nuclei with the theoretical prediction using nCTEQ15 PDFs.

4.3 The QCD improved parton model

In the modern framework of QCD, the parton model can be justified without using the impulse approximation, but the more precise concept of factorization, which separates the long distance and short distance physics at a certain scale μ_F, the factorization scale. It can be proven for certain processes [22] such as DIS or Drell-Yan that the hadronic cross sections can be split up into process dependent perturbatively calculable partonic cross sections and process independent parton distribution functions. The factorization result for Drell-Yan is for instance

$$\mathrm{d}\sigma^H_{AB}(P_A, P_B) = \sum_{a,b} \int_0^1 \mathrm{d}x_a \int_0^1 \mathrm{d}x_b \, f_{a/A}(x_a, \mu_\mathrm{F}^2) f_{b/B}(x_b, \mu_\mathrm{F}^2) \mathrm{d}\sigma_{ab}(x_a P_A, x_b P_B, \mu_\mathrm{F}^2), \tag{4.5}$$

which is the familiar result from the parton model, but the parton distributions and the partonic cross section have gained an additional dependency on the factorization scale μ_F. This scale defines the boundary between the short and long distance physics, and is not determined a priori, but has to be chosen carefully according to the kinematics of the process. It is for Drell-Yan or DIS usually chosen to be $\mu_\mathrm{F}^2 = Q^2$.

The implementation of QCD into the parton model enforces this scale dependency, because it allows for interactions between the partons. If we consider as example DIS, when probing the proton with a photon, beginning at a certain scale Q_0^2, a point-like parton might be resolved by the photon. At a higher scale Q^2, as finer structure is observed, the quark might have radiated a collinear gluon that was not visible at Q_0^2 before interacting with the photon. Thus, the photon interacts with a quark that carries less momentum. As a result, the partonic cross section depends on the scale $\mu_\mathrm{F}^2 = Q^2$. The probabilities for such partonic interactions are called splitting functions $P_{ij}(\frac{x}{z})$,

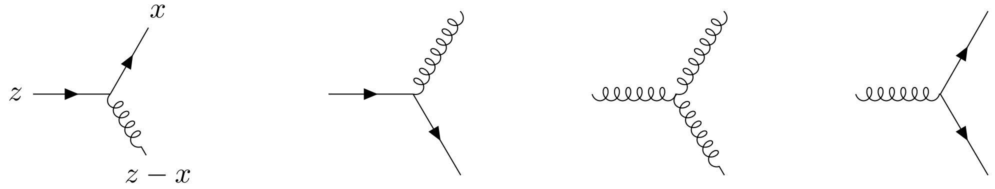

P_{qq} $\qquad$ P_{gq} $\qquad$ P_{gg} $\qquad$ P_{qg}

where $P_{ij}(\frac{x}{z})$ gives the probability of a parton j radiating a collinear quark or gluon and becoming a parton i with momentum fraction $\frac{x}{z}$. The splitting functions can be calculated in QCD, and are given at leading-order by

$$P_{ij}^{(0)}(x) = \delta_{ij}\delta(1-x),$$

which is the naive parton model result. In first non-trivial order, one finds

$$
\begin{aligned}
P^{(1)}_{q_iq_j} = P^{(1)}_{\bar{q}_i\bar{q}_j} &= \delta_{ij} C_F \left(\frac{1+x^2}{(1-x)_+} + \frac{3}{2}\delta(1-x) \right) \\
P^{(1)}_{gq_i} = P^{(1)}_{g\bar{q}_i} \equiv P^{(1)}_{gq} &= C_F \left(\frac{1+(1-x)^2}{x} \right) \\
P^{(1)}_{q_ig} = P^{(1)}_{\bar{q}_ig} \equiv P^{(1)}_{qg} &= T_F \left(x^2 + (1-x)^2 \right) \\
P^{(1)}_{gg} &= 2C_A \left(\frac{x}{(1-x)_+} + (1-x)\left(x + \frac{1}{x} \right) \right) + \frac{11C_A - 4n_fT_F}{6}\delta(1-x).
\end{aligned}
$$

Here, the plus distribution $[f(x)]_+$ is used, as defined in Appendix A.6. The splitting functions govern the scale evolution of the PDFs by the famous DGLAP [24, 25, 26] equations

$$
\frac{\mathrm{d}\mu_{\mathrm{F}} f_i(x_a, \mu_{\mathrm{F}}^2)}{\mathrm{d}\ln\left(\mu_f^2\right)} = \frac{\alpha_s}{2\pi} \sum_j \int_x^1 \frac{\mathrm{d}y}{y} f_j(y, \mu_{\mathrm{F}}^2) P_{ij}(\frac{x}{y}),
$$

where the P_{ij} is the splitting function to all orders. The DGLAP equations are a consequence of the fact, that the hadronic cross section to all orders should not depend on the factorization scale, as stated in (4.5). We will see later at the end of the NLO calculation, how collinear divergences are accompanied by the splitting functions.

5 Drell-Yan cross section

We now come to the calculation of the Drell-Yan process up to next-to-leading order in QCD. As shown in section 4.2 the hadronic cross section factorizes as

$$\mathrm{d}\sigma^H_{AB} = \sum_{a,b} \int_0^1 \mathrm{d}x_a \int_0^1 \mathrm{d}x_b \, f_{a/A}(x_a) f_{b/B}(x_b) \mathrm{d}\sigma_{ab}(x_a P_A, x_b P_B), \tag{5.1}$$

where $\mathrm{d}\sigma_{ab}$ is the perturbatively calculable partonic cross section. In this section, we will start by computing this at leading-order for various scenarios. Then the virtual and the real QCD-corrections will be calculated. This will still not lead to a finite result because of the quarks in the initial state. We will therefore switch to a more inclusive quantity, the hadronic cross section, in order to absorb the remaining singularities into renormalized PDFs.

Before we begin, it is helpful to look at the general structure of the Green's function we need to calculate. As there is no four-vertex for fermions and there are no possible vertices for the t and u channels, the leading-order Feynman diagram will have the form:

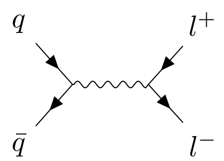

This can be compared to the general form of a four-point Green's function (2.10) to infer that the Green's function (to all orders) only consists of the following connected Green's function

$G_{\mathrm{c,tr}} =$ 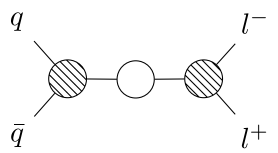 . (5.2)

The vertex functions here contain all possible connected (and truncated) vertex graphs, and can be expanded in the respective coupling strengths. The same can be done for the propagator. The leading-order terms will then be given by the basic vertex given by the Feynman rules and the free propagator for the exchange boson, thus resulting in the above Feynman diagram. This will be the starting point for our calculation.

5.1 Leading-order partonic cross section

We will calculate the leading-order partonic cross section $\sigma^{(0)}_{q\bar{q}}$ first for the special case of photon exchange in D dimensions. Then a generic case with general couplings will be examined in $D = 4$ dimensions. Although the calculation in D dimensions is not necessary for the pure LO cross section, the solution becomes useful when calculating NLO contributions in dimensional regularization.

For the leading-order cross section, we can simply use the appropriate vertex rule for the vertex function, and the corresponding propagator rule for the exchanged boson.

5.1.1 Photon production

We first look at the partonic Drell-Yan process $q\bar{q} \to \gamma \to l^+l^-$, where a photon is exchanged. The diagram for this is

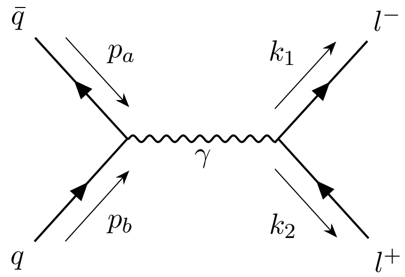

.

Using the Feynman rules, we get the transition matrix

$$i\mathcal{M} = \delta_{ij} \left[\bar{v}(p_a)(Q_f e)\gamma_\mu u(p_b)\right] \frac{-i}{q^2} \left[\bar{u}(k_1)(-e)\gamma^\mu v(k_2)\right].$$

where δ_{ij} is a color conserving factor for the quark vertex. To compute the unpolarized cross section, we have to average (sum) over the spin- and color degrees of freedom of the initial (final) particles. This results in the color factor

$$\frac{1}{N_\mathrm{C}^2} \sum_{i,j} \delta_{ij} = \frac{1}{N_\mathrm{C}},$$

such that the amplitude is given by

$$|\overline{\mathcal{M}}|^2 = \frac{1}{N_\mathrm{C}} \frac{1}{4} \sum_{\text{spins}} |\mathcal{M}|^2 = \frac{Q_f^2 e^4}{N_\mathrm{C} q^4} H_{\mu\nu} L^{\mu\nu}.$$

The factor of $\frac{1}{4}$ accounts for the number of combinations of incoming quark spins. We include the corresponding factor and spin summation in the tensors $H^{\mu\nu}$and $L^{\mu\nu}$. The tensors then read

$$H^{\mu\nu} = \frac{1}{2} \mathrm{Tr}\Big[(\not{p}_a + m_a)\gamma^\mu(\not{p}_b - m_b)\gamma^\nu\Big]$$
$$L^{\mu\nu} = \frac{1}{2} \mathrm{Tr}\Big[(\not{k}_1 + m_1)\gamma^\mu(\not{k}_2 - m_2)\gamma^\nu\Big].$$

The traces over the Dirac matrices can be evaluated using the trace identities for D-dimensions (see Appendix A.3), yielding

$$\begin{aligned} H^{\mu\nu} &= 2\left[p_a^\mu p_b^\nu + p_a^\nu p_b^\mu - g^{\mu\nu}\left(p_a \cdot p_b + m_a m_b\right)\right] \\ L^{\mu\nu} &= 2\left[k_1^\mu k_2^\nu + k_1^\nu k_2^\mu - g^{\mu\nu}\left(k_1 \cdot k_2 + m_1 m_2\right)\right]. \end{aligned} \tag{5.3}$$

When contracting both tensors, keeping in mind that $g^{\mu\nu} g_{\mu\nu} = D$, we get

$$\begin{aligned} H_{\mu\nu} L^{\mu\nu} = 8\Big[&(p_a \cdot k_1)(p_b \cdot k_2) + (p_a \cdot k_2)(p_b \cdot k_1) + m_1 m_2 (p_a \cdot p_b) + m_a m_b (k_1 \cdot k_2) + 2 m_1 m_2 m_a m_b\Big] \\ &+ 4(D-4)\Big[(p_a \cdot p_b)(k_1 \cdot k_2) + m_1 m_2 (p_a \cdot p_b) + m_a m_b (k_1 \cdot k_2) + m_1 m_2 m_a m_b\Big]. \end{aligned} \tag{5.4}$$

Now, we have reduced the transition amplitude to an expression involving only the particle masses and scalar products of initial and final state momenta. To further reduce these scalar products to simpler kinematical variables we use the center-of-mass system (CMS), where energy squared is given by

$$s = q^2 = (p_a + p_b)^2 = (k_1 + k_2)^2 .$$

Note that until we go to the hadronic level, all kinematic variables are understood to be at partonic level. The distinction between for instance the hadronic CMS energy squared $(P_a + P_b)^2$ will be introduced later, when it is needed. The partonic CMS kinematics allow us to compute the scalar products

$$p_a \cdot p_b = \frac{1}{2}\left(s - m_a^2 - m_b^2\right), \qquad k_1 \cdot k_2 = \frac{1}{2}\left(s - m_1^2 - m_2^2\right).$$

The remaining scalar products have to be calculated explicitly

$$\begin{aligned} p_a \cdot k_1 &= E_a E_1 - |\vec{p}_a||\vec{k}_1| \cos\theta & \qquad p_b \cdot k_2 &= E_b E_2 - |\vec{p}_b||\vec{k}_2| \cos\theta \\ p_a \cdot k_2 &= E_a E_2 + |\vec{p}_a||\vec{k}_2| \cos\theta & \qquad p_b \cdot k_1 &= E_b E_1 + |\vec{p}_b||\vec{k}_1| \cos\theta. \end{aligned}$$

The energies and momenta can be related to s and the masses of the incoming and outgoing particles as

$$\begin{aligned} E_1 &= \frac{s + m_1^2 - m_2^2}{2\sqrt{s}}, & \qquad E_2 &= \frac{s - m_1^2 + m_2^2}{2\sqrt{s}}, & \qquad |\vec{k}_1| = |\vec{k}_2| &= \frac{\lambda_{12}^{\frac{1}{2}}}{2\sqrt{s}} \\ E_a &= \frac{s + m_a^2 - m_b^2}{2\sqrt{s}}, & \qquad E_b &= \frac{s - m_a^2 + m_b^2}{2\sqrt{s}}, & \qquad |\vec{p}_a| = |\vec{p}_b| &= \frac{\lambda_{ab}^{\frac{1}{2}}}{2\sqrt{s}}, \end{aligned}$$

where we used the abbreviation

$$\lambda_{ij} = \lambda(s, m_i^2, m_j^2).$$

Inserting this into $H_{\mu\nu} L^{\mu\nu}$, the only unknown kinematic variable is the CMS angle θ

$$H_{\mu\nu} L^{\mu\nu} = a \cos^2\theta + b \cos\theta + c,$$

where the coefficients are given by

$$a = \frac{1}{s^2} \lambda_{12} \lambda_{ab},$$

$$b = -\frac{2}{s^2}\left(m_1^2 - m_2^2\right)\left(m_a^2 - m_b^2\right)\lambda^{1/2}\left(s, m^2{}_1, m^2{}_2\right)\lambda^{1/2}\left(s, m^2{}_a, m^2{}_b\right),$$

and

$$\begin{aligned}c = 4&\left[\left(s - m_1^2 - m_2^2\right)m_a m_b + \left(s - m_a^2 - m_b^2\right)m_1 m_2 + 4 m_a m_b m_1 m_2\right] \\ &+ \frac{1}{s^2}\left(s + m_1^2 - m_2^2\right)\left(s - m_1^2 + m_2^2\right)\left(s + m_a^2 - m_b^2\right)\left(s - m_a^2 + m_b^2\right) \\ +(D-4)&\left[\left(s - m_a^2 - m_b^2\right)\left(s - m_1^2 - m_2^2\right) + 4\left(s - m_1^2 - m_2^2\right)m_a m_b + 4\left(s - m_a^2 - m_b^2\right)m_1 m_2\right].\end{aligned}$$

We can now write down the differential cross section for this process using

$$\mathrm{d}\sigma_{q\bar{q}}^{(0)} = \frac{1}{F}|\overline{\mathcal{M}}|^2 \mathrm{dPS}^{(2)} = \frac{1}{F}\frac{Q_f^2 e^4}{N_\mathrm{C} q^4} H_{\mu\nu} L^{\mu\nu} \mathrm{dPS}^{(2)}.$$

Inserting the phase space element (see Appendix A.4), we obtain

$$\frac{\mathrm{d}\sigma_{q\bar{q}}^{(0)}}{\mathrm{d}\cos\theta \mathrm{d}\phi} = \frac{1}{16\pi^2}\frac{(4\pi)^\varepsilon}{\Gamma(1-\varepsilon)}\frac{1}{\sqrt{s}}\left(\frac{\lambda_{12}^{\frac{1}{2}}}{2\sqrt{s}}\right)^{1-2\varepsilon}\left(1 - \cos^2\theta\right)^{-\varepsilon}\frac{1}{F}\frac{Q_f^2 e^4}{N_\mathrm{C} q^4} H_{\mu\nu} L^{\mu\nu},$$

where the phase-space element is given in $D = 4 - 2\varepsilon$. The total cross section is obtained by integrating out the solid angle $\mathrm{d}\cos\theta \mathrm{d}\phi$

$$\sigma_{q\bar{q}}^{(0)} = \frac{1}{8\pi}\frac{(4\pi)^\varepsilon}{\Gamma(1-\varepsilon)}\frac{1}{\sqrt{s}}\left(\frac{\lambda_{12}^{\frac{1}{2}}}{2\sqrt{s}}\right)^{1-2\varepsilon}\frac{1}{F}\frac{Q_f^2 e^4}{N_\mathrm{C} s^2}\int_{-1}^{1}\left(1 - \cos^2\theta\right)^{-\varepsilon} H_{\mu\nu} L^{\mu\nu} \mathrm{d}\cos.$$

Only the quadratic and constant terms of $H_{\mu\nu}L^{\mu\nu}$ contribute to the integral, and give a gamma function

$$\begin{aligned}\int_{-1}^{1}\left(1 - y^2\right)^{-\varepsilon} H_{\mu\nu} L^{\mu\nu} \mathrm{d}y &= \int_{-1}^{1}\left(1 - y^2\right)^{-\varepsilon}\left(a y^2 + c\right)\mathrm{d}y \\ &= \frac{\sqrt{\pi}}{2}\frac{\Gamma(1-\varepsilon)}{\Gamma(\frac{5-2\varepsilon}{2})}\left(a + (D-1)c\right).\end{aligned}$$

Together with $F = 2\lambda_{ab}^{\frac{1}{2}}$ this leads to the general result

$$\sigma_{q\bar{q}}^{(0)} = \frac{\sqrt{\pi}}{16\pi\Gamma(\frac{5-2\varepsilon}{2})}(4\pi)^\varepsilon\frac{1}{\sqrt{s}}\left(\frac{\lambda_{12}^{\frac{1}{2}}}{2\sqrt{s}}\right)^{1-2\varepsilon}\frac{1}{2\lambda_{ab}^{\frac{1}{2}}}\frac{Q_f^2 e^4}{N_\mathrm{C} q^4}\left[a + (D-1)c\right], \tag{5.5}$$

from which the cross section in D dimensions for any mass combinations can be calculated. We consider the following two special cases:

No masses

If we neglect all masses, then the Källén functions reduce to $\lambda_{12} = \lambda_{ab} = s^2$, which reduces the coefficients of (5.5) to $a = s^2$ and $c = (D-3)s^2$. The cross section then collapses to

$$\begin{aligned}\sigma_{q\bar{q}}^{(0)} &= \frac{\sqrt{\pi}}{16\pi\Gamma(\frac{5-2\varepsilon}{2})}(4\pi)^{\varepsilon}\frac{1}{\sqrt{s}}\left(\frac{s}{2\sqrt{s}}\right)^{1-2\varepsilon}\frac{1}{2s}\frac{Q_f^2e^4}{N_\mathrm{C}s^2}\left[1+(D-1)(D-3)\right]s^2\\ &= \frac{\pi Q_f^2\alpha^2}{N_\mathrm{C}s}\left(\frac{4\pi}{s}\right)^{\varepsilon}\frac{\sqrt{\pi}(D-2)^2}{2^{2-2\varepsilon}\Gamma(\frac{5-2\varepsilon}{2})}\\ &= \frac{4\pi Q_f^2\alpha^2}{3N_\mathrm{C}s}\left(\frac{4\pi}{s}\right)^{\varepsilon}\frac{3\sqrt{\pi}(1-\varepsilon)^2}{2^{2-2\varepsilon}\Gamma(\frac{5-2\varepsilon}{2})}.\end{aligned}$$

Here, we have factored out the well-known Born cross section in $D = 4$ dimensions

$$\sigma_\mathrm{B} = \frac{4\pi Q_f^2\alpha^2}{3N_\mathrm{C}s},$$

to which this result reduces for $\varepsilon \to 0$. The important result in D-dimensions therefore is

$$\sigma_{q\bar{q}}^{(0)} = \sigma_\mathrm{B}\left(\frac{4\pi}{s}\right)^{\varepsilon}\frac{3\sqrt{\pi}(1-\varepsilon)^2}{2^{2-2\varepsilon}\Gamma(\frac{5-2\varepsilon}{2})}, \tag{5.6}$$

which we will need later for the NLO calculation.

Equal masses for incoming and outcoming particles

We also consider the case in $D = 4$ where $m_a = m_b = m_\mathrm{i}$ and $m_1 = m_2 = m_\mathrm{f}$. The Källén functions then reduce to

$$\lambda_{12}^{\frac{1}{2}} = s - 4m_\mathrm{f}^2,\ \ \lambda_{ab}^{\frac{1}{2}} = s - 4m_\mathrm{i}^2,$$

and a short calculation gives

$$\frac{a+3c}{3} = \left(1+\frac{2m_\mathrm{i}}{s}\right)\left(1+\frac{2m_\mathrm{f}}{s}\right).$$

Using this in (5.5), we obtain the result

$$\sigma_{q\bar{q}}^{(0)} = \frac{4Q_f^2\alpha^2\pi}{3N_\mathrm{C}s}\sqrt{\frac{s-4m_\mathrm{f}^2}{s-4m_\mathrm{i}^2}}\left(1+\frac{2m_\mathrm{i}}{s}\right)\left(1+\frac{2m_\mathrm{f}}{s}\right).$$

5.1.2 Generic exchange particles and interference

We generalize the above calculation to the case where n channels for the Drell-Yan process $q\bar{q} \to l^+l^-$ exist, each corresponding to a transition matrix $\mathcal{M}_i$. Then the total transition matrix is simply the sum

$$\mathcal{M} = \mathcal{M}_1 + ... + \mathcal{M}_n,$$

and the transition amplitude can be written as

$$|\mathcal{M}|^2 = |\mathcal{M}_1|^2 + ... + |\mathcal{M}_n|^2 + \sum_{a<b} 2\,\mathrm{Re}\left(\mathcal{M}_a\mathcal{M}_b^*\right),$$

where additional interference terms of the form $2\,\mathrm{Re}\left(\mathcal{M}_a\mathcal{M}_b^*\right)$ appear. To compute this in the most generic way, we construct the diagram

$$\mathcal{M}_a\mathcal{M}_b^* =$$

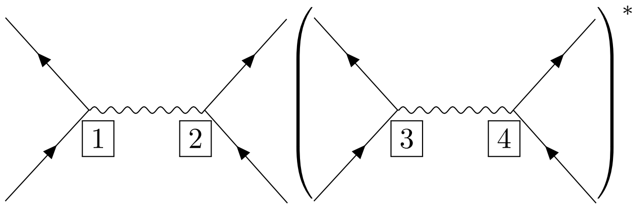

,

where we have introduced general couplings

$$\boxed{i} = \gamma^\mu g_i = \gamma^\mu \left(g_i^{\mathrm{L}} P_{\mathrm{L}} + g_i^{\mathrm{R}} P_{\mathrm{R}}\right)$$

with left- and right-handed parts g_i^{L} and g_i^{R}. Using these couplings, we can for instance compute the transition amplitudes for $\gamma-$, $W-$ or $Z-$exchange using the appropriate left- and right-handed couplings $g_i^{\mathrm{L}/R}$, given in table 5.1.

Table 5.1: Left- and right- handed couplings of photon, W and Z.

	γ	W	Z
g_i^{L}	$Q_f e$	$\frac{g}{\sqrt{2}}$	$\frac{g}{\cos\theta}\frac{1}{2}\left(V_f + A_f\right)$
g_i^{R}	$Q_f e$	0	$\frac{g}{\cos\theta}\frac{1}{2}\left(V_f - A_f\right)$

Here, V_f and A_f are the respective vector- and axial coupling to the fermion f at the vertex, given by

$$\begin{aligned} V_f &= T_f^3 - 2\sin^2\theta_{\mathrm{W}} Q_f \\ A_f &= T_f^3. \end{aligned}$$

Proceeding with the generic couplings, the diagrams give

$$\mathcal{M}_a\mathcal{M}_b^* = \frac{1}{\left(s - M_a^2\right)\left(s - M_b^2\right)} X_{\mu\nu} Y^{\mu\nu},$$

where M_a and M_b are the masses of the exchange bosons in the corresponding diagram, and the tensors are given by

$$\begin{aligned} X^{\mu\nu} &= \frac{1}{2}\mathrm{Tr}\Big[(\not{p}_a + m_a)\gamma^\mu g_1(\not{p}_b - m_b)\gamma^\nu g_3\Big] \\ Y^{\mu\nu} &= \frac{1}{2}\mathrm{Tr}\Big[(\not{k}_1 + m_1)\gamma^\mu g_2(\not{k}_2 - m_2)\gamma^\nu g_4\Big]. \end{aligned}$$

We proceed now in $D = 4$ dimensions, as we will not compute NLO corrections for this generic diagram.
The traces yield a result similar to (5.3),

$$\begin{aligned} X^{\mu\nu} = \left(g_1^{\mathrm{L}} g_3^{\mathrm{L}} + g_1^{\mathrm{R}} g_3^{\mathrm{R}}\right)\left(p_a^\mu p_b^\nu + p_a^\nu p_b^\mu - g^{\mu\nu} p_a \cdot p_b\right) - \left(g_1^{\mathrm{L}} g_3^{\mathrm{R}} + g_1^{\mathrm{R}} g_3^{\mathrm{L}}\right) g^{\mu\nu} m_a m_b \\ + i\left(g_1^{\mathrm{L}} g_3^{\mathrm{L}} - g_1^{\mathrm{R}} g_3^{\mathrm{R}}\right)\varepsilon^{\mu\nu}_{\ \ \delta\sigma} p_a^\delta p_b^\sigma, \end{aligned}$$

and

$$Y^{\mu\nu} = \left(g_2^{\mathrm{L}} g_4^{\mathrm{L}} + g_2^{\mathrm{R}} g_4^{\mathrm{R}}\right)\left(k_1^\mu k_2^\nu + k_1^\nu k_2^\mu - g^{\mu\nu} k_1 \cdot k_2\right) - \left(g_2^{\mathrm{L}} g_4^{\mathrm{R}} + g_2^{\mathrm{R}} g_4^{\mathrm{L}}\right) g^{\mu\nu} m_1 m_2 \\ + i\left(g_2^{\mathrm{L}} g_4^{\mathrm{L}} - g_2^{\mathrm{R}} g_4^{\mathrm{R}}\right) \varepsilon^{\mu\nu}_{\delta\sigma} k_1^\delta k_2^\sigma ,$$

where additional anti-symmetric terms appear. Contracting these in $D = 4$ gives

$$\begin{aligned} X_{\mu\nu} Y^{\mu\nu} = {} & 4\left(p_a \cdot k_1\right)\left(p_b \cdot k_2\right) \underbrace{\left(g_1^{\mathrm{L}} g_2^{\mathrm{R}} g_3^{\mathrm{L}} g_4^{\mathrm{R}} + g_1^{\mathrm{R}} g_2^{\mathrm{L}} g_3^{\mathrm{R}} g_4^{\mathrm{L}}\right)}_{c_1} \\ & + 4\left(p_a \cdot k_2\right)\left(p_b \cdot k_1\right) \underbrace{\left(g_1^{\mathrm{L}} g_2^{\mathrm{L}} g_3^{\mathrm{L}} g_4^{\mathrm{L}} + g_1^{\mathrm{R}} g_2^{\mathrm{R}} g_3^{\mathrm{R}} g_4^{\mathrm{R}}\right)}_{c_2} \\ & + 2\left(p_a \cdot p_b\right) m_1 m_2 \underbrace{\left(g_1^{\mathrm{L}} g_3^{\mathrm{L}} + g_1^{\mathrm{R}} g_3^{\mathrm{R}}\right)\left(g_2^{\mathrm{L}} g_4^{\mathrm{R}} + g_2^{\mathrm{R}} g_4^{\mathrm{L}}\right)}_{c_3} \\ & + 2\left(k_1 \cdot k_2\right) m_a m_b \underbrace{\left(g_1^{\mathrm{L}} g_3^{\mathrm{R}} + g_1^{\mathrm{R}} g_3^{\mathrm{L}}\right)\left(g_2^{\mathrm{L}} g_4^{\mathrm{L}} + g_2^{\mathrm{R}} g_4^{\mathrm{R}}\right)}_{c_4} \\ & + 4 m_1 m_2 m_a m_b \underbrace{\left(g_1^{\mathrm{L}} g_3^{\mathrm{R}} + g_1^{\mathrm{R}} g_3^{\mathrm{L}}\right)\left(g_2^{\mathrm{L}} g_4^{\mathrm{R}} + g_2^{\mathrm{R}} g_4^{\mathrm{L}}\right)}_{c_5} . \end{aligned} \tag{5.7}$$

This result has the same form as $H_{\mu\nu} L^{\mu\nu}$, but with different coefficients. Hence, we can use the result from above to get

$$\sigma = \frac{1}{16\pi s} \frac{1}{\left(s - M_a^2\right)\left(s - M_b^2\right)} \frac{\lambda_{12}^{\frac{1}{2}}}{\lambda^{\frac{1}{2}}\left(s, m_a^2, m_b^2\right)} \frac{a + 3c}{3} .$$

Here, the prefactor does not yet include the couplings, because they were included in $X_{\mu\nu} Y^{\mu\nu}$ and will therefore be contained in a and c. Inserting the kinematics in (5.7), we get the coefficients

$$a = \left(c_1 + c_2\right) \frac{\lambda_{12} \lambda_{ab}}{4 s^2} ,$$

$$b = \frac{\lambda_{12} \lambda_{ab}}{2 s^2} c_2\left(s^2 - \left(m_1^2 - m_2^2\right)\left(m_a^2 - m_b^2\right)\right) - c_1\left(s^2 + \left(m_1^2 - m_2^2\right)\left(m_a^2 - m_b^2\right)\right) ,$$

and

$$c = 4\left(c_1 + c_2\right) E + c_3\left(s - m_a^2 - m_b^2\right) m_1 m_2 + c_4\left(s - m_1^2 - m_2^2\right) m_a m_b + 4 c_5 M ,$$

where $E = E_a E_b E_1 E_2$ and $M = m_a m_b m_1 m_2$.

By setting $g_{1,3}^{\mathrm{L/R}} = Q_f e$ and $g_{2,4}^{\mathrm{L/R}} = -e$, this, collapses to the QED cross section σ_{B}. In the next section we will calculate explicitly the special case of γ - Z interference.

$\gamma - Z$ Interference

The total $\gamma - Z$ amplitude is given by

$$\left|\mathcal{M}_{\gamma - Z}\right|^2 = \left|\mathcal{M}_\gamma\right|^2 + \left|\mathcal{M}_Z\right|^2 + 2\,\mathrm{Re}\left(\mathcal{M}_\gamma \mathcal{M}_Z^*\right) ,$$

where $\mathcal{M}_\gamma$ and $\mathcal{M}_Z$ are the diagrams with photon and Z-exchange, respectively. We have already calculated the photon diagram, so we start with $|\mathcal{M}_Z|^2$. Therefore, we set

$$g_1^{\mathrm{L/R}} = g_3^{\mathrm{L/R}} = g_q^{\mathrm{L/R}} = \frac{g}{\cos\theta_{\mathrm{W}}} \frac{1}{2} \left(V_q \pm A_q\right),$$

and

$$g_2^{\mathrm{L/R}} = g_4^{\mathrm{L/R}} = g_l^{\mathrm{L/R}} = \frac{g}{\cos\theta_{\mathrm{W}}} \frac{1}{2} \left(V_l \pm A_l\right),$$

where V and A denote the vector and axial couplings for the incoming quarks and the lepton pair, respectively. This yields the coefficients

$$\begin{aligned} a = c = a_{ZZ} &= \frac{s^2}{4}(c_1 + c_2) \\ &= \frac{s^2}{4} \left[(g_q^{\mathrm{L}})^2 + (g_q^{\mathrm{R}})^2\right] \left[(g_l^{\mathrm{L}})^2 + (g_l^{\mathrm{R}})^2\right] \\ &= \frac{s^2}{16} \frac{g^4}{\cos^4\theta_{\mathrm{W}}} \left(V_q^2 + A_q^2\right) \left(V_l^2 + A_l^2\right), \end{aligned}$$

and

$$\begin{aligned} b = b_{ZZ} &= \frac{s^2}{2} (c_2 - c_1) \\ &= \frac{s^2}{2} \left[(g_q^{\mathrm{L}})^2 - (g_q^{\mathrm{R}})^2\right] \left[(g_l^{\mathrm{L}})^2 - (g_l^{\mathrm{R}})^2\right] \\ &= \frac{s^2}{2} \frac{g^4}{\cos^4\theta_{\mathrm{W}}} A_q A_l V_q V_l. \end{aligned}$$

As a result, we have the transition amplitude

$$|\mathcal{M}_Z|^2 = \frac{1}{\chi\chi^*} \left\{a_{ZZ} \left(1 + \cos^2\theta\right) + b_{ZZ} \cos\theta\right\},$$

where $\frac{1}{\chi}$ is the propagator of the Z boson, or

$$\chi = \left(s - M_z^2 + iM_Z\Gamma_Z\right),$$

with the finite resonance width Γ_Z of the Z boson. For the interference term, we set g_1 and g_2 to the appropriate couplings for the Z

$$\begin{aligned} g_1^{\mathrm{L/R}} &= g_q^{\mathrm{L/R}} = \frac{g}{\cos\theta_{\mathrm{W}}} \frac{1}{2} \left(V_q \pm A_q\right) \\ g_2^{\mathrm{L/R}} &= g_l^{\mathrm{L/R}} = \frac{g}{\cos\theta_{\mathrm{W}}} \frac{1}{2} \left(V_l \pm A_l\right), \end{aligned}$$

and g_3 and g_4 to the photon couplings

$$\begin{aligned} g_3^{\mathrm{L/R}} &= Q_f e \\ g_4^{\mathrm{L/R}} &= e. \end{aligned}$$

In this way, we get

$$\mathcal{M}_\gamma \mathcal{M}_Z^* = \frac{1}{s\chi} \left\{ a_{\text{if}} \left(1 + \cos^2\theta\right) + b_{\text{if}} \cos\theta \right\},$$

where

$$\begin{aligned} a_{\text{if}} &= \frac{g^2}{\cos^2\theta_{\text{W}}} \frac{s^2}{4} Q_f e^2 V_q V_l \\ b_{\text{if}} &= \frac{g^2}{\cos^2\theta_{\text{W}}} \frac{s^2}{2} Q_f e^2 A_q A_l. \end{aligned}$$

Summing up $|\mathcal{M}_\gamma|^2$, $|\mathcal{M}_Z|^2$ and $2\,\text{Re}(\mathcal{M}_\gamma \mathcal{M}_Z^*)$ results in

$$|\mathcal{M}_{\gamma Z}|^2 = 16\pi^2\alpha^2 m_0 \left(1 + \cos^2\theta\right) + m_1 \cos\theta, \tag{5.8}$$

where the coefficients m_0 and m_1 are combinations of the vector and axial couplings of the quarks and leptons,

$$\begin{aligned} m_0 &= Q_f^2 - 2Q_f V_l V_q \chi_1 + \left(V_q^2 + A_q^2\right)\left(V_l^2 + A_l^2\right)\chi_2 \\ m_1 &= -4\chi_1 Q_f A_q A_l + 8\chi_2 A_q A_l V_q V_l. \end{aligned}$$

and χ_1 and χ_2 are given by

$$\begin{aligned} \chi_1 &= \frac{\sqrt{2} G_{\text{F}} M_Z^2}{16\pi\alpha} \frac{s(s - M_Z)^2}{(s - M_Z^2)^2 + \Gamma_Z^2 M_Z^2} \\ \chi_2 &= \left(\frac{\sqrt{2} G_{\text{F}} M_Z^2}{16\pi\alpha}\right)^2 \frac{s^2}{(s - M_Z^2)^2 + \Gamma_Z^2 M_Z^2}, \end{aligned}$$

where we used the Fermi coupling constant $G_{\text{F}} = \frac{\sqrt{2}}{8} \frac{g^2}{m_{\text{W}}^2}$. From (5.8), the differential cross section can be written as

$$\frac{\text{d}\sigma}{\text{d}\Omega} = \frac{1}{16\pi^2} \frac{1}{4N_{\text{C}} s} |\mathcal{M}_{\gamma Z}|^2 = \frac{\alpha^2}{4N_{\text{C}} s} \left(m_0 \left(1 + \cos^2\theta\right) + m_1 \cos\theta\right). \tag{5.9}$$

For $m_0 = 1$ and $m_1 = 0$, this is the QED result (only photon exchange), which is symmetric in the angle θ. The different coupling of the Z to left- and right-handed fermions introduces an asymmetry through the term m_1. This drops out in the integrated cross section

$$\sigma = \frac{4\pi\alpha^2}{3N_{\text{C}} s} A_0 = \sigma_{\text{B}} m_0.$$

5.2 Virtual Corrections

The next step for the NLO cross section is including the virtual (loop) corrections to the vertex functions and propagators, where we are interested in corrections of $\mathcal{O}(\alpha_s)$. Considering again (5.2), we realize that there are no such corrections for the propagator of the exchange boson, as the electroweak mediators do not couple to gluons. Nor are there corrections to the lepton vertex, as the gluons do not couple to the colorless leptons. Therefore, the only part that receives a correction is the quark vertex, which we will calculate in the next subsection.

5.2.1 Quark vertex correction

There is only one vertex correction diagram of $\mathcal{O}(\alpha_s)$,

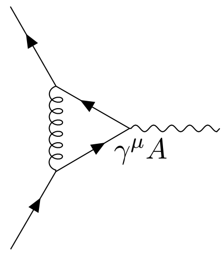

where, as before, A is an generic coupling of the form

$$A = A^{\mathrm{L}} P_{\mathrm{L}} + A^{\mathrm{R}} P_{\mathrm{R}}.$$

The matrix element including the external legs, reads

$$\begin{aligned}
i\mathcal{M} &= T^a_{ik} T^a_{kj} (-i g^{\alpha\beta}) \mu^{4-D} \int \frac{\mathrm{d}^D q}{(2\pi)^D} \bar{v}(p_a) \frac{i g_s \gamma^\alpha \, i(\not{q} + \not{p}_a) \, i\gamma^\mu A \, i(\not{q} - \not{p}_b) \, i g_s \gamma^\beta}{q^2 \, (q+p_a)^2 \, (q-p_b)^2} u(p_3) \\
&= g_s^2 C_{\mathrm{F}} \mu^{4-D} \frac{i}{(4\pi)^2} \int_q \frac{\bar{v}(p_a) \, \gamma^\alpha (\not{q} + \not{p}_a) \gamma^\mu A (\not{q} - \not{p}_b) \gamma_\alpha \, u(p_b)}{q^2 \, (q+p_a)^2 \, (q-p_b)^2} \\
&= \bar{v}(p_a) i \Gamma^\mu u(p_b),
\end{aligned}$$

with Γ^μ being the vertex function

$$\Gamma^\mu = \frac{g_s^2}{(4\pi)^2} C_{\mathrm{F}} \int_q \frac{\gamma^\alpha (\not{q} + \not{p}_a) \gamma^\mu A (\not{q} - \not{p}_b) \gamma_\alpha}{q^2 \, (q+p_a)^2 \, (q-p_b)^2}.$$

Using the relation

$$\gamma^\alpha \gamma^\mu \gamma^\nu \gamma^\rho \gamma_\alpha = -2 \gamma^\rho \gamma^\nu \gamma^\mu + (4-D) \, \gamma^\mu \gamma^\nu \gamma^\rho,$$

the numerator can be simplified to

$$N^\mu = -2 \left(\not{q} - \not{p}_b \right) \gamma^\mu \left(\not{q} + \not{p}_a \right) A + (4-D) \left(\not{q} + \not{p}_a \right) \gamma^\mu \left(\not{q} - \not{p}_b \right) A.$$

The Dirac structures can be further simplified to

$$\begin{aligned}
(\not{q} - \not{p}_b) \gamma^\mu (\not{q} + \not{p}_a) &= -q^2 \gamma^\mu + 2 \not{q} q^\mu + \not{q} \gamma^\mu \not{p}_a - \not{p}_b \gamma^\mu \not{q} - \not{p}_b \gamma^\mu \not{p}_a \\
(\not{q} + \not{p}_a) \gamma^\mu (\not{q} - \not{p}_b) &= -q^2 \gamma^\mu + 2 \not{q} q^\mu - \not{q} \gamma^\mu \not{p}_b + \not{p}_a \gamma^\mu \not{q} - \not{p}_a \gamma^\mu \not{p}_b,
\end{aligned}$$

where we used the fact that the quarks are massless. The numerator thus simplifies to

$$N^\mu(q) = \left[(D-2) q^2 \gamma^\mu + \not{q} \left(2(2-D) q^\mu + 4 p_b - 4 p_a \right) + \gamma^\mu \left(4 p_a q - 4 p_b q - 4 p_a p_2 \right) \right] A.$$

To solve the q-integral, we introduce Feynman parameters x and y as

$$\Gamma^\mu = \frac{g_s^2}{(4\pi)^2} C_{\mathrm{F}} \int_q 2 \int_0^1 \mathrm{d}x \int_0^{1-x} \mathrm{d}y \frac{N^\mu(q)}{\left[(q + x p_a - y p_b)^2 + s x y \right]^3},$$

and shift the integral to

$$\Gamma^\mu = 2\frac{g_s^2}{(4\pi)^2}C_\mathrm{F}\int_q\int \mathrm{d}x\mathrm{d}y\frac{N^\mu(q - x_1p_a + yp_b)}{\left[q^2 + sxy\right]^3},$$

where, in N^μ, terms linear in q can be neglected, such that we obtain

$$\Gamma^\mu = 2\frac{g_s^2}{(4\pi)^2}C_\mathrm{F}\int_q\int \mathrm{d}x\mathrm{d}y\frac{\gamma^\mu\left[(D-2)q^2 + s\left(2x + 2y + (2-D)xy - 2\right)\right] + \not{q}2(2-D)q^\mu}{\left[q^2 + sxy\right]^3}A.$$

The tensor structure in the last term can be eliminated by using the identity

$$\int_q q^\mu q^\nu f(q) = \frac{g^{\mu\nu}}{D}\int_q q^2 f(q).$$

This reduces the integral to

$$\Gamma^\mu = 2\frac{g_s^2}{(4\pi)^2}C_\mathrm{F}\gamma^\mu A\int \mathrm{d}x\mathrm{d}y\int_q\frac{\frac{(D-2)}{D}q^2 + s\left(2x + 2y + (2-D)xy - 2\right)}{\left[q^2 + sxy\right]^3}.$$

This integral is now solvable using the generic integral formula. It consist of two parts $\Gamma^\mu = \Gamma_1^\mu + \Gamma_2^\mu$. First the part Γ_1^μ proportional to q^2

$$\Gamma_1^\mu = 2\frac{g_s^2}{(4\pi)^2}C_\mathrm{F}\int_q\int \mathrm{d}x\mathrm{d}y\frac{\gamma^\mu(D-2)q^2}{\left[q^2 + sxy\right]^3},$$

is considered. This can be decomposed into the generic integrals

$$\int_q \frac{q^2}{\left[q^2 + sxy\right]^3} = \int_q \frac{1}{\left[q^2 + sxy\right]^2} - \int_q \frac{sxy}{\left[q^2 + sxy\right]^3}.$$

Using (3.2), this yields

$$\begin{aligned}\int_q \frac{q^2}{\left[q^2 + sxy\right]^3} &= \left(4\pi\mu^2\right)^{\frac{4-D}{2}}(-sxy)^{\frac{D}{2}-2}\left(\Gamma(2-\frac{D}{2}) - \frac{\Gamma(3-\frac{D}{2})}{2}\right)\\ &= \left(4\pi\mu^2\right)^{\varepsilon}(-sxy)^{-\varepsilon}\frac{1}{2\varepsilon}(2-\varepsilon)\Gamma(1+\varepsilon).\end{aligned}$$

Here, we encounter a UV-divergence originating in $\Gamma(2-\frac{D}{2})$, as the gamma functions would converge for $D > 4$. The remaining expression has to be integrated over x and y, resulting in a Beta function,

$$\begin{aligned}\int_0^1 \mathrm{d}x\int_0^{1-x}(xy)^{-\varepsilon} &= \int_0^1 \mathrm{d}x\int_0^1 \mathrm{d}y\left[x(1-x)y\right]^{-\varepsilon}(1-x)\\ &= \frac{1}{1-\varepsilon}B(1-\varepsilon, 2-\varepsilon) = \frac{1}{1-\varepsilon}\frac{\Gamma(1-\varepsilon)\Gamma(2-\varepsilon)}{\Gamma(3-2\varepsilon)}.\end{aligned}$$

Collecting the results for the first part, this results in

$$\begin{aligned}\Gamma_1^\mu &= 2\frac{g_s^2}{(4\pi)^2}C_\mathrm{F}\gamma^\mu A\left(\frac{4\pi\mu^2}{-s}\right)^\varepsilon\Gamma(1+\varepsilon)\frac{\Gamma(1-\varepsilon)\Gamma(2-\varepsilon)}{\Gamma(3-2\varepsilon)}\frac{4(1-\varepsilon)}{4-2\varepsilon}\frac{1}{2\varepsilon}(2-\varepsilon)\\ &= 2\frac{g_s^2}{(4\pi)^2}C_\mathrm{F}\gamma^\mu A\left(\frac{4\pi\mu^2}{-s}\right)^\varepsilon\Gamma(1+\varepsilon)\frac{\Gamma(1-\varepsilon)\Gamma(2-\varepsilon)}{\Gamma(3-2\varepsilon)}\left(\frac{1}{\varepsilon_\mathrm{UV}} - 1\right).\end{aligned}$$

We again made the UV-divergence explicit by denoting $\varepsilon = \varepsilon_{\mathrm{UV}}$. For the second part, we can directly apply the formula for the generic integral, yielding

$$\Gamma_2^\mu = 2\frac{g_s^2}{(4\pi)^2} C_{\mathrm{F}} \gamma^\mu A \left(\frac{4\pi\mu^2}{-s}\right)^\varepsilon \int \mathrm{d}x\mathrm{d}y \; [2x + 2y + (2-D)xy - 2] \, (-xy)^{-1-\varepsilon} \frac{\Gamma(1+\varepsilon)}{2}.$$

In an analogous calculation the x and y integral result in

$$I = \int \mathrm{d}x\mathrm{d}y \, [2x + 2y + (2-D)xy - 2] \, (-xy)^{-1-\varepsilon} = -2B(1-\varepsilon, 2-\varepsilon) + \frac{2}{1-\varepsilon} B(1-\varepsilon, 2-\varepsilon) + \frac{2}{\varepsilon} B(-\varepsilon, 2-\varepsilon).$$

Here the last two Beta functions contain a IR-divergence, as the corresponding expressions would converge for $D < 4$ (or $\varepsilon > 0$). We can simplify this integral in the same fashion as above to

$$I = \frac{\Gamma(1-\varepsilon)\Gamma(2-\varepsilon)}{\Gamma(3-2\varepsilon)} \left(-\frac{4}{\varepsilon_{\mathrm{IR}}^2} - 2\right),$$

where this time $\varepsilon = \varepsilon_{\mathrm{IR}}$. Thus, the second part is given as

$$\Gamma_2^\mu = \frac{g_s^2}{(4\pi)^2} \left(4\pi\mu^2\right)^\varepsilon C_{\mathrm{F}} \gamma^\mu A \, \Gamma(1+\varepsilon) \frac{\Gamma(1-\varepsilon)\Gamma(2-\varepsilon)}{\Gamma(3-2\varepsilon)} \left(-\frac{4}{\varepsilon_{\mathrm{IR}}^2} - 2\right),$$

so that the total vertex correction sums up to

$$\Gamma^\mu = \frac{g_s^2}{(4\pi)^2} C_{\mathrm{F}} \gamma^\mu A \left(\frac{4\pi\mu^2}{-s}\right)^\varepsilon \Gamma(1+\varepsilon) \frac{\Gamma(1-\varepsilon)\Gamma(2-\varepsilon)}{\Gamma(3-2\varepsilon)} \left(-\frac{4}{\varepsilon_{\mathrm{IR}}^2} + \frac{2}{\varepsilon_{\mathrm{UV}}} - 4\right).$$

We reduce this to the final form

$$\Gamma^\mu = \frac{\alpha_s}{4\pi} C_{\mathrm{F}} \gamma^\mu \left(A^{\mathrm{L}} P_{\mathrm{L}} + A^{\mathrm{R}} P_{\mathrm{R}}\right) \left(\frac{4\pi\mu^2}{-s}\right)^\varepsilon \Gamma(1+\varepsilon) \frac{\Gamma^2(1-\varepsilon)}{\Gamma(1-2\varepsilon)} \left(-\frac{2}{\varepsilon_{\mathrm{IR}}^2} - \frac{4}{\varepsilon_{\mathrm{IR}}} + \frac{1}{\varepsilon_{\mathrm{UV}}} - 8 + \mathcal{O}(\varepsilon)\right), \tag{5.10}$$

where three types of divergences appear. The infrared divergences are caused by the gluon as a massless particle in the loop. Both infrared poles result from the momentum region in the loop integral, where the gluon is collinear ($\vec{q} \propto \vec{p}_{a/b}$) to one of the incoming quarks. The double pole $\frac{2}{\varepsilon_{\mathrm{IR}}^2}$ is caused by the momentum region, where in addition the gluon is soft ($q = 0$). As explained in section 3.7, these divergences can only be canceled by including real emission diagrams, where the single collinear pole will even remain on partonic level. It can only be canceled in the total Drell-Yan cross section by renormalizing the PDFs.

At last, there is the UV-divergence, which can be eliminated by renormalization. This will be done in the next section.

5.2.2 Renormalized vertex correction

In section 3.5 it was shown, that the UV-divergences can be canceled by renormalizing the parameters of the theory. To specify the appropriate parameter, we note that the vertex graph is nothing else but a contribution to the three-point Green's function which results from the interaction term

$$\mathcal{L} = \bar{\psi} B_\mu \gamma^\mu \left(A^{\mathrm{L}} P_{\mathrm{L}} + A^{\mathrm{R}} P_{\mathrm{R}} \right) \psi.$$

Here B_μ is an electroweak gauge boson with the generic coupling

$$\gamma^\mu A = \gamma^\mu \left(A^{\mathrm{L}} P_{\mathrm{L}} + A^{\mathrm{R}} P_{\mathrm{R}} \right).$$

As we will not consider electroweak corrections in our calculation, neither the coupling A, nor the field B_μ need to be renormalized. Hence, the only source for a counterterm can be the quark fields ψ. The counterterm Lagrangian will therefore be

$$\mathcal{L} = \delta_\psi \bar{\psi}_{\mathrm{R}} \not{B} \psi_{\mathrm{R}} \left(A^{\mathrm{L}} P_{\mathrm{L}} + A^{\mathrm{R}} P_{\mathrm{R}} \right),$$

such that

$$\Gamma^\mu_{\mathrm{R}} = \Gamma^\mu + \delta_\psi \gamma^\mu \left(A^{\mathrm{L}} P_{\mathrm{L}} + A^{\mathrm{R}} P_{\mathrm{R}} \right).$$

The counterterm δ_ψ has already been determined in the MS-scheme in section 3.5. In section 3.6, it was shown that depending on the renormalization of the two-point function there appears an additional factor from the residuum of the two-point function in the S-matrix. It is therefore convenient, to renormalize the two-point function in the on-shell scheme, where this factor equals one. The counterterm in this scheme is given by

$$\delta_\psi = \left. \frac{\mathrm{d}\Sigma(\not{p})}{\mathrm{d}\not{p}} \right|_{\not{p}=m_p},$$

where m_p is the physical mass of the quark, which we set to zero. To compute this, we can start at expression (3.3), where we introduced Feynman parameters for the self-energy

$$\Sigma(\not{p}) = -C_{\mathrm{F}} \frac{g_s^2}{(4\pi)^2} \int_q \int_0^1 \mathrm{d}x \frac{(2-D)\not{p}x}{\left[q^2 + p^2 x(1-x) + i\varepsilon\right]^2}.$$

The derivative then reads

$$\left. \frac{\mathrm{d}\Sigma(\not{p})}{\mathrm{d}\not{p}} \right|_{\not{p}=0} = -C_{\mathrm{F}} \frac{g_s^2}{(4\pi)^2} \int_q \int_0^1 \mathrm{d}x \frac{(2-D)x}{\left[q^2 + i\varepsilon\right]^2} = -C_{\mathrm{F}} \frac{g_s^2}{(4\pi)^2} \int_q \frac{(2-D)}{\left[q^2 + i\varepsilon\right]^2},$$

which is a scaleless integral, with IR- and UV-divergence that formally cancel in dimensional regularization. We want to separate these in order to check the individual cancellation of the different divergences later. This can be accomplished by going to the euclidean integral and introducing a scale Λ:

$$\begin{aligned} \int_q \frac{1}{\left[q^2 + i\varepsilon\right]^2} &= \frac{(2\pi\mu)^{4-D}}{\pi^2} \int \mathrm{d}^D q_{\mathrm{E}} \frac{1}{q_{\mathrm{E}}^4} \\ &= \frac{(2\pi\mu)^{2\varepsilon}}{\pi^2} \left(\Omega_D \int_0^\Lambda \mathrm{d}q_{\mathrm{E}} q_{\mathrm{E}}^{1-2\varepsilon_{\mathrm{IR}}} + \Omega_D \int_\Lambda^\infty \mathrm{d}q_{\mathrm{E}} q_{\mathrm{E}}^{1-2\varepsilon_{\mathrm{UV}}} \right). \end{aligned}$$

Here we made explicit that the first integral converges for $\varepsilon = \varepsilon_{\mathrm{IR}} < 0$, whereas the second integral converges for $\varepsilon = \varepsilon_{\mathrm{UV}} > 0$. The integrals can now be solved individually

$$\int \mathrm{d}^D q_{\mathrm{E}} \frac{1}{q_{\mathrm{E}}^4} = \Omega_D \left(\ln \Lambda - \frac{1}{2\varepsilon_{\mathrm{IR}}} + \mathcal{O}(\varepsilon_{\mathrm{IR}}) \right) - \Omega_D \left(\ln \Lambda - \frac{1}{2\varepsilon_{\mathrm{UV}}} + \mathcal{O}(\varepsilon_{\mathrm{UV}}) \right).$$

Each of the integrals diverges individually, but the sum vanishes because of $\varepsilon_{\mathrm{IR}} = \varepsilon_{\mathrm{UV}}$. Neglecting terms of order ε, this can be used to define

$$\int_q \frac{1}{[q^2 + i\varepsilon]^2} = \frac{1}{\varepsilon_{\mathrm{UV}}} - \frac{1}{\varepsilon_{\mathrm{IR}}},$$

where we keep the discrimination of UV- and IR-divergence. Accordingly, the counterterm δ_ψ takes the form

$$\delta_\psi = -C_{\mathrm{F}} \frac{g_s^2}{(4\pi)^2} \left(\frac{1}{\varepsilon_{\mathrm{UV}}} - \frac{1}{\varepsilon_{\mathrm{IR}}} \right).$$

Adding this to the regularized vertex correction (5.10), the UV-divergences cancel and we arrive at a UV-finite result

$$\Gamma^\mu_{\mathrm{R}} = \frac{\alpha_s}{4\pi} C_{\mathrm{F}} \gamma^\mu \left(A^{\mathrm{L}} P_{\mathrm{L}} + A^{\mathrm{R}} P_{\mathrm{R}} \right) \left(\frac{4\pi\mu^2}{-s} \right)^\varepsilon \Gamma(1+\varepsilon) \frac{\Gamma^2(1-\varepsilon)}{\Gamma(1-2\varepsilon)} \left(-\frac{2}{\varepsilon_{\mathrm{IR}}^2} - \frac{3}{\varepsilon_{\mathrm{IR}}} - 8 + \mathcal{O}(\varepsilon) \right).$$

5.2.3 Cross section with virtual corrections

The α_s correction for the partonic Drell-Yan cross section results from the interference of the LO diagram $\mathcal{M}_0$ and the same diagram with the replacement

$$\gamma^\mu A \to \Gamma^\mu_{\mathrm{R}} = \gamma^\mu A\, f(s),$$

where

$$f(s) = \frac{\alpha_s}{4\pi} C_{\mathrm{F}} \left(\frac{4\pi\mu^2}{-s} \right)^\varepsilon \Gamma(1+\varepsilon) \frac{\Gamma^2(1-\varepsilon)}{\Gamma(1-2\varepsilon)} \left(-\frac{2}{\varepsilon_{\mathrm{IR}}^2} - \frac{3}{\varepsilon_{\mathrm{IR}}} - 8 + \mathcal{O}(\varepsilon) \right).$$

As these diagrams have the same kinematical structure, the cross section $\sigma^{\mathrm{v}}_{q\bar{q}}$ for this interference diagram will be simply given by the LO cross section, corrected by the real part $f(s)$:

$$\sigma^{\mathrm{v}}_{q\bar{q}} = 2\sigma^{(0)}_{q\bar{q}} \,\mathrm{Re}\left[f(s) \right],$$

where we used the D-dimensional result from (5.6). We only take the real part of $f(s)$ as $\sigma^{(0)}_{q\bar{q}}$ is real, however, imaginary parts are hidden in the expansion of $(-1)^\varepsilon$ in $f(s)$,

$$f(s) = \frac{\alpha_s}{4\pi} C_{\mathrm{F}} \left(\frac{4\pi\mu^2}{s} \right)^\varepsilon \Gamma(1+\varepsilon) \frac{\Gamma^2(1-\varepsilon)}{\Gamma(1-2\varepsilon)} \left(-\frac{2}{\varepsilon_{\mathrm{IR}}^2} - \frac{3-2i\pi}{\varepsilon_{\mathrm{IR}}} - 8 - 3i\pi + \pi^2 + \mathcal{O}(\varepsilon) \right).$$

By furthermore expanding

$$\Gamma(1+\varepsilon)\Gamma(1-\varepsilon) = 1 + \frac{\pi^2 \varepsilon^2}{6} + \mathcal{O}(\varepsilon),$$

and by inserting $\sigma_{q\bar{q}}^{(0)}$ from (5.6), we arrive at the renormalized cross section

$$\sigma_{q\bar{q}}^{\mathrm{v}} = 2\sigma_{\mathrm{B}} \frac{\alpha_s}{4\pi} C_{\mathrm{F}} \gamma^{\mu} \left(\frac{4\pi\mu^2}{s} \right)^{2\varepsilon} D(\varepsilon) \left(-\frac{2}{\varepsilon_{\mathrm{IR}}^2} - \frac{3}{\varepsilon_{\mathrm{IR}}} - 8 + \frac{2\pi^2}{3} + \mathcal{O}(\varepsilon) \right). \tag{5.11}$$

Here, we abbreviated the prefactor

$$D(\varepsilon) = \frac{3\sqrt{\pi}(1-\varepsilon)^2}{2^{2-2\varepsilon}\Gamma\left(\frac{5-2\varepsilon}{2}\right)} \frac{\Gamma(1-\varepsilon)}{\Gamma(1-2\varepsilon)} = 1 + \left(\frac{2}{3} - 2 \right) \gamma_{\mathrm{E}} + \mathcal{O}(\varepsilon^2). \tag{5.12}$$

The UV-divergences have canceled, as they should, but there still remain a double and single infrared singularity. For this reason, real contributions have to be accounted for, which will be done in the next section.

5.3 Real Corrections

As explained before, the process we calculated so far cannot be distinguished from processes, in which additional soft and collinear particles are emitted. The two possibilities for the emission of another particle, are the emission of a gluon from an initial quark

$$q\bar{q} \to g l^+ l^-,$$

and quark-gluon scattering with the emission of a final state quark

$$qg \to q l^+ l^-.$$

We also have to account for this second process, as in the hadronic cross section one sums over all initial parton combinations.

5.3.1 Real gluon emission

The diagrams for the process $q\bar{q} \to g l^+ l^-$ are

$i\mathcal{M} =$ 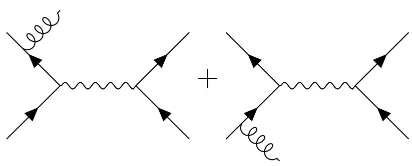

and the matrix element reads

$$i\mathcal{M}_{qq} = Q_f e^2 g_s \mu^{3(4-D)/2} \left[\bar{v}(p_b) S^{\mu\alpha} u(p_a) \right] T_{ij}^a \varepsilon_\alpha^* \frac{-i}{q^2} \left[\bar{u}(k_2) \gamma_\mu v(k_3) \right],$$

where we defined

$$S^{\mu\alpha} = S_a^{\mu\alpha} - S_b^{\mu\alpha} = \gamma^\mu \frac{1}{\not{p}_a - \not{k}_1} \gamma^\alpha - \gamma^\alpha \frac{1}{\not{p}_b - \not{k}_1} \gamma^\mu.$$

Only the hadronic part in the first bracket is modified in comparison to the LO diagram. As before, the amplitude will thus, separate into a leptonic and a hadronic part,

$$|\overline{\mathcal{M}_{qq}}|^2 = \frac{1}{4}\frac{1}{N^2}\sum_a \mathrm{Tr}[T_a T_a]\frac{Q_f^4 e^4 g_s^2 \mu^{3(4-D)}}{q^4} H^{\mu\nu} L_{\mu\nu},$$

where, analogous to the LO calculation, we have the leptonic tensor

$$\begin{aligned} L^{\mu\nu} &= \mathrm{Tr}[\not{k}_2 \gamma^\mu \not{k}_3 \gamma^\nu] \\ &= 4\left[k_2^\mu k_3^\nu + k_2^\nu k_3^\mu - g^{\mu\nu} k_2 \cdot k_3\right], \end{aligned}$$

and the modified hadronic tensor

$$H^{\mu\nu} = \mathrm{Tr}[\not{p}_b S^{\mu\alpha} \not{p}_a S_\alpha^{\ \nu}].$$

In this case, the invariant mass of the lepton pair is given by

$$Q^2 = q^2 = (p_a + p_b - k_1)^2.$$

The color factor in this diagram sums up to

$$\frac{1}{N_\mathrm{C}^2}\mathrm{Tr}[T_a T_a] = \frac{1}{N_\mathrm{C}^2} T_F \delta_{aa} = \frac{N_\mathrm{C}^2 - 1}{N_\mathrm{C}^2} T_F = \frac{C_F}{N_\mathrm{C}}.$$

To evaluate the tensors for the massless case, it is useful to work with the Mandelstam-like variables

$$s = (p_a + p_b)^2, \ \ t = (p_a - k_1)^2, \ \ \ u = (p_b - k_1)^2,$$

which fulfill the relation

$$s + t + u = q^2.$$

Using these variables, we split the hadronic tensor up into the different contributions from the sum in $S^{\mu\alpha}$,

$$\begin{aligned} H_a^{\mu\nu} &= \frac{1}{t^2}\mathrm{Tr}[\not{p}_b S_a^{\mu\alpha} \not{p}_a S_a^{\alpha\nu}] \\ &= -\frac{2(2-D)}{t}\left(2k_1^\mu p_b^\nu + 2k_1^\nu p_b^\mu + u g^{\mu\nu}\right) \\ H_b^{\mu\nu} &= \frac{1}{u^2}\mathrm{Tr}[\not{p}_b S_b^{\mu\alpha} \not{p}_a S_b^{\alpha\nu}] \\ &= -\frac{2(2-D)}{u}\left(2k_1^\mu p_a^\nu + 2k_1^\nu p_a^\mu + t g^{\mu\nu}\right), \end{aligned}$$

and

$$H_{ab}^{\mu\nu} = H_{ba}^{\mu\nu} = -\frac{1}{tu}\mathrm{Tr}[\not{p}_b S_a^{\mu\alpha} \not{p}_a S_a^{\alpha\nu}].$$

In terms of these tensors the amplitude thus can be written as

$$\begin{aligned} |\overline{\mathcal{M}_{qq}}|^2 &= |\overline{\mathcal{M}_a}|^2 + |\overline{\mathcal{M}_b}|^2 + 2\,\mathrm{Re}(\mathcal{M}_a \mathcal{M}_b^*) \\ &= \frac{C_F Q_f^2}{4N_\mathrm{C}}\frac{e^4 g_s^2 \mu^{3(4-D)}}{q^4}\left(H_a^{\mu\nu} + H_b^{\mu\nu} + 2H_{ab}^{\mu\nu}\right) L_{\mu\nu} \\ &= \frac{C_F}{4N_\mathrm{C}}\frac{Q_f^2 e^4 g_s^2 \mu^{3(4-D)}}{q^4} H^{\mu\nu} L_{\mu\nu}. \end{aligned}$$

The cross section can be obtained by integrating the amplitude in the three-particle phase space

$$\begin{aligned}\sigma^{\mathrm{r}}_{q\bar{q}} &= \frac{1}{F}\int |\overline{\mathcal{M}}|^{2} \mathrm{dPS}^{(3)}\\ &= \frac{C_F}{4N_{\mathrm{C}}}Q_f^2 e^4 g_s^2 \mu^{3(4-D)}\frac{1}{2s}\int H_{\mu\nu}\frac{L^{\mu\nu}}{q^4}\mathrm{dPS}^{(3)}\\ &= \frac{3}{2}\pi\sigma_{\mathrm{B}} C_F\, g_s^2\mu^{3(4-D)}\int H_{\mu\nu}\frac{L^{\mu\nu}}{q^4}\mathrm{dPS}^{(3)}.\end{aligned}$$

Here the LO cross section $\sigma_{\mathrm{B}} = \frac{4\alpha^2 Q_f^2}{3N_C s}$ was factored out for later convenience.

Leptonic integration

As the k_2 and k_3 dependence of $|\overline{\mathcal{M}}|^{2}$ lies only in $L^{\mu\nu}$, these variables can be integrated out first. Therefore, we define

$$I_L^{\mu\nu} = \int \frac{\mathrm{d}^{D-1}k_2}{(2\pi)^{D-1}2E_2}\frac{\mathrm{d}^{D-1}k_3}{(2\pi)^{D-1}2E_3}L^{\mu\nu}(2\pi)^D\delta^{(D)}(q-k_2-k_3).$$

The integral can be calculated by exploiting the fact that after the integration, $I_L^{\mu\nu}$can only depend on q and can therefore be decomposed as

$$I_L^{\mu\nu} = a(q^2)q^2 g^{\mu\nu} + b(q^2)q^\mu q^\nu.$$

The coefficients can be determined by contracting this equation with $g^{\mu\nu}$and $q^\mu q^\nu$, respectively,

$$\begin{aligned} g_{\mu\nu}I_L^{\mu\nu} &= (D\,a+b)q^2\\ q_\mu q_\nu I_L^{\mu\nu} &= (a+b)q^4. \end{aligned} \tag{5.13}$$

The left-hand sides of these equations can easily be computed. From the first equation, we have

$$\begin{aligned} g_{\mu\nu}I_L^{\mu\nu} &= 4(2-D)\int \frac{\mathrm{d}^{D-1}k_2}{(2\pi)^{D-1}2E_2}\frac{\mathrm{d}^{D-1}k_3}{(2\pi)^{D-1}2E_3}k_2\cdot k_3(2\pi)^D\delta^{(D)}(q-k_2-k_3)\\ &= 4(2-D)\int \frac{\mathrm{d}^{D-1}k_2}{(2\pi)^{D-2}}\frac{1}{2}\delta(q-2E_2). \end{aligned}$$

The remaining integral can be computed by introducing spherical coordinates

$$\mathrm{d}^{D-1}k_2 = |\vec{k}_2|^{D-2}\mathrm{d}|\vec{k}_2|\,\mathrm{d}\Omega_{D-1} = E_2^{D-2}\mathrm{d}E_2\mathrm{d}\Omega_{D-1},$$

where we have used the fact that the leptons are assumed massless, and therefore $E_1 = k_1^0 = |\vec{k}_1|$. Using the formula for the solid angle from Appendix A.5, we get

$$g_{\mu\nu}I_L^{\mu\nu} = 2(2-D)\frac{q^{D-2}}{(4\pi)^{D-2}}\frac{\pi^{\frac{D-1}{2}}}{\Gamma(\frac{D-1}{2})}.$$

In the same fashion, we can derive

$$q_\mu q_\nu I_L^{\mu\nu} = (2-D)\frac{q^D}{(4\pi)^{D-2}}\frac{\pi^{\frac{D-1}{2}}}{\Gamma(\frac{D-1}{2})}.$$

By now solving the system of equations (5.13) the result is

$$\begin{aligned} I_L^{\mu\nu} &= \frac{D-2}{2^{2D-4}\,\pi^{(D-3)/2}\,\Gamma(\frac{D+1}{2})}q^{D-4}\left(q^\mu q^\nu - q^2 g^{\mu\nu}\right) \\ &= \frac{D-2}{2^{2D-4}\,\pi^{(D-3)/2}\,\Gamma(\frac{D+1}{2})}q^{D-4} f^{\mu\nu}, \end{aligned}$$

where $f^{\mu\nu}$ was defined for simplicity. Thus, the integral for the cross section reduces considerably to

$$\sigma^{\mathrm{r}}_{q\bar{q}} = \frac{1}{2}\pi\sigma_{\mathrm{B}} N C_F\, g_s^2 \int \frac{\mathrm{d}^{D-1}k_1}{(2\pi)^{D-1}2E_1}\frac{1}{q^4}H_{\mu\nu}I_L^{\mu\nu}. \tag{5.14}$$

Hadronic integration

Now, the gluon momentum k_1 still has to be integrated out. The integral reads

$$\int \frac{\mathrm{d}^{D-1}k_1}{(2\pi)^{D-1}2E_1}\frac{1}{q^4}H_{\mu\nu}I_L^{\mu\nu} \tag{5.15}$$

and our goal is to transform this integral to simpler kinematical variables. As the leptonic momenta have been integrated out in this expression, we can consider the remaining integration in the CMS system $p_a + p_b \to q + k_1$:

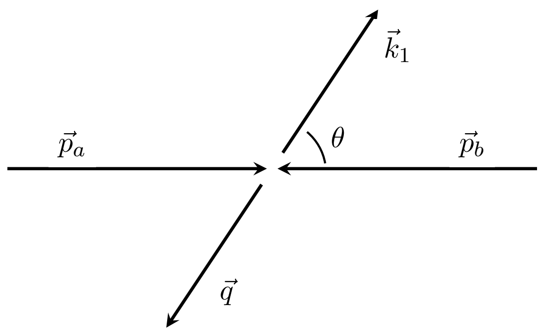

where θ is the angle between $\vec{p}_a$ and the gluon momentum $\vec{k}_1$. We can now introduce spherical coordinates in the same way as for the leptonic part

$$\mathrm{d}^{D-1}k_1 = |\vec{k}_1|^{D-2}\mathrm{d}|\vec{k}_1|\,\mathrm{d}\Omega_{D-1} = E_1^{D-2}\mathrm{d}E_1\mathrm{d}\Omega_{D-1}.$$

By using momentum conservation

$$q^2 = (p_a + p_b - k_1)^2 = s - 2(p_a+p_b)k_1 = s - 2\sqrt{s}E_1,$$

we can furthermore change the integration variable E_1 to q^2. With

$$E_1 = \frac{s-q^2}{2\sqrt{s}}, \quad \mathrm{d}E_1 = -\frac{\mathrm{d}q^2}{2\sqrt{s}},$$

the transformation reads

$$\frac{\mathrm{d}^{D-1}k_1}{(2\pi)^{D-1}2E_1} = -\frac{1}{2^{D-1}s^{(D-2)/2}}\left(s-q^2\right)^{D-3}\mathrm{d}q^2\,\frac{1}{(2\pi)^{D-1}}\mathrm{d}\Omega_{D-1}. \tag{5.16}$$

Now the integration is already written in terms of one convenient kinematical variable, the momentum transfer q. We try to further transform the integral over the solid angle

$$I_\Omega = \frac{1}{(2\pi)^{D-1}}\int \mathrm{d}\Omega_{D-1} H_{\mu\nu} I_L^{\mu\nu}. \tag{5.17}$$

Using (A.1) from Appendix A.5, we can reduce the phase space integration to

$$\frac{1}{(2\pi)^{D-1}}\int \mathrm{d}\Omega_{D-1} = \frac{\pi^{-D/2}}{2\Gamma(\frac{D-2}{2})}\int_0^1 \mathrm{d}y\;[y(1-y)]^{\frac{D-4}{2}}, \tag{5.18}$$

where $y = (1+\cos\theta)/2$. So in total, (5.17) takes the final form

$$I_\Omega = \frac{\pi^{-D/2}}{2\Gamma(\frac{D-2}{2})}\int_0^1 \mathrm{d}y\;[y(1-y)]^{\frac{D-4}{2}}\,H_{\mu\nu}I_L^{\mu\nu},$$

where we can now insert the leptonic integral to arrive at

$$\begin{aligned} I_\Omega &= \frac{\pi^{-D/2}}{2\Gamma(\frac{D-2}{2})}\frac{D-2}{2^{2D-4}\,\pi^{(D-3)/2}\,\Gamma(\frac{D+1}{2})}q^{D-4}\int_0^1 \mathrm{d}y\;[y(1-y)]^{\frac{D-4}{2}}\,H_{\mu\nu}f^{\mu\nu} \\ &= \frac{(4\pi)^{2\varepsilon}}{16\pi^{5/2}}\frac{(1-\varepsilon)}{\Gamma(1-\varepsilon)\Gamma(\frac{5-2\varepsilon}{2})}q^{D-4}\int_0^1 \mathrm{d}y\;[y(1-y)]^{-\varepsilon}\,H_{\mu\nu}f^{\mu\nu}. \end{aligned} \tag{5.19}$$

Performing the integration

To be able to perform the integration

$$\int_0^1 \mathrm{d}y\;[y(1-y)]^{-\varepsilon}\,H_{\mu\nu}f^{\mu\nu} \tag{5.20}$$

in (5.19), we express $H_{\mu\nu}f^{\mu\nu}$ in dimensionless quantities. In terms of the variables s, t and u that we introduced, its contributions are given by

$$\left(H_a^{\mu\nu}+H_b^{\mu\nu}\right)f_{\mu\nu} = -2(D-2)\left[(D-2)q^2\left(\frac{t}{u}+\frac{u}{t}\right)+2s\right],$$

and

$$\left(2H_{\mathrm{if}}^{\mu\nu}\right)f_{\mu\nu} = -4(D-2)\left[(D-4)q^2 - s + s\frac{2q^4}{tu}\right],$$

which sum up to

$$H_{\mu\nu}f^{\mu\nu} = -8(1-\varepsilon)\left[s\frac{2q^4}{tu} - 2\varepsilon q^2 + (1-\varepsilon)q^2\left(\frac{t}{u}+\frac{u}{t}\right)\right]. \tag{5.21}$$

The angular variable y is already dimensionless, and q^2 can be rendered dimensionless by switching to $z = \frac{q^2}{s}$. The transformations between the kinematics read

$$\begin{aligned}
s &= (p_a+p_b)^2 = \frac{q^2}{z} \\
t &= (p_a-k_1)^2 = -2p_a k_1 = -\sqrt{s}|\vec{k}_1|\ (1-\cos\theta) = \frac{-q^2}{z}(1-z)(1-y) \\
u &= (p_b-k_1)^2 = \frac{-q^2}{z}(1-z)y.
\end{aligned}$$

In the new variables (5.21) becomes

$$H_{\mu\nu}f^{\mu\nu} = -16(1-\varepsilon)q^2\left[\frac{z}{(1-z)^2}\frac{1}{y(1-y)} - \varepsilon + \frac{(1-\varepsilon)}{2}\left(\frac{1-y}{y}+\frac{y}{1-y}\right)\right]. \tag{5.22}$$

As $(1-z)$ denotes the momentum fraction of the emitted gluon, we see that the first expression is singular when the gluon is emitted softly ($z=1$). Furthermore, when the gluon is emitted collinearly to one of the quarks, we have $y=1$ (because of $\cos\theta = 1$). Therefore the first term contains a soft and collinear singularity. Keeping this in mind, we can integrate over y, where the following integrals will occur:

$$\begin{aligned}
\int_0^1 \mathrm{d}y\ \ [y(1-y)]^{-\varepsilon}\,\frac{1}{y(1-y)} &= \int_0^1 \mathrm{d}y\ y^{-\varepsilon-1}(1-y)^{-\varepsilon-1} \\
&= B(-\varepsilon,-\varepsilon) = \frac{\Gamma^2(-\varepsilon)}{\Gamma(-2\varepsilon)} = \frac{-2}{\varepsilon}\frac{\Gamma^2(1-\varepsilon)}{\Gamma(1-2\varepsilon)},
\end{aligned}$$

$$\int_0^1 \mathrm{d}y\ \ [y(1-y)]^{-\varepsilon} = B(1-\varepsilon,1-\varepsilon) = \frac{\Gamma^2(1-\varepsilon)}{\Gamma(2-2\varepsilon)} = \frac{1}{1-2\varepsilon}\frac{\Gamma^2(1-\varepsilon)}{\Gamma(1-2\varepsilon)},$$

$$\begin{aligned}
\int_0^1 \mathrm{d}y\ \ [y(1-y)]^{-\varepsilon}\left(\frac{1-y}{y}+\frac{y}{1-y}\right) &= B(-\varepsilon,2-\varepsilon) + B(2-\varepsilon,-\varepsilon) = 2B(-\varepsilon,2-\varepsilon) \\
&= 2\frac{\Gamma(-\varepsilon)\Gamma(2-\varepsilon)}{\Gamma(2-2\varepsilon)} = -2\frac{1-\varepsilon}{\varepsilon(1-2\varepsilon)}\frac{\Gamma^2(1-\varepsilon)}{\Gamma(1-2\varepsilon)}.
\end{aligned}$$

Inserting these in (5.20) results in

$$\begin{aligned}
\int_0^1 \mathrm{d}y\ \ [y(1-y)]^{-\varepsilon}\,H_{\mu\nu}f^{\mu\nu} &= 16(1-\varepsilon)\frac{\Gamma^2(1-\varepsilon)}{\Gamma(1-2\varepsilon)}q^2\left[\frac{2}{\varepsilon}\frac{z}{(1-z)^2} + \frac{1}{1-2\varepsilon}\varepsilon + \frac{(1-\varepsilon)^2}{\varepsilon(1-2\varepsilon)}\right] \\
&= 16(1-\varepsilon)\frac{\Gamma^2(1-\varepsilon)}{\Gamma(1-2\varepsilon)}q^2\left[\frac{2}{\varepsilon}\frac{z}{(1-z)^2} + \frac{1}{1-2\varepsilon}\left(\varepsilon + \frac{(1-\varepsilon)^2}{\varepsilon}\right)\right].
\end{aligned}$$

Collecting all factors, the integral over the solid angle therefore gives

$$
\begin{aligned}
I_\Omega &= \frac{(4\pi)^{2\varepsilon}}{16\pi^{5/2}} \frac{16(1-\varepsilon)^2\Gamma(1-\varepsilon)}{\Gamma(\frac{5-2\varepsilon}{2})\Gamma(1-2\varepsilon)} q^{D-4} q^2 \left[\frac{2}{\varepsilon}\frac{z}{(1-z)^2} + \frac{1}{1-2\varepsilon}\left(\varepsilon + \frac{(1-\varepsilon)^2}{\varepsilon}\right)\right] \\
&= \frac{(4\pi)^{2\varepsilon}}{\pi^{5/2}} \frac{(1-\varepsilon)^2\Gamma(1-\varepsilon)}{\Gamma(\frac{5-2\varepsilon}{2})\Gamma(1-2\varepsilon)} q^{D-2} \left[\frac{2}{\varepsilon}\frac{z}{(1-z)^2} + \frac{1}{1-2\varepsilon}\left(\varepsilon + \frac{(1-\varepsilon)^2}{\varepsilon}\right)\right].
\end{aligned}
$$

Differential cross section

With (5.14) and (5.16) we can write the cross section differential in q^2 :

$$
\begin{aligned}
\frac{\mathrm{d}\sigma^{\mathrm{r}}_{q\bar{q}}}{\mathrm{d}q^2} &= -\frac{3}{2}\pi\sigma_{\mathrm{B}} C_F\, g_s^2 \mu^{3(4-D)} \frac{\left(s-q^2\right)^{D-3}}{2^{D-1} s^{(D-2)/2}} \frac{I_\Omega}{q^4} \\
&= -\frac{3}{2}\pi\sigma_{\mathrm{B}} C_F\, g_s^2 \mu^{6\varepsilon}\, 2^{-3+2\varepsilon} s^{-\varepsilon}(1-z)^{1-2\varepsilon}\frac{I_\Omega}{q^4} \\
&= -\sigma_{\mathrm{B}} \frac{g_s^2}{4\pi^2} C_F\, \mu^{6\varepsilon}\, (4\pi)^{2\varepsilon} D(\varepsilon) s^{-\varepsilon}(1-z)^{1-2\varepsilon} q^{D-6} \left[\frac{2}{\varepsilon}\frac{z}{(1-z)^2} + \frac{1}{1-2\varepsilon}\left(\varepsilon + \frac{(1-\varepsilon)^2}{\varepsilon}\right)\right] \\
&= -4\frac{\sigma_{\mathrm{B}}}{q^2} \frac{g_s^2}{(4\pi)^2} C_F \left(\frac{4\pi\mu^{3\varepsilon}}{q^2}\right)^{2\varepsilon} D(\varepsilon)\, z^{\varepsilon}(1-z)^{1-2\varepsilon} \left[\frac{2}{\varepsilon}\frac{z^2}{(1-z)^2} + \frac{1}{1-2\varepsilon}\left(\varepsilon + \frac{(1-\varepsilon)^2}{\varepsilon}\right) z\right].
\end{aligned}
$$

Contributions of $\mathcal{O}(\varepsilon)$ in the last term can be dropped, resulting in

$$
\frac{\mathrm{d}\sigma^{\mathrm{r}}_{q\bar{q}}}{\mathrm{d}q^2} = -4\frac{\sigma_{\mathrm{B}}}{q^2}\frac{\alpha_s}{4\pi} C_F \left(\frac{4\pi\mu^{3\varepsilon}}{q^2}\right)^{2\varepsilon} D(\varepsilon)\,(1-z)^{-1-2\varepsilon}\frac{z^{\varepsilon}}{\varepsilon}\left[1+z^2\right], \tag{5.23}
$$

where we used the same abbreviation $D(\varepsilon)$ as we did for the virtual correction (5.12)

$$
D(\varepsilon) = \frac{3\sqrt{\pi}(1-\varepsilon)^2}{2^{2-2\varepsilon}\Gamma\left(\frac{5-2\varepsilon}{2}\right)} \frac{\Gamma(1-\varepsilon)}{\Gamma(1-2\varepsilon)} = 1 + \mathcal{O}(\varepsilon).
$$

In the result (5.23), there are singularities for $z \to 1$ if we take $\varepsilon \to 0$. We can make these singularities manifest in ε with the help of the plus-distribution using the identity

$$
(1-z)^{-1-2\varepsilon} = -\frac{1}{2\varepsilon}\delta(1-z) + \frac{1}{(1-z)_+} - 2\varepsilon\left(\frac{\ln(1-z)}{1-z}\right)_+ + \mathcal{O}(\varepsilon).
$$

Using this expansion and expanding $z^{\varepsilon} = 1 + \varepsilon \ln z + \mathcal{O}(\varepsilon)$ as usual, we end up with

$$
\begin{aligned}
\frac{\mathrm{d}\sigma^{\mathrm{r}}_{q\bar{q}}}{\mathrm{d}q^2} = 2\frac{\sigma_{\mathrm{B}}}{q^2}\frac{\alpha_s}{2\pi} C_F \left(\frac{4\pi\mu^{3\varepsilon}}{q^2}\right)^{2\varepsilon} D(\varepsilon)\Bigg[&\frac{1}{\varepsilon^2}\delta(1-z) - \frac{1}{\varepsilon}\frac{1+z^2}{(1-z)_+} \\
&+ 2(1+z^2)\left(\frac{\ln(1-z)}{1-z}\right)_+ - \frac{1+z^2}{(1-z)_+}\ln z\Bigg],
\end{aligned}
$$

where we used that $z = 1$ in terms containing the delta function $\delta(1-z)$. Here, the soft collinear ($\frac{1}{\varepsilon^2}$) and the collinear singularity ($\frac{1}{\varepsilon}$) are now manifest at $z = 1$. This can now be combined with the virtual corrections. From (5.11), the virtual corrections can be written differential in q^2 as

$$\frac{\mathrm{d}\sigma^{\mathrm{v}}_{q\bar{q}}}{\mathrm{d}q^2} = \delta(1-z)\frac{\sigma_{\mathrm{B}}}{q^2}\frac{\alpha_s}{2\pi}C_{\mathrm{F}}\left(\frac{4\pi\mu^3}{s}\right)^{2\varepsilon} D(\varepsilon)\left(-\frac{2}{\varepsilon^2_{\mathrm{IR}}} - \frac{3}{\varepsilon_{\mathrm{IR}}} - 8 + \frac{2\pi^2}{3} + \mathcal{O}(\varepsilon)\right).$$

By adding this to the real contribution the double poles cancels, resulting in

$$\frac{\mathrm{d}\sigma^{\mathrm{r}}_{q\bar{q}}}{\mathrm{d}q^2} + \frac{\mathrm{d}\sigma^{\mathrm{v}}_{q\bar{q}}}{\mathrm{d}q^2} = \frac{\sigma_{\mathrm{B}}}{q^2}\frac{\alpha_s}{2\pi}\left(\frac{4\pi\mu^{3\varepsilon}}{q^2}\right)^{2\varepsilon} D(\varepsilon)\left[-\frac{2}{\varepsilon}P^{(1)}_{qq}(z) + R_1(z)\right],$$

where the splitting function $P^{(1)}_{qq}(z)$ occurs by combination of the collinear singularities of the virtual and the real correction. Thus, there remains the collinear singularity together with a finite part

$$R_1(z) = C_F\left[\delta(1-z)\left(\frac{2\pi^2}{3} - 8\right) + 4(1+z^2)\left(\frac{\ln(1-z)}{1-z}\right)_+ 2\frac{1+z^2}{(1-z)_+}\ln z\right].$$

5.3.2 Quark-gluon scattering

Lastly, there is the quark-gluon scattering $qg \to l^- l^+ q$. The corresponding diagrams are

$i\mathcal{M} =$

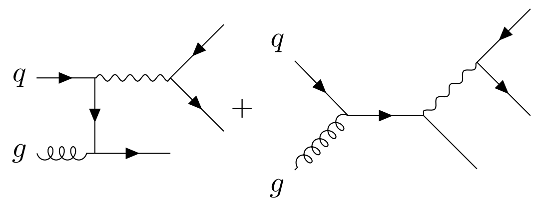

with the matrix elements

$$i\mathcal{M}_s = Q_f e^2 g_s \mu^{3(4-D)/2}\frac{1}{s}\left[\bar{u}(k_1)\gamma^\mu(\not{p}_a + \not{p}_b)\gamma^\alpha u(p_a)\right] T^a_{ij}\varepsilon_\alpha \frac{-i}{q^2}\left[\bar{u}(k_2)\gamma_\mu v(k_3)\right],$$

for the $s-$channel and

$$i\mathcal{M}_u = Q_f e^2 g_s \mu^{3(4-D)/2}\frac{1}{-u}\left[\bar{u}(k_1)\gamma^\alpha(\not{p}_b - \not{k}_1)\gamma^\mu u(p_a)\right] T^a_{ij}\varepsilon_\alpha \frac{-i}{q^2}\left[\bar{u}(k_2)\gamma_\mu v(k_3)\right]$$

for the $u-$channel. Again, the leptonic part is unmodified. Therefore, the same procedure as before can be used. The only modifications are the hadronic traces, which here sum up to

$$H_{\mu\nu}f^{\mu\nu} = -8(1-\varepsilon)\left[-\frac{2tq^4}{su} + 2\varepsilon q^2 - (1-\varepsilon)q^2\left(\frac{t}{s} + \frac{s}{t}\right)\right], \tag{5.24}$$

and the color factor, which gives

$$\frac{1}{N_{\mathrm{C}}(N^2_{\mathrm{C}} - 1)}\sum_a \mathrm{Tr}[T^a T^a] = \frac{T_F}{N}.$$

The calculation of the hadronic integral can be performed in a similar fashion as above, resulting in

$$\int_0^1 \mathrm{d}y \;\; [y(1-y)]^{-\varepsilon} H_{\mu\nu} f^{\mu\nu} = -16(1-\varepsilon)\frac{\Gamma^2(1-\varepsilon)}{\Gamma(1-2\varepsilon)} q^2 \frac{1}{2}\left[2z\frac{1-\varepsilon}{\varepsilon(1-2\varepsilon)} - \frac{1}{\varepsilon}\frac{1}{1-z} + \frac{1-z}{2-\varepsilon}\right].$$

Using this, together with the modified color factor, we can directly translate the result for the cross section from before (5.23) into the quark-gluon cross section

$$\frac{\mathrm{d}\sigma^{\mathrm{r}}_{qg}}{\mathrm{d}q^2} = \frac{\sigma_{\mathrm{B}}}{q^2}\frac{\alpha_s}{2\pi} T_F \left(\frac{4\pi\mu^{3\varepsilon}}{q^2}\right)^{2\varepsilon} D(\varepsilon) z^{\varepsilon}(1-z)^{1-2\varepsilon}\left[2z\frac{1-\varepsilon}{\varepsilon(1-2\varepsilon)} - \frac{1}{\varepsilon}\frac{1}{1-z} + \frac{1-z}{2-\varepsilon}\right].$$

This time, there is no need for the plus distribution and by expanding we find that the gluon-quark splitting function $P^{(1)}_{qg}(z)$ appears,

$$\frac{\mathrm{d}\sigma^{\mathrm{r}}_{qg}}{\mathrm{d}q^2} = \frac{\sigma_{\mathrm{B}}}{q^2}\frac{\alpha_s}{2\pi}\left(\frac{4\pi\mu^{3\varepsilon}}{q^2}\right)^{2\varepsilon} D(\varepsilon)\left[-\frac{1}{\varepsilon}P^{(1)}_{qg}(z) + R_2(z)\right],$$

together with a residual part

$$R_2(z) = -\frac{3z^2}{2} + z + \frac{1}{2} + \left(z^2 + (1-z)^2\right)\ln\frac{(1-z)^2}{z}.$$

5.4 The finite hadronic cross section

Having now calculated all virtual and real contributions to NLO, we can first collect the important results. In the $q\bar{q}$ channel, we obtained the NLO correction

$$\begin{aligned}\frac{\mathrm{d}\tilde{\sigma}^{(1)}_{q\bar{q}}}{\mathrm{d}q^2} &= \frac{\mathrm{d}\sigma^{\mathrm{r}}_{q\bar{q}}}{\mathrm{d}q^2} + \frac{\mathrm{d}\sigma^{\mathrm{v}}_{q\bar{q}}}{\mathrm{d}q^2}\\ &= \frac{\sigma_{\mathrm{B}}}{q^2}\frac{\alpha_s}{2\pi}\left(\frac{4\pi\mu^{3\varepsilon}}{q^2}\right)^{2\varepsilon} D(\varepsilon)\left[-\frac{2}{\varepsilon}P^{(1)}_{qq}(z) + R_1(z)\right].\end{aligned}$$

We also had to account for the real contribution of the channel $qg \to ql^+l^-$

$$\frac{\mathrm{d}\tilde{\sigma}^{(1)}_{qg}}{\mathrm{d}q^2} = \frac{\sigma_{\mathrm{B}}}{q^2}\frac{\alpha_s}{2\pi}\left(\frac{4\pi\mu^{3\varepsilon}}{q^2}\right)^{2\varepsilon} D(\varepsilon)\left[-\frac{1}{\varepsilon}P^{(1)}_{qg}(z) + R_2(z)\right],$$

where there are no leading diagrams and therefore no virtual corrections. Both results are still collinearly divergent, which will be denoted by a tilde ($\mathrm{d}\tilde{\sigma}$). Our goal is to find a finite cross section for the Drell-Yan process. To this end, it is useful to think about the physical nature of the remaining singularity. It originates in an initial quark that emits a soft and collinear gluon. As the momentum of the soft gluon goes to zero, the propagator of the quark becomes infinite. However, the propagator corresponds to the propagation time of the particle. We can therefore think of the process as happening on two different time scales: First, the quark emits a soft gluon and propagates for a long time (going to infinity). Then, on a short time scale the hard scattering takes place, when both initial quarks form a highly virtual exchange particle. This is why the cross section is the product of the Born cross section for the hard scattering and the respective splitting function P_{ij}. It is just given by the combined probability of the collinear splitting and the cross section without splitting for the remaining process.

Recalling the assumption for the factorization of the hadronic cross section, one gets an idea how to consistently treat the collinear singularity. It was assumed that all physics describing the interactions of the partons on large timescales should be contained in the PDFs. Thus, the PDFs should be redefined, such that the collinear splitting is contained in them, instead of the cross section. After all, this is well justified, as only the hadronic cross section is guaranteed to be a finite observable, while the PDFs and the hard cross section are not. Therefore, we can denote the factorization result for the Drell-Yan process as

$$\mathrm{d}\sigma^{H}_{AB}(s) = \sum_{a,b} \int_0^1 \mathrm{d}y_a \int_0^1 \mathrm{d}y_b\, \overline{f}_a(y_a, \mu_\mathrm{F}^2)\overline{f}_b(y_b, \mu_\mathrm{F}^2)\mathrm{d}\tilde{\sigma}_{ab}(y_a y_b s, \mu_\mathrm{F}^2), \tag{5.25}$$

in terms of bare PDFs $\overline{f}$, that are supposed to absorb the divergence in the collinear divergent partonic cross section $\mathrm{d}\tilde{\sigma}_{ab}$. The notation $\overline{f}_{a/A}$ was simplified to $\overline{f}_a$ for readability and we adopted the kinematics

$$\begin{aligned} s^2 &= (P_A + P_B)^2 \\ \hat{s}^2 &= (x_a P_A + x_b P_B)^2 = (x_a x_b s)^2. \end{aligned}$$

Now we need to find a way to separate the singular part of $\mathrm{d}\tilde{\sigma}_{ab}$ such that it can be absorbed into the PDFs in the above convolution. This is very similar to the multiplicative renormalization procedure for UV-divergences, only that in this case the IR-divergences cannot be eliminated by a simple multiplicative constant. Instead of counterterms, we define transition functions

$$\Gamma_{ij}(z) = \delta_{ij}\delta(1-z) + \frac{\alpha_s}{2\pi}\Gamma^{(1)}_{ij}(z) + \mathcal{O}(\alpha_s^2), \tag{5.26}$$

such that the collinear divergent partonic cross section $\mathrm{d}\tilde{\sigma}_{ab}$ is obtained from the finite partonic cross $\mathrm{d}\sigma_{ab}$ by the convolution

$$\mathrm{d}\tilde{\sigma}_{ab}(\hat{s}) = \sum_{l,m} \int_0^1 \mathrm{d}z_a \int \mathrm{d}z_b\, \Gamma_{al}(z_a)\mathrm{d}\sigma_{lm}(z_a z_b \hat{s}, \mu_\mathrm{F}^2)\Gamma_{bm}(z_b). \tag{5.27}$$

The first term in the transition function (5.26) reproduces the parton model, where the partonic cross section does not need to renormalized, thus $\mathrm{d}\tilde{\sigma}_{ab} = \mathrm{d}\sigma_{ab}$. The second term $\Gamma^{(1)}_{ij}(z)$ is used to absorb the divergences of order α_s, which we will demonstrate later. We try to include the transition functions into the bare PDFs. By inserting (5.27) into (5.25), we find

$$\mathrm{d}\sigma^{H}_{AB}(s) = \sum_{a,b,l,m} \int \mathrm{d}y_a \mathrm{d}z_a\, \overline{f}_a(y_a, \mu_\mathrm{F}^2)\Gamma_{al}(z_a) \int \mathrm{d}y_b \mathrm{d}z_b \overline{f}_b(y_b, \mu_\mathrm{F}^2)\Gamma_{bm}(z_b)\mathrm{d}\sigma_{lm}(y_a y_b \hat{s}, \mu_\mathrm{F}^2). \tag{5.28}$$

The product of bare PDF and transition functions can be decoupled using $\delta-$functions, respectively, such that the hadronic cross section can be written in terms of the finite partonic cross section $\mathrm{d}\sigma_{lm}$ as

$$\mathrm{d}\sigma^{H}_{AB}(s) = \sum_{l,m} \int \mathrm{d}x_a \mathrm{d}x_b\, f_l(x_a, \mu_\mathrm{F}^2) f_m(x_b, \mu_\mathrm{F}^2)\mathrm{d}\sigma_{lm}(x_a x_b \hat{s}, \mu_\mathrm{F}^2). \tag{5.29}$$

Here we defined the renormalized PDFs

$$
\begin{aligned}
f_{l/A}(x_a,\mu_\mathrm{F}^2) &= \sum_a \int_0^1 \mathrm{d}y_a \int_0^1 \mathrm{d}z_a\, \delta(x_a - y_a z_a)\overline{f}_a(y_a,\mu_\mathrm{F}^2)\Gamma_{al}(z_a) \\
f_{m/B}(x_b,\mu_\mathrm{F}^2) &= \sum_b \int_0^1 \mathrm{d}y_b \int_0^1 \mathrm{d}z_b\, \delta(x_b - y_b z_b)\overline{f}_b(y_b,\mu_\mathrm{F}^2)\Gamma_{bm}(z_b).
\end{aligned}
$$

Since the hadronic cross section is finite, and the partonic cross section was rendered finite ($\mathrm{d}\tilde{\sigma} \to \mathrm{d}\sigma$ in our notation), the renormalized PDFs have to be finite as a consequence, and can be considered to be the PDFs extracted by experiments. The scale dependence is completely given by the fact that the hadronic cross section does not depend on the scale, which leads to the DGLAP equations for the PDFs given in section 4.3.

This procedure can now be used to arrive at the finite result for the hadronic Drell-Yan cross section. From (5.26) the relation between the finite and singular partonic cross section can be read off by expanding

$$
\begin{aligned}
\mathrm{d}\tilde{\sigma}_{ab}(\hat{s},\mu_\mathrm{F}^2) &= \mathrm{d}\tilde{\sigma}_{ab}^{(0)}(\hat{s}) + \frac{\alpha_s}{2\pi}\mathrm{d}\tilde{\sigma}_{ab}^{(1)}(\hat{s},\mu_\mathrm{F}^2) + \mathcal{O}(\alpha_s^2) \\
\mathrm{d}\sigma_{ab}(\hat{s},\mu_\mathrm{F}^2) &= \mathrm{d}\sigma_{ab}^{(0)}(\hat{s}) + \frac{\alpha_s}{2\pi}\mathrm{d}\sigma_{ab}^{(1)}(\hat{s},\mu_\mathrm{F}^2) + \mathcal{O}(\alpha_s^2) \\
\Gamma_{ij}(z) &= \delta_{ij}\delta(1-z) + \frac{\alpha_s}{2\pi}\Gamma_{ij}^{(1)}(z) + \mathcal{O}(\alpha_s^2),
\end{aligned}
$$

and then collecting terms. In lowest-order, one gets the result $\mathrm{d}\tilde{\sigma}_{ab}^{(0)} = \mathrm{d}\sigma_{ab}^{(0)}$, as leading-order partonic cross sections are finite. In order of α_s, the result is

$$
\mathrm{d}\tilde{\sigma}_{ab}^{(1)}(\hat{s},\mu_\mathrm{F}^2) = \mathrm{d}\sigma_{ab}^{(1)}(\hat{s},\mu_\mathrm{F}^2) + \sum_l \int_0^1 \mathrm{d}z_a \Gamma_{al}^{(1)}(z_a)\mathrm{d}\sigma_{lb}^{(0)}(z_a\hat{s}) + \sum_m \int_0^1 \mathrm{d}z_b \Gamma_{bm}^{(1)}(z_b)\mathrm{d}\sigma_{am}^{(0)}(z_b\hat{s}).
$$

Using $\mathrm{d}\tilde{\sigma}_{ab}^{(0)} = \mathrm{d}\sigma_{ab}^{(0)}$ from the lowest-order, this can be inverted yielding

$$
\mathrm{d}\sigma_{ab}^{(1)}(\hat{s},\mu_\mathrm{F}^2) = \mathrm{d}\tilde{\sigma}_{ab}^{(1)}(\hat{s},\mu_\mathrm{F}^2) - \sum_l \int_0^1 \mathrm{d}z_a \Gamma_{al}^{(1)}(z_a)\mathrm{d}\tilde{\sigma}_{lb}^{(0)}(z_a\hat{s}) - \sum_m \int_0^1 \mathrm{d}z_b \Gamma_{bm}^{(1)}(z_b)\mathrm{d}\tilde{\sigma}_{am}^{(0)}(z_b\hat{s}).
\tag{5.30}
$$

With this renormalization procedure, we can finally write down the finite partonic cross sections for the two real channels we have calculated. First, we recall that the LO cross section can be written as

$$
\frac{\mathrm{d}\sigma_{q\bar{q}}^{(0)}(\hat{s})}{\mathrm{d}q^2} = \sigma_\mathrm{B}(\hat{s})\delta(\hat{s}-q^2).
$$

Now using (5.30), the collinear finite NLO cross section for the $q\bar{q}-$channel can be obtained by

$$
\frac{\mathrm{d}\sigma_{q\bar{q}}^{(1)}(\hat{s},\mu_\mathrm{F}^2)}{\mathrm{d}q^2} = \frac{\mathrm{d}\tilde{\sigma}_{q\bar{q}}^{(1)}(\hat{s},\mu_\mathrm{F}^2)}{\mathrm{d}q^2} - 2\int_0^1 \mathrm{d}x\; \Gamma_{q\bar{q}}^{(1)}(x)\frac{\mathrm{d}\sigma_{q\bar{q}}^{(0)}(x\hat{s})}{\mathrm{d}q^2},
\tag{5.31}
$$

with the subtraction

$$
\Gamma_{q\bar{q}}^{(1)}(x) = -\frac{1}{\varepsilon}P_{q\bar{q}}^{(1)}(x).
\tag{5.32}
$$

The final result is

$$\begin{aligned}\frac{\mathrm{d}\sigma_{q\bar{q}}(\hat{s},\mu_{\mathrm{F}}^2)}{\mathrm{d}q^2} &= \frac{\mathrm{d}\sigma^{(0)}_{q\bar{q}}(\hat{s})}{\mathrm{d}q^2} + \frac{\mathrm{d}\tilde{\sigma}^{(1)}_{q\bar{q}}(\hat{s},\mu_{\mathrm{F}}^2)}{\mathrm{d}q^2} - \frac{2}{\varepsilon}P^{(1)}_{qq}(z) \\ &= \frac{\sigma_{\mathrm{B}}(\hat{s})}{q^2}\left(\delta(1-z) + \frac{\alpha_s}{2\pi}R_1(z)\right).\end{aligned}$$

In the $qg-$channel, (5.30) collapses to

$$\begin{aligned}\mathrm{d}\sigma^{(1)}_{qg}(\hat{s},\mu_{\mathrm{F}}^2) &= \mathrm{d}\tilde{\sigma}^{(1)}_{qg}(\hat{s},\mu_{\mathrm{F}}^2) - \sum_m \int_0^1 \mathrm{d}z_b \Gamma^{(1)}_{gm}(z_b)\mathrm{d}\tilde{\sigma}^{(0)}_{qm}(z_b\hat{s}) \\ &= \mathrm{d}\tilde{\sigma}^{(1)}_{qg}(\hat{s},\mu_{\mathrm{F}}^2) - \int_0^1 \mathrm{d}z_b \Gamma^{(1)}_{g\bar{q}}(z_b)\mathrm{d}\tilde{\sigma}^{(0)}_{q\bar{q}}(z_b\hat{s}),\end{aligned}$$

because there is no leading-order $qg-$diagram, such that $\mathrm{d}\tilde{\sigma}^{(0)}_{gi} = 0$. Therefore we can choose

$$\Gamma^{(1)}_{g\bar{q}}(z) = -\frac{1}{\varepsilon}P^{(1)}_{g\bar{q}}(z) = -\frac{1}{\varepsilon}P^{(1)}_{qg}(z),$$

leading to the finite result

$$\begin{aligned}\frac{\mathrm{d}\tilde{\sigma}_{qg}(\hat{s},\mu_{\mathrm{F}}^2)}{\mathrm{d}q^2} &= \frac{\mathrm{d}\tilde{\sigma}^{(1)}_{qg}(\hat{s},\mu_{\mathrm{F}}^2)}{\mathrm{d}q^2} - \frac{1}{\varepsilon}P^{(1)}_{qq}(z) \\ &= \frac{\sigma_{\mathrm{B}}(\hat{s})}{q^2}\frac{\alpha_s}{2\pi}R_2(z).\end{aligned}$$

These are the final results of this thesis, which can be used with the formula (5.29) to calculate the IR-safe hadronic cross section with known renormalized parton distribution functions. Inversely, using these results, PDFs can be determined in a scheme given by the subtraction that is used in (5.32).

6 Conclusion

The aim of this thesis was to calculate the cross section of the Drell-Yan process with all analytic details using the theory of quantum chromodynamics (QCD) and the QCD-improved parton model for describing the hadronic interaction. For this purpose, the basic procedure of how cross section can be extracted from a given quantum field theory was shown. The Green's function as the essential object containing the physical structure of the theory was introduced and it was sketched how it can be calculated using perturbation theory.

The most important features of QCD were discussed briefly and the possible appearance of different types of divergences during perturbative calculation was explained. We presented techniques for regularizing and renormalizing the theory, thus removing the UV-divergences. In order to apply QCD to hadronic collisions, the parton model was introduced with focus on deep inelastic scattering (DIS) and the Drell-Yan process. In the context of DIS, we discussed parton distribution functions (PDFs). Various aspects of the phenomenology of the Drell-Yan process were discussed, such as the impact of strange quark PDFs, nuclear PDFs or the sensitivity to electroweak observables. It was shown how QCD can be incorporated into the parton model, where the factorization result for the Drell-Yan process was stated and the splitting functions introduced.

Using these theoretical foundations, we computed the leading-order contributions to the partonic cross section in a generic way and analyzed various specific scenarios. The next-to-leading order virtual loop contributions were calculated in dimensional regularization in the on-shell scheme, where ultraviolet- (UV) and infrared- (IR) singularities were explicitly distinguished. Thus the cancellation of UV-divergences by the renormalization of the quark wave function was shown, where the IR-divergences remained. We argued that real emissions which cannot be distinguished from the leading-order process had to be considered. Hence, the processes $q\bar{q} \to gl^-l^+$ and $qg \to ql^-l^+$ were included where the calculation was performed in a general framework not relying on current conservation or other simplifications. The addition of these processes canceled the remaining IR-double pole, however collinear single poles remained.

In the final section of this thesis it was explained, why this remaining divergence can be expected and how to treat it by renormalizing the PDFs. We gave a justification for the renormalization and introduced the systematic procedure to render the partonic cross section finite at any order. At last, we applied it to the real contributions and calculated the IR-finite cross section for the Drell-Yan process.

A Summary of formulae for regularization

A.1 Gamma and Beta function

The gamma function is an extension of the factorial function, with its argument shifted down by 1, to real and complex numbers. For positive integers, it is defined as

$$\Gamma(n) = (n-1)!$$

For complex numbers z with $\mathrm{Re}(z) > 0$ it can be defined as

$$\Gamma(z) = \int_0^\infty x^{z-1} e^{-x}\, dx$$

and fulfills the useful property

$$\Gamma(z+1) = z\Gamma(z).$$

The function has poles for negative integers starting with $z = 0$ and can be expanded as

$$\Gamma(z) = \frac{1}{z} - \gamma_\mathrm{E} + \tfrac{1}{2}\left(\gamma_\mathrm{E}^2 + \frac{\pi^2}{6}\right) z + O(z^2),$$

where γ_E is the Euler–Mascheroni constant defined by

$$\gamma = \lim_{n\to\infty}\left(-\ln n + \sum_{k=1}^{n} \frac{1}{k}\right)$$

In loop calculation one very often encounters the Beta function which is defined by

$$\mathrm{B}(x,y) = \int_0^1 t^{x-1}(1-t)^{y-1}\,\mathrm{d}t$$

for $\mathrm{Re}(x), \mathrm{Re}(y) > 0$. It is symmetric in its arguments and closely related to the gamma function by

$$\mathrm{B}(x,y) = \frac{\Gamma(x)\,\Gamma(y)}{\Gamma(x+y)}.$$

A.2 Feynman Parametrization

When solving loop integrals in quantum field theory, it is often helpful to introduce Feynman parameters, which are simple identities of the form

$$
\begin{aligned}
\frac{1}{AB} &= \int_0^1 \frac{\mathrm{d}x}{[xA+(1-x)B]^2} \\
\frac{1}{ABC} &= 2\int_0^1 \mathrm{d}x \int_0^{1-x} \frac{\mathrm{d}y}{[A(x-y)+(1-x)B+Cy]^3},
\end{aligned}
$$

which are special cases of the general formula

$$
\frac{1}{A_1...A_n} = \int_0^1 \mathrm{d}x_1...\mathrm{d}x_n \delta(1-\sum_i x_i \frac{(n-1)!}{[A_1x_1+...+A_nx_n]^n}.
$$

A.3 Dirac algebra in D dimensions

For calculation of Feynman diagrams with fermions in dimensional regularization, we to modify the Dirac algebra to D dimensions. The anticommutation relation remains normalized to

$$
\{\gamma^\mu, \gamma^\nu\} = 2g^{\mu\nu}
$$

but identities that involve Lorentz-contractions change. They can all be derived by the anti-commutation relation, using $g^\mu_\mu = D$:

$$
\begin{aligned}
\gamma^\mu\gamma_\mu &= D \\
\gamma^\alpha\gamma^\mu\gamma_\alpha &= (2-D)\gamma^\mu \\
\gamma^\alpha\gamma^\mu\gamma^\nu\gamma_\alpha &= 4g^{\mu\nu} - (4-D)\gamma^\mu\gamma^\nu \\
\gamma^\alpha\gamma^\mu\gamma^\nu\gamma^\rho\gamma_\alpha &= -2\gamma^\rho\gamma^\nu\gamma^\mu + (4-D)\gamma^\mu\gamma^\nu\gamma^\rho \\
\gamma^\alpha\gamma^\mu\gamma^\nu\gamma^\rho\gamma^\sigma\gamma_\alpha &= -2\gamma^\sigma\gamma^\rho\gamma^\nu\gamma^\mu + 2\gamma^\rho\gamma^\mu\gamma^\nu\gamma^\sigma - (4-D)\gamma^\mu\gamma^\nu\gamma^\rho\gamma^\sigma
\end{aligned}
$$

The trace identities do not change:

$$
\begin{aligned}
\mathrm{Tr}[\gamma^\mu] &= 0 \\
\mathrm{Tr}[\gamma^\mu\gamma^\nu] &= 4g^{\mu\nu} \\
\mathrm{Tr}[\gamma^\mu\gamma^\nu\gamma^\rho] &= 0 \\
\mathrm{Tr}[\gamma^\mu\gamma^\nu\gamma^\rho\gamma^\sigma] &= 4\left(g^{\mu\nu}g^{\sigma\rho} - g^{\mu\rho}g^{\nu\sigma} + g^{\mu\sigma}g^{\nu\rho}\right)
\end{aligned}
$$

A.4 Phase space in D dimensions

The n-particle phase space can be most conveniently written in the center of mass system (CMS), where $\vec{p}_a = -\vec{p}_b$. In D dimensions, the phase space element is given by

$$
\mathrm{dPS}^{(n)} = \frac{\mathrm{d}^{D-1}k_1}{(2\pi)^{D-1}2E_1} \cdot\cdots\cdot \frac{\mathrm{d}^{D-1}k_n}{(2\pi)^{D-1}2E_n} (2\pi)^D \delta^{(D)}(p_a+p_b-k_1-...-k_n).
$$

For $n = 2$ this can be transformed to

$$\mathrm{dPS}^{(2)} = \frac{1}{(2\pi)^{D-1}} \frac{1}{2\sqrt{s}} \frac{\pi^{(D-2)/2}}{\Gamma(\frac{D-2}{2})} \left(\frac{\lambda_{12}^{\frac{1}{2}}}{2\sqrt{s}} \right)^{D-3} \left(1 - \cos^2\theta\right)^{\frac{D-4}{2}} \mathrm{d}\cos\theta \mathrm{d}\phi,$$

or using $D = 4 - 2\varepsilon$

$$\mathrm{dPS}^{(2)} = \frac{1}{16\pi^2} \frac{(4\pi)^{\varepsilon}}{\Gamma(1-\varepsilon)} \frac{1}{\sqrt{s}} \left(\frac{\lambda_{12}^{\frac{1}{2}}}{2\sqrt{s}} \right)^{1-2\varepsilon} \left(1 - \cos^2\theta\right)^{-\varepsilon} \mathrm{d}\cos\theta \mathrm{d}\phi.$$

The kinematics schematically take the form

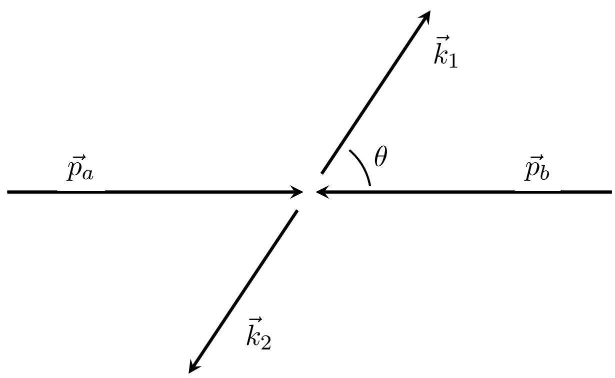

where the $z-$axis is conventionally chosen to $\vec{p}_a$, such that the the azimuthal angle θ coincides with the angle between $\vec{p}_a$ and $\vec{k}_1$.

A.5 Solid angle in D dimensions

Often we need to integrate over the solid angle

$$\mathrm{d}\Omega_D = \mathrm{d}\phi\,\mathrm{d}\theta_1 \sin\theta_1 ... \mathrm{d}\theta_{D-3} \sin^{D-3}\theta_{D-3}$$

by either integrating all variables out, or leaving out one angle, usually $\theta = \theta_{D-3}$. This can be done with the help of

$$\begin{aligned}\int_0^{\pi} \sin^n\theta \mathrm{d}\theta &= \int_0^1 2^n y^{\frac{n-1}{2}} (1-y)^{\frac{n-1}{2}} \mathrm{d}y \\ &= \sqrt{\pi} \frac{\Gamma(\frac{n+1}{2})}{\Gamma(\frac{n+2}{2})},\end{aligned}$$

where we introduced $y = (1+\cos\theta)/2$. In the first case, one gets the solid angle in D-dimensions,

$$\begin{aligned}\int \mathrm{d}\Omega_D = \Omega_D &= 2\pi\sqrt{\pi}^{D-2} \frac{\Gamma(1)\Gamma(\frac{3}{2})}{\Gamma(\frac{3}{2})\Gamma(2)} ... \frac{\Gamma(\frac{D-1}{2})}{\Gamma(\frac{D}{2})} \\ &= 2\frac{\pi^{D/2}}{\Gamma(\frac{D}{2})}.\end{aligned}$$

In the second case, the remaining integration is

$$\int \mathrm{d}\Omega_D = \Omega_{D-1} \int_0^1 2^{D-3} y^{\frac{D-3}{2}} (1-y)^{\frac{D-3}{2}} \mathrm{d}y. \tag{A.1}$$

A.6 The plus distribution

The plus distribution is useful to define integrals $\int_0^1 \mathrm{d}x\, f(x)$ for functions that have a pole at $x = 1$. It is defined as

$$\int \frac{f(x)}{(1-x)_+} \mathrm{d}x = \int_0^1 \frac{f(x) - f(1)}{1-x} \mathrm{d}x,$$

such that

$$\frac{1}{(1-x)_+} = \frac{1}{1-z} \quad \text{for } z \neq 1.$$

These two conditions define the distribution uniquely for any limits of integration.

B Feynman Rules for the electroweak sector

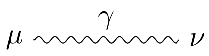

$$= \frac{-ig^{\mu\nu}}{k^2 + i\varepsilon}$$

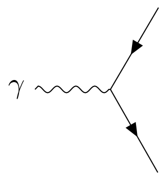

$$= -ie\gamma^\mu$$

$$= \frac{-i\left(g^{\mu\nu} - \frac{p^\mu p^\nu}{M_{W,Z}^2}\right)}{k^2 - M_{W,Z}^2 + i\varepsilon}$$

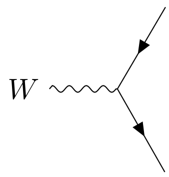

$$= i\frac{g}{\sqrt{2}}\gamma^\mu \frac{1-\gamma_5}{2}$$

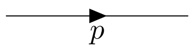

$$= \frac{i(\not{p} + m_f)}{p^2 - m_f^2 + i\varepsilon}$$

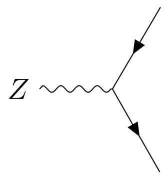

$$= i\frac{g}{\cos\theta_{\mathrm{W}}}\gamma^\mu \left(g_V^f - g_A^f\gamma_5\right)$$

The couplings for the $Z-$boson are given as

$$\begin{aligned} g_V^f &= \frac{1}{2}T_f^3 - Q_f \sin^2\theta_{\mathrm{W}} \\ g_A^f &= \frac{1}{2}T_f^3. \end{aligned}$$

Bibliography

[1] UA1 collaboration, G. Arnison et al, *Phys. Lett.* B122, 103 (1983); UA2 collaboration, G. Banner et al., *Phys. Lett.* B122 (1983), 476.

[2] F. Abe et al. (CDF Collaboration), *Phys. Rev. Lett.* 74, 2626 (1995); D0 Collaboration, S. Abachi et al., *Phys. Rev. Lett.* 74 (1995), 2632.

[3] CMS Collaboration, *Phys. Lett. B* 716, 30 (2012); ATLAS Collaboration, *Phys. Lett.* B716, 1 (2012).

[4] Böhm, Manfred, Ansgar Denner, and Hans Joos, "Gauge theories of the strong and electroweak interaction," *Springer Science & Business Media* (2012).

[5] T. Muta, "Foundations of Quantum Chromodynamics," *World Scientific Publishing Co Pte Ltd* (1987).

[6] G. 't Hooft and M. Veltman, "Regularization and renormalization of gauge fields," *Nuclear Physics B* 44 no. 1, (1972) 189 - 213. `http://www.sciencedirect.com/science/article/pii/0550321372902799`.

[7] F. Bloch and A. Nordsieck, "Note on the radiation field of the electron," *Phys. Rev.* 52 (1937) 54–59. `http://link.aps.org/doi/10.1103/PhysRev.52.54`.

[8] T. Kinoshita, "Mass singularities of Feynman amplitudes," *J. Math. Phys. 3* (1962) 650–677.

[9] T. Lee and M. Nauenberg, "Degenerate systems and mass singularities," *Phys. Rev.* 133 (1964) B1549–B1562.

[10] J. Bjorken, "Asymptotic sum rules at infinite momentum," *Phys. Rev.* 179 (1969), 1547–1553. `http://link.aps.org/doi/10.1103/PhysRev.179.1547.`

[11] DULAT, Sayipjamal, et al., "New parton distribution functions from a global analysis of quantum chromodynamics," *Phys. Rev. D* 93 (2016), 033006.

[12] E. D. Bloom; et al., "High-Energy Inelastic e–p Scattering at 6° and 10°," *Physical Review Letters. 23* (1969), 930–934.

[13] J.H. Christenton et al., "Observation of Massive Muon Pairs in Hadron Collisions," *Phys. Rev. Lett.* 25 (1970), 1523–1526. `doi:10.1103/PhysRevLett.25.1523.`

[14] S. Drell and T.-M. Yan, "Partons and their Applications at High-Energies," *Annals Phys.* 66 (1971), 578.

[15] C. Callan and D. Gross, "High-energy electroproduction and the constitution of the electric current," *Phys. Rev. Letters.* 22 (1969), 156–159. http://link.aps.org/doi/10.1103/PhysRevLett.22.156.

[16] T. Aaltonen et al. (CDF Collaboration), *Phys. Rev. Lett.* 108, 151803.

[17] S. Chatrchyan et al. (CMS Collaboration), *Phys.Rev. D* 84, 112002 (2011), 1110.2682.

[18] Khachatryan, V., Sirunyan, A.M., Tumasyan, A. et al. *Eur. Phys. J. C* (2016) 76,325. `https://doi.org/10.1140/epjc/s10052-016-4156-z`

[19] A. Kusina et al., "Strange quark parton distribution functions and implications for Drell-Yan boson production at the LHC," *Phys. Rev. D* 85 (2012), 094028.

[20] Han, Tao. "Collider Phenomenology:. Basic Knowledge and Techniques," *Physics in D* $\geq$ *4, TASI 2004.*

[21] K. Kovarik et al., *Phys. Rev. D 93*, 085037 (2016).

[22] Collins, John C., Davison E. Soper, and George Sterman, "Factorization of hard processes in QCD," *Adv. Ser. Direct. High Energy Phys 5* (1989): 1-91.

[23] R. K. Ellis, H. Georgi, M. Machacek, H. D. Politzer and G. G. Ross, "Factorization and the Parton Model in QCD," *Phys. Lett. 78B* (1978) 281. `doi:10.1016/0370-2693(78)90023-0`

[24] Altarelli, G. and G. Parisi, "Asymptotic Freedom in Parton Language". *Nucl. Phys. B* 126 (1977), 298–318.

[25] Yu.L. Dokshitzer, *Sov. Phys. JETP* 46 (1977), 641-653.

[26] V.N. Gribov, L.N. Lipatov, *Sov. J. Nucl. Phys.* 15 (1972), 438-450.

[27] C. Patrignani et al. (Particle Data Group), *Chin. Phys. C*, 40, 100001 (2016).

[28] Ingo Bojak, "NLO QCD corrections to the polarized photoproduction and hadroproduction of heavy quarks.", No. hep-ph/0005120, 2000.

Danksagung

Ich möchte zum Schluss allen danken, die mich unterstützt und zu dieser Arbeit beigetragen haben:

- Ich danke Prof. Dr. Michael Klasen für die Übernahme des Referats dieser Arbeit und die Möglichkeit, sie in seiner Arbeitsgruppe verfassen zu können. Auch danken möchte ich für die freundliche Aufnahme und dafür, dass ich die Möglichkeit bekam, bei beiden Retreats des Graduiertenkollegs teilnehmen zu dürfen.
- Mein besonderer Dank gilt Dr. Karol Kovařík für die Themenstellung und die intensive Betreuung. Ich habe durch diese Arbeit sehr viel gelernt, was ohne die vielen Diskussionen und Erklärungen nicht möglich gewesen wäre. Danke für die Geduld, die investierte Zeit und den Zuspruch in schwierigen Phasen. Ich hoffe die Arbeit lebt weiter im Hitchhiker's!
- Ich danke meinen Bürokollegen Marthijn und Lasse, ohne die meine Zeit in der Arbeitsgruppe nur halb so unterhaltsam gewesen wäre. Ich werde die bösen Bienen und den niederländischen Humor auf jeden Fall vermissen!
- Dem restlichen Teil der (erweiterten) Arbeitsgruppe, insbesondere Sonja, Saskia und Daniel danke ich für die warmherzige Aufnahme, die entspannte Atmosphäre in der Gruppe, die interessanten Diskussionen und den freundlichen, hilfsbereiten Umgang miteinander.
- Zuletzt: Danke Isa, dafür dass du mich mit Geist und Herz unterstützt und mich in jedem Zustand ertragen hast. Danke für das schonungslose Korrekturlesen und die geduldige Auseinandersetzung mit allen Problemen, die es bei der Arbeit gab.